REPAIR OF BIPYRIMIDINE PHOTOPRODUCTS AT TELOMERES OF ULTRAVIOLET LIGHT IRRADIATED MAMMALIAN CELLS

by

Dhvani Parikh

BS, St. Xavier's College, India, 2004

MS, Gujarat University, India, 2006

MS, Environmental Health Sciences, New York University, 2009

Submitted to the Graduate Faculty of

Graduate School of Public Health in partial fulfillment

Of the requirements for the degree of

Doctor of Philosophy

University of Pittsburgh

2014

UNIVERSITY OF PITTSBURGH

Graduate School of Public Health

This dissertation was presented

By

Dhvani Parikh

It was defended on

November 12, 2014

And approved by

Chairperson: Aaron Barchowsky, PhD, Professor, Department of Environmental and Occupational Health, Graduate School of Public Health, University of Pittsburgh

Ben Van Houten, PhD, Professor, Department of Pharmacology and Chemical Biology, School of Medicine, University of Pittsburgh

Peter Di, PhD, Assistant Professor, Department of Environmental and Occupational Health, Graduate School of Public Health, University of Pittsburgh

Dissertation Advisor: Patricia Lynn Opresko, PhD, Associate Professor, Department of Environmental and Occupational Health, Graduate School of Public Health, University of Pittsburgh

Patricia Lynn Opresko, PhD

Aaron Barchowsky, PhD

REPAIR OF BIPYRIMIDINE PHOTOPRODUCTS AT TELOMERES OF ULTRAVIOLET LIGHT IRRADIATED MAMMALIAN CELLS

Dhvani Parikh, PhD

University of Pittsburgh, 2014

Abstract

Telomeres at chromosome ends promote genome stability, survival, and proliferation in cells, and prevent degenerative diseases and cancer in humans. Human telomeres are 10-15 kilobases long and consist of about 1500 tandem TTAGGG repeats. Six telomeric proteins form a shelterin complex that protects the telomeres from being recognized as a chromosome break, thereby preventing inappropriate repair and chromosome fusions. Telomeric DNA sequences are vulnerable to ultraviolet light (UV)-induced damage. UV creates primarily two types of photoproducts within DNA: cyclobutane pyrimidine dimers (CPDs) and 6-4 photoproducts (6-4 PPs). Unrepaired photoproducts can stall or block DNA replication and transcription, or if tolerated and bypassed, can introduce mutations that cause genomic instability which can drive carcinogenesis. In genomic DNA, these potentially harmful cellular effects are avoided through a specialized nucleotide excision repair (NER) pathway that removes photoproducts and restores normal DNA.

This dissertation investigated if photoproducts also form at chromosome ends and if they are repaired over time by NER. We exposed skin fibroblasts BJ-hTERT (NER proficient) and XP-A (NER deficient) to 10 J/m^2 UVC which induces CPD and 6-4 PP lesions. We

then extracted genomic and telomeric DNA from these fibroblasts and measured the rate of lesion disappearance. Post UVC exposure, BJ-hTERT cells repaired all detectable telomeric 6-4 PPs by six hours and telomeric CPDs by two days. However, XP-A cells did not repair telomeric 6-4 PPs. We observed that unrepaired photoproducts inhibit telomere TRF1 protein binding to telomeric DNA *in vitro*, and that cellular UVC irradiation of NER deficient cells causes telomere aberrations. Our novel findings have uncovered the presence and importance of a major DNA repair pathway at telomeres and increase our understanding of how unrepaired bulky adducts at telomeres may impact telomere structure and function. Telomere maintenance is essential in protection against age-related diseases and cancer in humans. The public health relevance of our study thus, relates to its potential usefulness in developing biomarkers of toxicology for aging and cancer.

TABLE OF CONTENTS

LIST OF TABLES

LIST OF FIGURES

ACKNOWLEDGEMENTS

Foremost thank you to Dr. Aaron Barchowsky for seeing potential in me at the Society of Toxicology meeting in 2009 and for offering me an opportunity to pursue this program. Utmost thanks goes to Dr. Ben Van Houten for his leadership, genuine interest in my work and encouraging guidance that got me from one goalpost to the next. Many thanks to Dr. Peter Di for his interest in my work and for providing thoughtful suggestions in committee meetings.

Thanks to my mentor Dr. Patricia Opresko for accepting me as a PhD student in her lab and for giving me great opportunities to succeed ever since. I thank her for being there from Day One and for keeping morale high through tough research times. I also thank her for being a fair, encouraging and involved mentor, and for being an excellent scientist and an inspiring, strong leader in the field.

Thanks to former and present lab mates especially Dr. Rama Damerla, Noah Buncher, Justin Lormand and Melinda Sager and lab neighbors Dr. Michelangelo Giuseppe and Joel Njah, M.D. for a helpful lab environment. Thanks especially to all the manuscript co-authors Drs. Hong Wang, Connor Murphy and Elise Fouquerel for their

brainstorming, time and efforts. Also thanks to Dr. Shikhar Uttam for assistance with biostatistical analysis. Thanks to the staff at Pitt who made non-academic tasks easier.

Thanks to my science teachers and mentors from high school and college in India; their efforts and ideas fired in me a long lasting curiosity and ambition for research.

Thanks to my brave parents who found time and energy to help me unconditionally, amidst starting a new, tough life in a foreign country at this age.

Thanks to my husband Dhruv Gami who moved to Pittsburgh from Washington D.C. and patiently supported my ambition day after day despite his own demanding career. Half of the credit for my work successes belongs to him.

Thanks to my family, my parents-in-law in India and my elder sister in Canada who gave me all the encouragement I needed, over long distance while fully understanding my inability to visit and spend time with them all these years.

Lastly, thanks to the One above who made it all possible and worth it.

ABBREVIATIONS

6-4 PP	(6-4) pyrimidine-pyrimidone
8-oxoG	8-oxoguanine
ALT	alternative lengthening of telomeres
ATR	ataxia telangiectasia and Rad3-related protein
ATM	ataxia telangiectasia mutated
CPD	cyclobutane pyrimidine dimer
CSA	Cockayne syndrome A
CSB	Cockayne syndrome B
DDB	DNA damage binding protein
d-loop	displacement loop
DDR	DNA damage response
ds	double strand
DSB	double-strand breaks
HR	homologous recombination
IARC	International Agency for Research on Cancer
KD	knock down
KO	knock out
MMR	mismatch repair
MRN	Mre11-Rad50-Nbs1
NHEJ	non-homologous end joining
PCNA	Proliferating cell nuclear antigen
Polη	Polymerase η
POT1	Protection of telomeres protein 1
pRB	Retinoblastoma protein
RAP1	Repressor/activator site binding protein
ROS	reactive oxygen species
RPA	Replication protein A
sh	short hairpin
ss	single strand
SSB	single strand breaks
t-loop	telomeric loop
TERC	telomere RNA component
TERRA	telomeric repeat containing RNA
TERT	telomere reverse transcriptase

TFIIH	transcription factor II human
TIN2	TRF1 interacting nuclear factor 2
TLS	translesion synthesis
TPP1	POT1-TIN2 organizing protein
TRF1	Telomeric repeat binding factor 1
TRF2	Telomeric repeat binding factor 2
UV	ultraviolet light
XPA	xeroderma pigmentosum group A
XPB	xeroderma pigmentosum group B
XPC	xeroderma pigmentosum group C
XPD	xeroderma pigmentosum group D
XPE	xeroderma pigmentosum group E
XPF	xeroderma pigmentosum group F
XPG	xeroderma pigmentosum group G
XPV	xeroderma pigmentosum group V (variant)

1 INTRODUCTION

1.1 TELOMERES: AN OVERVIEW

1.1.1 Beginning of the end

The word “telomere” first used in the 1940’s comes from combining two Greek roots – “telos” meaning “end” and “meros” meaning “part or segment”, signifying terminal parts of linear chromosomes [1] . The first studies for telomeres began in the 1970s when Elizabeth Blackburn mapped *Tetrahymena thermophila* DNA and discovered a series of hexanucleotide repeat sequences at the terminal ends of the chromosomes. Blackburn and Jack Szostak discovered that telomeres are conserved protective structures when they found that inserting the isolated terminal sequences from *Tetrahymena thermophila* chromosomes into linearized yeast plasmid was able to prevent the linear DNA from being degraded in yeast [2].

1.1.2 A solution to the end replication problem

The discovery of the enzyme telomerase helped solve the then-existing dilemma of replication at the very ends of the chromosomes, defined as the “end-replication” problem [3]. Briefly, DNA replication is asymmetric in that the two daughter strands are synthesized differently because of the specific DNA polymerase 5’->3’ directional activity

that adds nucleotides at a free 3' OH of an RNA primer that is bound to the template/parent DNA. Therefore, the leading strand is synthesized continuously from the primer in the 5'-> 3' direction while the lagging strand (3'->5') is synthesized discontinuously with several primers in the form of short Okazaki fragments. The primers are removed by an RNase enzyme and the Okazaki fragments are sealed with ligase [4]. The lagging strand synthesis presents a problem for replication at telomeres. The extreme ends of the chromosome after the removal of the final RNA primer cannot be replicated, causing shortening at the terminus with each round of cell division. The reverse transcriptase telomerase is able to resolve the problem in cells that express this enzyme. Telomerase elongates the parent 3' strand further with its RNA template providing an extended template at the very end of the chromosome for synthesis of the lagging daughter strand by the DNA polymerase in a 5'->3' direction [4].

A search for an enzyme that lengthens telomeric DNA in *Tetrahymena thermophila* extracts revealed a novel activity of the "telomere terminal transferase" (telomerase), as shown by Blackburn and Greider [5]. Subsequently, telomerase was shown to have an RNA component (TERC) that in combination with its catalytic protein component (TERT: Telomerase Reverse Transcriptase) adds repeats *de novo* to the 3' end of the chromosomes [6]. Blackburn, Greider and Szostak were collectively awarded the Nobel Prize in Medicine in 2009 for their exciting and groundbreaking work in the discovery of telomeres and telomerase.

1.1.3 **Electron microscopy examination of telomeres and the discovery of telomere looping**

Telomeres in humans consist of 10-14 kilobases (kb) of double-stranded 5' TTAGGG/5'CCCTAA tandem repeats, and terminate with a single stranded 3' overhang that averages 100 nucleotides (see Fig. 1) [7]. In yet another startling discovery in the telomere field, Jack Griffith and colleagues in 1999 published evidence for a duplex lariat structure in isolated telomeres when viewed under an electron microscope, now commonly referred to as 't-loops' [8] (see Fig. 1). The authors concluded that the telomere loops back upon itself with the 3' G rich single stranded overhang invading the double stranded repeats and forming a smaller displacement loop or D loop (Fig. 1). The overall result is that the 3' end is sequestered preventing the telomere from being recognized as a free end or a DNA double strand break (DSB). Broken chromosome end structures generally invite DNA damage responses and excision or resection activity elsewhere in the genome [9].

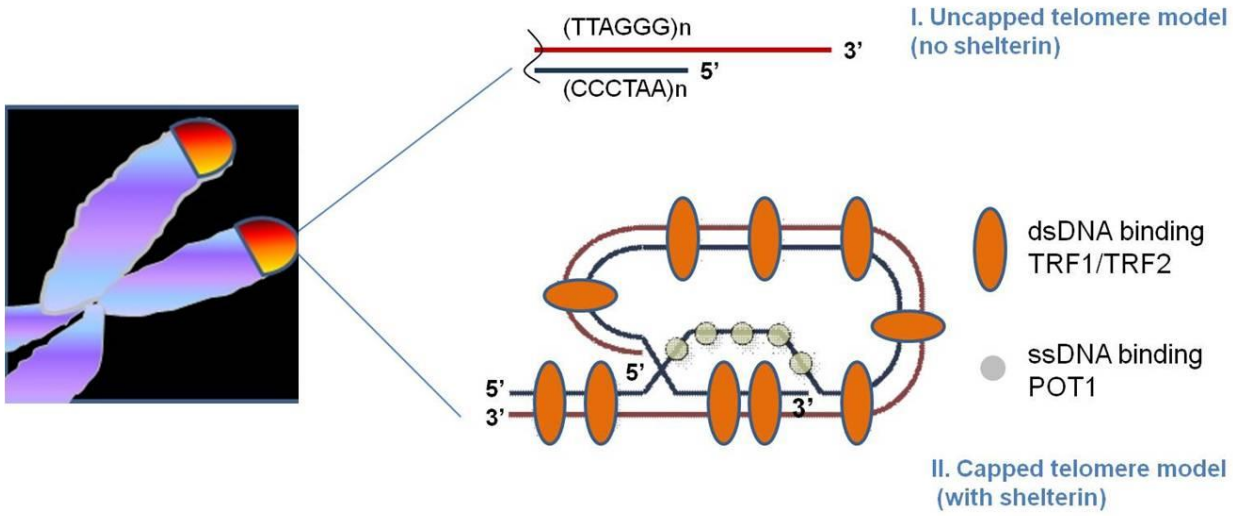

Figure 1 represents two scenarios for a chromosome end. The uncapped model is regarded to be telomeric double stranded DNA structure with a free 3' overhang, and may be deficient in shelterin protein binding. The capped telomeric model shows part of the shelterin protein complex that directly binds to the DNA, namely TRF1, TRF2 and POT1, and shows the looped structure that sequesters the 3' end. The three other shelterin proteins are RAP1, TPP1 and TIN2 and do not bind directly to the DNA (see section 1.1.4 for details).

Figure 1: Telomere models

1.1.4 **Current paradigm of telomeres with shelterin and associated proteins**

Telomeres are a complex of DNA and proteins. DNA repeats at telomeres co-exist with a 6-member protein complex named “shelterin” by Titia de Lange [7]. Shelterin proteins include:

- Telomeric repeat binding factors 1 and 2 (TRF1 and TRF2) that bind to double stranded telomeric DNA.
- Repressor activator site binding protein 1 (RAP1) that binds to and interacts with TRF2 directly.
- Protection of telomeres 1 (POT1) that binds to single stranded telomeric DNA.
- TIN2 POT1 organizing protein (TPP1) that binds to POT1 and TIN2.
- TRF2 and TRF1 interacting nuclear protein 2 (TIN2) that bridges together TRF1, TRF2 and TPP1.

Some non-telomeric accessory factors were also found to associate with the shelterin complex via pulldown experiments [9]. These include Ku 70/80, XPF-ERCC1, Apollo, and the Mre11 complex (Mre11/Rad50/Nbs1), which generally function in overall genomic DNA repair and maintenance.

1.1.5 **Role of shelterin in preserving telomere integrity**

The current paradigm for telomere structure *in vitro* is the capped shelterin-DNA model with the t-loops being formed and maintained partly by TRF2, which binds near the 3’ telomeric overhang [10]. TRF1 on the other hand is required for efficient replication and

to prevent fork stalling at telomeres [11]. Additionally, loss of TRF2 and other shelterin components can lead to uncapping and activation of inappropriate DNA damage response pathways at telomeres [12, 13]. Two of these DNA damage response pathways involve checkpoint signaling by ATM (ataxia telangiectasia mutated) kinase, which is activated by double strand breaks (DSBs), or ATR (ataxia telangiectasia and Rad3 related) kinase, which is activated by single strand breaks (SSBs) [13]. Importantly, when shelterin protein TRF1 was deleted in mice, the ATR kinase checkpoint was activated and the mice exhibited a fragile telomere phenotype [11]. Fragile telomeres are apparent as multiple telomeric signals or foci at a chromosome end [11]**.** NHEJ (non-homologous end joining) and HR (homologous recombination) pathways that repair double strand breaks elsewhere in the genome are normally repressed at telomeres by shelterin proteins RAP1/TRF2 and POT1 respectively [14] [15, 16], to prevent end-to-end chromosome fusions arising from illicit end joining and recombination [17].

1.1.6 **Telomere length maintenance mechanisms and consequences of telomere dysfunction**

In germ line and stem cells, telomerase is required to maintain the telomeres. Loss of functional telomerase due to *TERT* or *TERC* mutations cause a variety of diseases including dyskeratosis congenita, pulmonary fibrosis, and aplastic anemia [18]. Failure to maintain telomere length causes gradual telomere shortening that along with oxidative stress and DNA damage responses are capable of inducing irreversible arrest in cell division (senescence) [19]. This is significant because there is some evidence that cellular senescence may contribute to cellular and organismal aging [20]. Average

telomere length has been widely studied as a possible biomarker for cellular health and aging, however, evidence indicates that a few critically short telomeres are sufficient to drive senescence and genome instability [21] [22]. Importantly, genomic instability arising from an accumulation of genomic damage and mutations is accepted as a hallmark of cancer and aging [23] [24].

Telomere maintenance is essential for continued cell proliferation. Interestingly, cancer cells maintain their telomere lengths either by upregulating telomerase [25], or by using a recombination based alternative lengthening of telomeres (ALT) pathway. Cells that use the ALT pathways have heterogenous telomere lengths and show a dysregulation of recombination at the telomeres [26].

1.2 **DNA DAMAGE AND REPAIR**

Cellular DNA is constantly subjected to various kinds of insults that are deleterious to the intact normal DNA structure. The sources for these insults can be classified as exogenous or endogenous. The endogenous sources including DNA hydrolysis, methylations, lipid peroxidation reactions and reactive oxygen species (ROS) introduce base damage in DNA [27]. Exogenous sources of insults come from the environment and include X-rays, ultraviolet (UV) light, chemicals such as polycyclic aromatic hydrocarbons, nitrates and even chemotherapeutics such as cisplatin (Pt) [28] (see Fig. 2). For the sake of clarity, the term DNA ‘lesion’ commonly refers to a modified structure

of DNA arising from existing or new bonds within the DNA, while the term ‘adduct’ applies to covalent joining of a foreign, non-cellular compound to DNA. Lesions and adducts in damaged DNA are repaired by specialized DNA repair pathways. Some major pathways are highlighted in Fig. 2.

Not all DNA repair pathways function similarly at telomeres as in the bulk genome. Importantly, double strand break repair is inhibited at normal telomeres by shelterin as mentioned previously (see section 1.1.5). In contrast, it is well established that base excision repair is functional at telomeres (see section 1.2.2). Whether NER functions at telomeres is controversial and is the central topic of investigation in this thesis (see section 1.3).

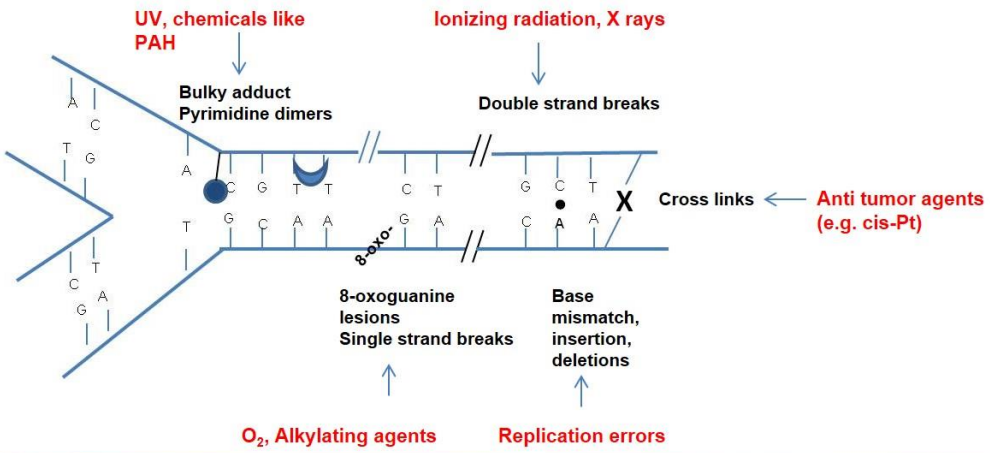

Type of DNA insult	Repair pathway Genomic	Repair pathway Telomeric
Bulky adduct/Pyrimidine dimers	NER	? Controversial
Double strand breaks	NHEJ/HR	No
Cross links	ICLR	?
Base mismatch/insertion/deletion	MMR	?
8-oxoguanine lesions/Single strand breaks	BER	Yes

Possible DNA damage types, sources and associated repair pathways in genomic and telomeric DNA. NER: nucleotide excision repair, NHEJ/HR: non-homologous end joining/homologous recombination, ICLR: Inter strand cross link repair, MMR: mismatch repair, BER: base excision repair.

Figure 2: DNA damage and repair pathways

1.2.1 **Ultraviolet light (UV) as a toxic agent**

Ultraviolet (UV) light is a major toxicant for life forms on earth. Solar UV radiation consists of three types of UV light based on their wavelengths of electromagnetic irradiation: UVA (from 320-400 nm), UVB (from 295-320 nm), and UVC (100-295 nm) (see Fig. 3). Of these, only UVA and some of UVB fully penetrates the earth's atmosphere. UV radiation from sun and tanning beds has been classified as a human carcinogen by the World Health Organization (WHO) and the Department of Health and Human Services [29]**.** The ozone barrier lining the earth's atmosphere is critical for absorbing all of the UVC radiation and most of the UVB light, thus offering protection from the harmful effects of UV exposures which include skin cancers and cataracts in humans [30] [31]. 95% of the UV light that penetrates the ozone layer is UVA light, while the remainder is UVB light. However, the risk for all types of UV exposure in causing adverse health effects is now increased in light of findings that human activities are causing a depletion of the ozone layer [32].

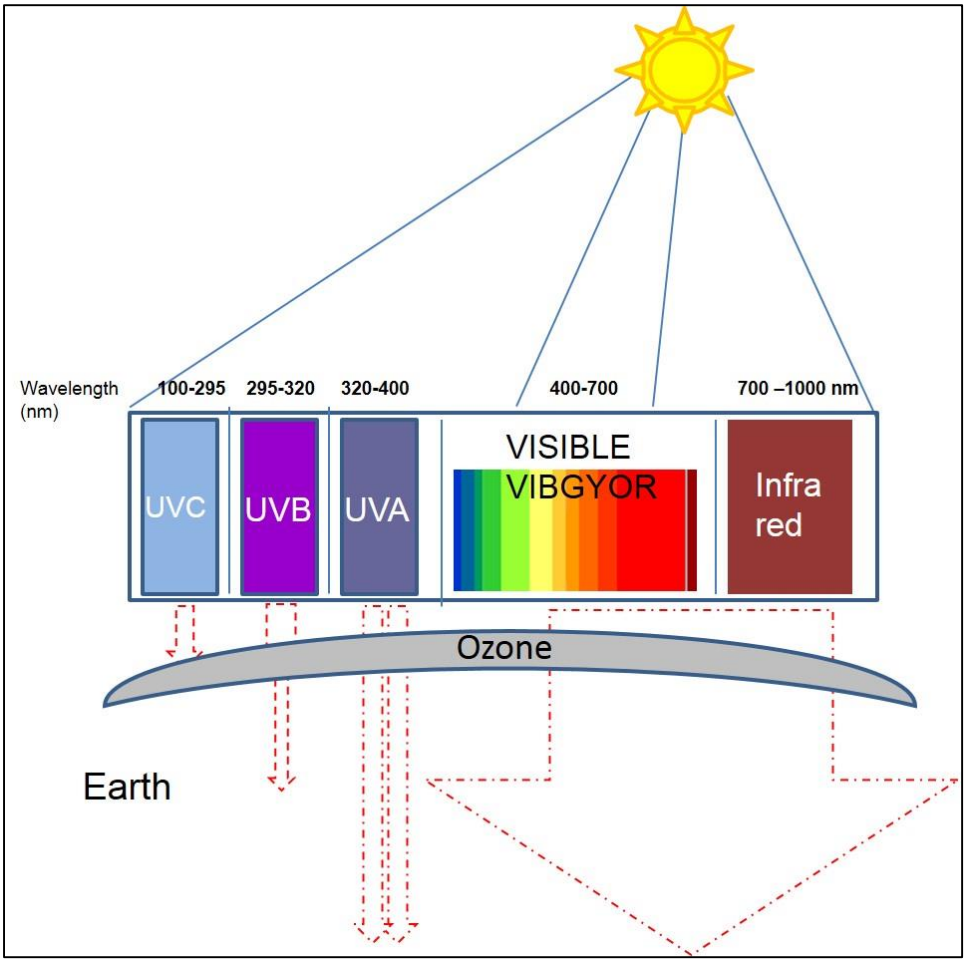

Splitting of solar radiation into components. The size of the red dashed arrows represents amount of entry into earth's atmosphere after ozone absorption. The broad red arrow indicates complete entry of visible and infra-red radiations into the earth's atmosphere.

Figure 3: Electromagnetic light spectrum

Because UV light has been a persistent toxicant since life originated, almost all life forms have evolved defense mechanisms to counteract UV damage. UV germicidal lamps are popular tools to precisely monitor and deliver damage to study these defense mechanisms in the field of DNA repair. For example, both UVA and UVB induce oxidative DNA base damage in addition to UV photoproducts, while UVC specifically generates photoproducts with very little oxidative base damage [33]. UVC is also more efficient at causing DNA damage because while proteins inside cells absorb very little at 260 nm, the absorption peak of cellular DNA is maximal at 260 nm, which matches closely the wavelength of the UVC germicidal lamp wavelength (254 nm).

1.2.2 **Oxidative base damage in DNA**

As mentioned previously (see section 1.2), oxidative DNA damage can be produced in the microenvironment of the cell endogenously by the creation of reactive oxygen species (ROS). ROS creates various kinds of DNA lesions, most prominently 8-oxoguanine (8-oxoG) [34]. Unrepaired 8-oxoguanine can potentially mispair with adenine eventually leading to G -> T transversions [35]. These mutagenic events are prevented by the efficient base excision repair (BER) pathway, which removes damaged bases in the global genome to restore normal DNA. In general, BER is a multi-step pathway that initiates with the action of specialized DNA glycosylase enzymes (such as Ogg1 and Nth1) that recognize damaged bases and cleave the N-glycosidic bond of the damaged base linked to the sugar-phosphate backbone, thereby creating an abasic or apurinic/apyrimidinic (AP) site. AP endonuclease enzyme further cuts the phospho-diester bond on 5’ side of abasic site, thereby creating a single strand break (SSB), a

free 3'OH group and a 5' dRP (deoxyribose phosphate). DNA polymerase beta has deoxyribophosphodiesterase (dRPase) activity in addition to polymerizing activity so it can process the 5' dRP end to yield a 5' phosphate (5' P) and add nucleotides at the 3' OH end [36]. Then, DNA ligase seals the SSB [37] to restore normal DNA.

Various studies have examined the effect of oxidative damage on telomeres. Guanine rich telomeres are highly susceptible to oxidative damage and chronic oxidative stress can accelerate telomeric shortening and the onset of cellular senescence as shown by Kurz, D.J. et al (2004) [38]. Oxidative damage (8-oxoGs) in telomeric DNA also disrupt binding of shelterin proteins TRF1 and TRF2 *in vitro* [39]. As mentioned previously, glycosylases such as Ogg1 and Nth1 remove oxidative lesions via BER pathway *in vivo*. Primary mouse embryonic fibroblasts (MEFs) were isolated from wild type ($Ogg1^{+/+}$) and Ogg1 deficient ($Ogg1^{-/-}$) mice and these isolated MEFs were either cultured in 20% oxygen or paraquat that induced oxidative stress, or normal 3% oxygen conditions to lessen oxidative stress [40]. The authors observed that high oxidative stress in $Ogg1^{-/-}$ primary MEFs enhanced telomeric DNA strand breaks and led to telomere strand losses, which was associated with an accumulation of oxidative lesions such as 2,6-diamino-4-hydroxy-5-formamidopyrimidine (FapyG) and 8-oxoGs normally removed by Ogg1 glycosylase [40]. A similar study was performed to test effect of Nth1 (Endonuclease III-like protein 1) deficiency on mice telomeres [41]. MEFs were isolated from wild type ($Nth1^{+/+}$) and knockout ($Nth1^{-/-}$) mice and treated with aphidicolin that induce replication stress and enhance telomere fragility [41]. The authors recorded a higher incidence of fragile telomeres and higher telomere sister chromatid exchanges in

primary MEFs isolated from Nth1 deficient mice compared to wild type control mice. The authors associated this increase in telomere fragility and T-SCEs with Nth1 deficiency and suggested that an accumulation of telomeric Endonuclease III-sensitive DNA lesions due to absence of Nth1 could be responsible for the observed telomere defects [41]. Thus, in both these studies, the removal of oxidative lesions by Ogg1 and Nth1 glycosylases via BER was shown to be important for maintaining telomeric integrity [40, 41]. In another related study, human AP endonuclease 1 (Ape1) was shown to have a key role in telomere maintenance [42]. Ape1 protein recognizes and processes apurinic/apyrimidinic (AP) sites in the base excision repair pathway of DNA. The authors performed telomere FISH assays in Ape1 depleted U2OS, BJ-hTERT and primary fibroblasts IMR90 cells and observed telomere end-to-end fusions and telomere losses [42]. This led to the conclusion that Ape1 deficiency was associated with telomere dysfunction [42]. Related to this, Ape1 depletion in U2OS and BJ-hTERT cells was also found to be associated with reduced TRF2 at telomeres which in turn was associated with activation of DNA damage responses at telomeres [42]. Thus, oxidative damage and repair have been well characterized at telomeres.

1.2.3 **UV-induced bulky lesions and repair in genomic DNA**

The majority of UV-induced DNA damage is in the form of cyclobutane pyrimidine dimers (CPDs) [43] [44]. CPDs are formed when adjacent pyrimidines (thymines/cytosines) link together covalently via formation of a four member ring structure resulting from saturation of pyrimidine 5, 6 carbon double bonds (see Fig. 4). Various stereo isoforms of CPDs are possible such as cis-syn, cis-anti, trans-syn or trans-anti. Double stranded B DNA forms mostly the cis-syn CPD when exposed to UV light, while single stranded DNA can form trans-syn dimers which generates a greater distortion in the helical structure [44]. CPDs are formed in a sequence context. Thymine-thymine (T<>T) CPDs are the most frequently formed, compared to cytosine-cytosine (C<>C) CPDs which are the least frequently formed. Thus, the overall frequency of CPD formation in a sequence context was observed to be T<>T: C<>T: T<>C: C<>C at a ratio of 68:13:16:3 [43, 45]. Pyrimidine (6-4) pyrimidone photoproducts **(**6-4 PPs) are formed when two pyrimidines link together covalently across the 4, 6 carbon double bonds. 6-4 PPs introduce a much more prominent distortion in the double helical structure of DNA than CPDs [46] but like CPDs they also form in a sequence context. 6-4 PPs form most frequently at TC and CC sites, and less frequently at TT and CT sites [47, 48]. In human telomeres, which consist of the sequence 5' TTAGGG/5' CCCTAA, CPDs and 6-4 PPs can form at the TTs, CCs, and CTs residues. Irradiation of an existing 6-4 PP lesion with 313-325 nm light can form Dewar isomer-derivatives considered to be a type of secondary damage [37]. The ratio of CPD to 6-4 PP formation upon UVC exposure of B-DNA was found to be 3:1 [49], while the ratio upon UVB exposure was found to be 8:1 [50].

CPDs and 6-4 PPs in some vertebrates (except mammals), bacteria and plants can be repaired via photoreactivation or photoreversal by specific chromophore containing enzymes called CPD or 6-4 PP photolyases [51]. Mammalian cells however lack photoreversing enzymes and repair the bulky photoproducts via the nucleotide excision repair (NER) pathway. Unrepaired UV damage in DNA can lead to irreversible nucleotide sequence changes in the genome, termed as mutations.

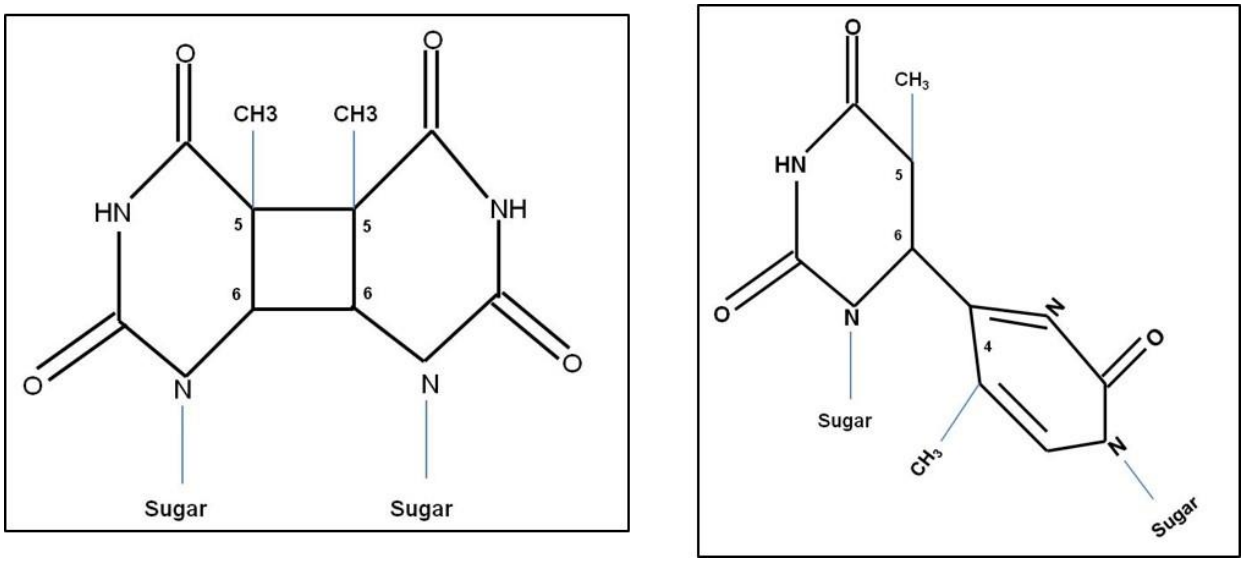

Left: Skeletal formula of thymine dimer showing joining across 5 and 6 double bonds. Right: Skeletal formula of pyrimidine (6-4) pyrimidine photoproduct showing joining across 4 and 6 bonds.

Figure 4: Structures of ultraviolet light induced CPDs and 6-4 PPs

1.2.4 **UV mutagenesis and photoproduct removal**

UV mutagenesis in DNA can be caused by multiple factors and mechanisms. Cytosine in DNA is unstable compared to other bases and can undergo hydrolytic deamination irreversibly to form uracil. Also, if cytosine is a part of a CPD, this increases the frequency of cytosine deamination to uracil [52]. At dipyrimidine sites, deamination of CC's can thus create uracil (UU) containing CPDs. Moreover, methylated cytosines deaminate at a greater rate than normal cytosines, which lead to conversion to thymine [53]. Also, UVB as part of sunlight induces CPDs preferentially at 5 methylcytosine dipyrimidine sites [54].

CPDs in general serve as impediments to replicative polymerases, which can cause stalling at replication forks, potentially leading to fork collapse into a double strand break and consequent cell death [55]. These events can be prevented by a DNA damage bypass/tolerance mechanism in cells known as translesion DNA synthesis. Specialized translesion polymerases are able to prevent fork collapse or can re-start stalled replication forks in an 'error-free' or 'error prone' way, depending on the type of lesion and the type of translesion polymerase recruited to the lesion [56]. Translesion polymerase eta (Pol η) can synthesize accurately across TT CPDs including those formed due to deamination of methyl cytosines at dipyrimidine CPD sites. The bypass is error-free in incorporating correctly adenines across thymines. However, it is deleterious to the cell because it can potentially cause C->T or CC->TT mutations, which are signature UV mutations, if bypass occurs at methylated cytosine CPDs that could

deaminate to TT CPDs [57]. Also, although Pol η is efficient at bypassing CPDs, it is ineffective at the bypass of 6-4 PPs.

Most of the UV-induced mutations are single base pair substitutions, that are concentrated at hotspots (non-random) and directed at the 3' residues of pyrimidine dinucleotides [58] [37, 59]. UVA and UVB generate a diverse spectrum of mutations in DNA. UVA generates photosensitizing reactions that produce oxidized bases that lead to G-> T transversions while UVB produces bulky lesions such as CPDs and 6-4 PPs that create single (C->T) or tandem (CC->TT) transition mutations [33]. However, recent studies point to UVA induced CPDs in whole human skin as the predominant lesions, as opposed to 8-oxo-7,8-dihydroguanine (8-oxoG), and report no formation of 6-4 PPs at thymine sites [60].

As mentioned earlier, removal of photoproducts from genomic DNA is critical because they impede progression of the normal replicative DNA polymerases during DNA replication. For example, CPDs introduce a helical distortion by bending the overall helical axis by 30° toward the major groove [61, 62]. CPDs are particularly deleterious due to poor recognition by the global genome excision repair pathway and therefore, exhibit longer persistence in the DNA compared to 6-4 PPs [63]. In normal cells 12 hours after UV exposure, about 50% of CPDs are removed from mammalian DNA [64-66]. On the other hand, 6-4 PPs which are more helix distorting than CPDs are recognized and removed at a much faster rate than CPDs. By 6 hours post UV exposure most of the 6-4 PPs are repaired in genomic DNA [49].

1.2.5 **Types of Nucleotide Excision Repair (NER)**

CPDs and 6-4 PPs are repaired in mammalian cells via the nucleotide excision repair (NER) pathway. Areas of genome that are transcriptionally silent or non-transcribing at any given time, are repaired by the Global Genome Repair (GGR) pathway while lesions within actively transcribing regions are repaired by the Transcription-Coupled Repair (TCR) pathway (reviewed in Friedberg *et al* [37] (see Fig. 5). The distinction between the two pathways lies in the initial steps of lesion recognition. The translocating RNA polymerase II (RNA pol II) in TCR senses a replication block in the template strand and stalls, following which it recruits TCR specific proteins Cockayne syndrome A (CSA) and Cockayne syndrome B (CSB). CSB strongly binds to RNA pol II at the site of stalling [67]. CSA is a substrate recognition factor that recruits ubiquitin proteases, nucleosome binding as well as scaffolding proteins, and is responsible for the degradation of CSB post damage recognition [68]. For GGR, the helix distortion is recognized by the main damage sensor protein complex XPC-H23RB, which binds to the lesion. Ultraviolet DNA damage binding protein (UV-DDB) complex facilitates recognition of a photoproduct lesion by flipping it out, which further kinks the DNA to create a ssDNA region for XPC binding [69].

After the lesion recognition step, the two NER pathways unite into a similar sequence of events. The transcription initiation factor complex TFIIH is recruited to the lesion site in association with its helicase subunits XPD and XPB which melt the duplex DNA around the lesion to form a ‘bubble’ structure [70, 71], followed by verification of the lesion in the damaged strand [72]. Next, a preincision complex is formed by recruiting proteins XPG,

RPA and XPA. XPG endonuclease is recruited by interaction with TFIIH [73]. Replication protein A (RPA) coats the undamaged single stranded DNA resulting from the open bubble structure [74]. XPA protein also binds to the damaged DNA strand and then recruits the heterodimer complex XPF-ERCC1 [75]. XPG and XPF-ERCC1 are structure-specific endonucleases that make dual incisions on the 3' and 5' ends of the lesion containing strand respectively, leading to the release of a 24-32 nucleotide single stranded piece of DNA [76]. Replication factor C (RFC) and proliferating cell nuclear antigen (PCNA) complex together facilitate loading of DNA polymerase to synthesize the new strand [77]. The Ligase III-XRCC1 complex carries out the final ligation step to seal the nick in the strand [78].

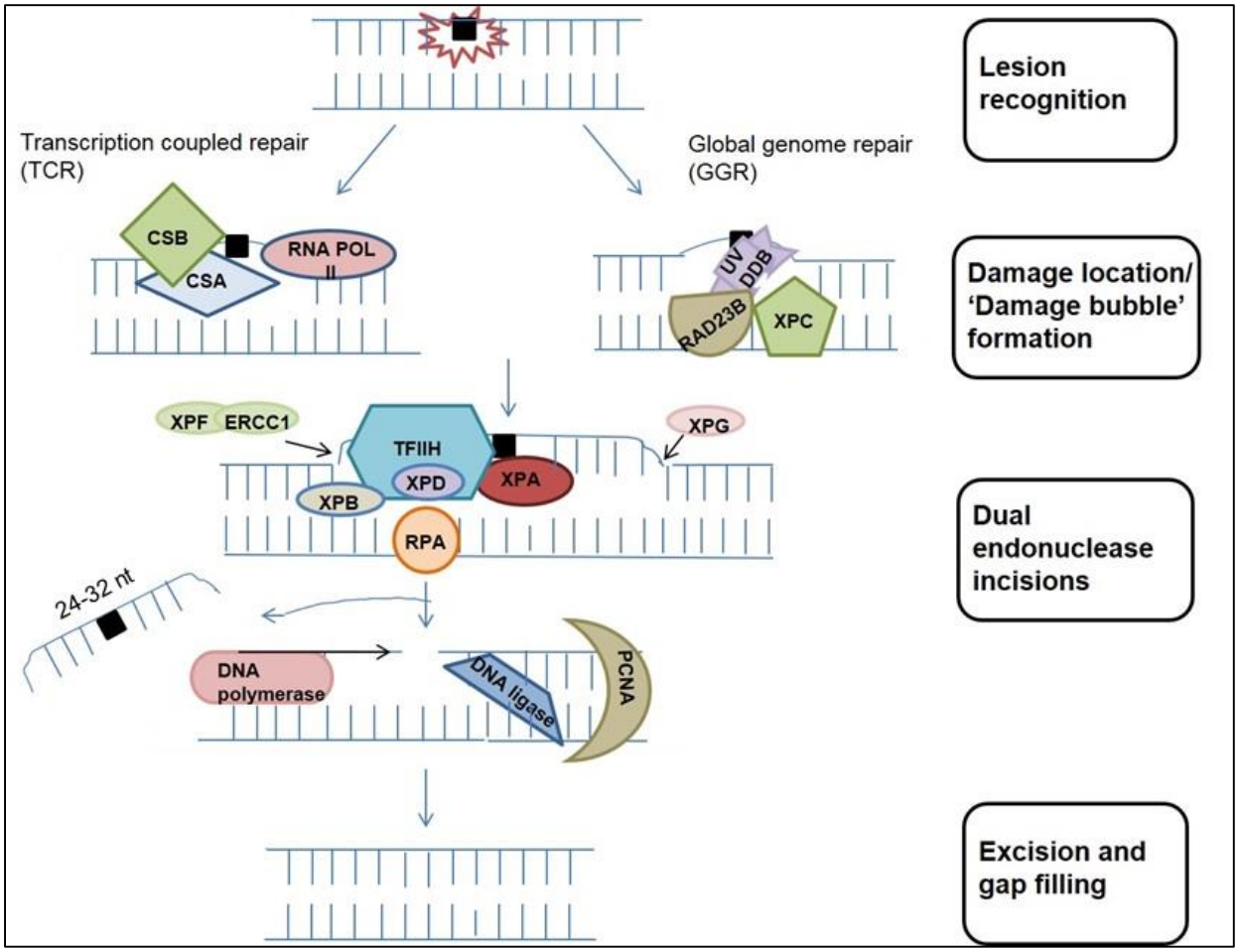

A replication/transcription blocking lesion may be formed in either a transcribing (left) or non-transcribing (right) region of genome, which determines initial recognition by two distinct NER pathways: transcription coupled repair (TCR- left) or global genome repair (GGR- right). Lesion recognition is achieved by a stalled RNA polymerase II along with recruitment of Cockayne syndrome A and B proteins (CSA and CSB) for TCR and by XPC-RAD23B, UV-DDB complex proteins for GGR. The remaining steps of the pathway are shared by TCR and GGR resulting in recruitment of NER proteins and TFIIH transcription complex, which ultimately results in removal of a 24-32 nucleotide damaged fragment containing the lesion. The ensuing gap is filled by DNA polymerase and the nick is sealed by the action of ligase.

Figure 5: Sequence of events in eukaryotic nucleotide excision repair (NER) pathway

1.2.6 **The case of no repair: XP and complications arising from lack of NER**

Defective or absent NER pathways cause xeroderma pigmentosum (XP), a rare autosomal recessive genetic disease that encompasses 8 disease subtypes which differ in severity depending on the affected complementation protein in the pathway. The first seven are classified as XP-A through XP-G and are caused by mutations in genes that encode or NER proteins. The eighth subtype (XP-V) is caused by a mutation in the gene that encodes Pol η (translesion polymerase) resulting in defective translesion synthesis past UV-induced lesions [79].

The absence of NER pathways causes diverse and severe adverse health effects. Primarily, NER deficiency causes a >10,000-fold increase in skin cancer risk, presumably due to an accumulation of mutations resulting from CPD and 6-4 PP photoproducts [80]. The frequency of XP is about one per one million people in the United States and Europe. XP patients sometimes have an average onset age of <10 years for the first skin cancer [80, 81]. XP patients are characterized by having greater skin sun sensitivity than normal people. Exposed areas of the skin, tongue, eyes and extremities are highly susceptible to sunburns and melanomas. Patients suffering from the more severe form of XP can also exhibit neurological abnormalities including developmental delay, loss in sensorineural hearing, the ability to walk, and neuronal atrophy and degeneration, caused by defects in XPA, XPB, XPD or XPG proteins [79]. Importantly, XPV patients lack translesion synthesis polymerase Pol η as opposed to lacking an NER pathway protein. These patients exhibit sun sensitivity and skin cancers similar to other XP patients, but possess a fully functional NER pathway [57].

While XP is primarily due to defects in any of the complementation proteins mentioned above, other related diseases are CS (Cockayne syndrome), TTD (Trichothiodystrophy) and a rarer combined XP/CS disorder. CS is an autosomal recessive disease thought to primarily arise from lack of transcription coupled repair (TCR). TCR occurs due to mutations in the genes encoding the DNA translocase Cockayne syndrome group B protein (CSB) or the ubiquitin ligase associated Cockyane syndrome group A (CSA) protein [82]. Thus, the CS patients suffer from transcription related problems in DNA and possess a dysfunctional TCR pathway but an intact cellular GGR pathway. Patients with CS suffer from severe growth arrest, premature aging like symptoms and developmental abnormalities. They have accelerated demyelination of neurons in the brain, microcephaly, sensorineural deafness and overall very low life expectancy (12 years) [83]. TTD is caused by very specific mutations in TTDA, XPB or XPD proteins which are part of the basal transcription complex TFIIH [79]. Patients suffering from these diseases exhibit severe phenotypes due to disruption in the basal transcriptional machinery and show features of CS phenotypes in varying degrees along with brittle hair and nails (reviewed in [81]).

1.2.7 **UV damage and NER at telomeres**

Knowledge about UV-induced damage and repair at telomeres has been limited to findings by just two previous studies done in the field. This could be because 1) telomeres are less than 0.02% of the bulk genome [84] and hence, there are limited techniques that can investigate telomeres with specificity and sensitivity and 2)

telomeres were only recently discovered to be actively transcribing regions of the genome raising the potential for TCR existence at telomeres [85]. A study by Rochette and Brash in 2010 first concluded that UV-induced CPDs are not removed from telomeres despite showing evidence for hypersensitivity of telomeres to CPD formation [86]. The implication was that telomeres tolerate lesions perhaps through translesion synthesis, which enables bypass of UV photoproducts in genomic DNA. However, an earlier study by Kruk *et al.* in 1995 measured rates of telomeric CPD repair along with repair rates in transcribing and non-transcribing genes, and concluded that the telomeric CPD repair rate resembles that of non-transcribed genes [87]. Slower or no repair of telomeric CPDs, compared to CPD repair in the bulk genome, has the potential to cause replication and transcription blocks in telomeres, which can further lead to genomic instability.

Effect of chronic UVB exposure on telomeres in mice was recently examined in a study that used an XP mouse model. XP mouse models generated by complete knockout of NER proteins are useful in understanding human XP diseases. XPC as mentioned previously, is a global genome repair (GGR) pathway protein whose deficiency leads to a defective NER pathway [88]. When the dorsal skin of XPC knockout mice was exposed to a chronic dose of 1.8 kJ/m^2 UVB and examined, the authors of the study discovered that chronic UVB increased telomere shortening and introduced greater fragility at telomeres compared to wild type mice [89]. This study was the first to examine and report deleterious effects of UV on telomeres in animal tissues, but could not conclusively answer if NER protects telomeres from UV-induced damage. This is because UVB

exposures were utilized which also induce oxidative damage, and XPC has also been implicated in base excision repair for removal of oxidative damage [90, 91].

Some studies have also examined NER protein XPF-ERCC1 behavior in presence of shelterin complex protein TRF2. In these studies, NER incision factor XPF-ERCC1 was found to localize to telomeres as well as to co-purify with shelterin protein TRF2 in pulldown experiments [92, 93]. Also, XPF-ERCC1 protects telomeres by repressing telomeric recombination events, but in the absence of TRF2 it cleaves the 3' overhang at telomeres thereby facilitating deleterious chromosome end-to-end fusions [92]. Preliminary data from our lab (see appendix) indicates that TRF2 can modulate activity of XPF-ERCC1 on a non-telomeric substrate.

1.3 **STATEMENT OF THE PROBLEM AND HYPOTHESIS**

Telomeric DNA is particularly susceptible to genotoxic stress because of 1) a high frequency of tandem pyrimidines that are hotspots for bulky photoproduct damage and guanines that are hotspots for oxidative damage [86] and 2) suppression of DNA double strand break repair pathways at telomeres [9, 14, 94]. UV is a ubiquitous source of DNA damage, is a complete carcinogen and has been used extensively to study B-DNA damage and repair [37]. Helix distorting DNA lesions such as UV-induced CPDs have the potential to cause cell death or mutagenesis by interfering with DNA transcription and replication. Organisms have evolved a transcription coupled NER pathway to more rapidly remove bulky lesions from transcriptionally active DNA [95]. Telomeres were very

recently shown to be actively transcribed into non-coding RNAs called telomeric repeat containing RNA (TERRA), which aid in telomere maintenance and prevent premature cellular senescence [96]. It is thus, important to investigate whether damage at dynamically transcribing telomeres is repaired, accumulates or is tolerated.

While oxidative damage and the base excision repair pathway are well characterized at telomeres [38, 40] (also summarized in 1.3), the status of UV-induced bulky damage and repair at telomeres is not clear. Studies investigating NER function at telomeres or interactions of NER proteins with telomeric proteins are limited to two NER proteins; XPC and XPF-ERCC1, as described in section 1.2.7. Stout and Blasco recently showed that UVB exposure of mice lacking NER protein XPC induced an increase in critically short telomeres, compared to exposed wild type mice. The authors also suggested that telomere lengths in double knockout mice (having a combined XPC and telomerase deficiency) were increased after UVB exposure perhaps due to activation of the alternative lengthening of telomeres pathway (ALT, described briefly in section 1.1.6) [89]. Thus, XPC and telomerase work together to maintain telomeres in mice upon UV exposure. Moreover, despite evidence for interactions of NER protein XPF-ERCC1 and shelterin protein TRF2 via co-immunoprecipitation experiments [92], it is unknown if XPF-ERCC1 and TRF2 directly interact to modulate each other's activity.

Two studies that examined UV-induced photoproduct removal at telomeres reported contrasting results. Kruk *et al* (1995) reported that the rate of CPD repair at telomeres after UV exposure was similar to that observed for non-transcribing genes [87]. Rochette

and Brash reported that telomeres are hypersensitive to UV-induced CPD formation, but refractory to CPD removal [86]. Additionally, these previous studies did not directly measure the potential role of NER proteins in telomeric CPD removal and used semi-quantitative methods to measure CPDs.

The objective of this research was to investigate the presence of a potential NER pathway operating at telomeres. My central hypothesis was that telomeres exhibit slower NER of UV-induced DNA damage, as compared to genomic DNA, and that UV photoproducts can affect shelterin integrity at telomeres. In order to address this hypothesis, the specific aims were 1) to determine what effect UV-induced photoproducts have on shelterin protein binding to telomeric DNA and 2) to measure repair kinetics of UVC-induced photoproducts at telomeres. For my first aim, I performed gel shift assays to test the effect of a CPD on binding of shelterin protein TRF1 to telomeric DNA. For my second aim, I developed, standardized and validated a novel and sensitive immuno-DNA spot blot based assay for telomeric lesion quantification. Knowledge about the formation and removal of photoproducts in telomeric DNA will advance our understanding of bulky lesion repair across the mammalian genome.

1.4 **STATEMENT OF PUBLIC HEALTH SIGNIFICANCE**

Nucleotide excision repair (NER) is the principal DNA repair pathway that removes a multitude of distinct types of bulky DNA lesions caused by major chemical mutagens. NER removes environmentally induced DNA insults such as benzo[a]pyrene adducts [97], polycyclic aromatic hydrocarbon adducts [98], 2-acetylaminoflourene adducts (dG-C8-AAF) [99], aristolactam (AL-DNA) adducts [100], aflatoxin B1 formamidopyrimidine adducts [101], chromium-DNA adducts [102] as well as chemotherapeutically induced cisplatin-DNA adducts [103]. However, the most well- studied and established bulky lesions repaired by NER remain the evolutionarily significant ultraviolet (UV) light induced cyclobutane pyrimidine dimers and 6-4 photoproducts.

Telomeric sequence is especially susceptible to UV photoproduct formation due to the presence of adjacent pyrimidines within each telomeric repeat. A recent study measured telomere lengths using quantitative fluorescence in situ hybridization in sun exposed and sun protected skin areas and found that basal cell telomeres were shorter in sun exposed epidermal areas with or without actinic keratosis as compared to telomeres in sun protected epidermal areas [104]. Unrepaired genomic DNA photoproducts serve as replication blocks that can further lead to mutations and genomic instability, which is a hallmark of cancer.

Our study aims to define clearly the picture of UV lesion formation and abolition at telomeres and to investigate in depth whether NER is truly functional in protecting telomeres from the adverse effects of these lesions. We foresee two distinct ways in which this study will contribute to improving human health. First, knowledge about a functional telomeric NER pathway will help elucidate novel strategies to preserve or upregulate NER protection of normal telomeres in the face of constant environmental stressors. Conversely, NER inhibition or modulation in cancer cells, combined with drug therapy can greatly sensitize tumors to killing [105, 106]. Second, knowledge from our study will inform about telomeric damage endpoints such as impaired shelterin binding to telomeres and telomeric dysfunction (telomere loss, fusions etc.) due to photoproducts. Telomere dysfunction can drive carcinogenesis in cells that lack tumor suppression and evade senescence. Unrepaired UV damage can drive senescence causing accelerated photo-aging [107]. Telomere maintenance is thus, essential in protection against age-related diseases and cancer in humans. Finally, telomeric DNA damage and toxicity is an emerging field and our novel techniques will allow future investigations into all the varied bulky adducts (outlined above) that could form at telomeres.

2 TELOMERES ARE PROFICIENT IN REMOVAL OF UV INDUCED PHOTOPRODUCTS VIA NUCLEOTIDE EXCISION REPAIR

2.1 ABSTRACT

UV irradiation induces photoproducts in the genome that if left unrepaired can interfere with DNA replication and transcription, and ultimately lead to mutations or chromosome breaks. Telomeric TTAGGG/CCCTAA repeats at chromosome ends are enriched for dipyrimidine sites that are prone to UV-induced cyclobutane pyrimidine dimers (CPD) and pyrimidine (6-4) pyrimidone (6-4 PP) photoproduct formation. To examine the efficiency of CPD and 6-4 PP formation and removal at telomeres, we irradiated BJ-hTERT fibroblasts with UVC and purified telomeres from genomic DNA extracted at various repair times. Photoproducts were quantitated by immuno-spot blotting. Using this approach we observed approximately 2-fold fewer photoproducts in telomeres, compared to the bulk genome. CPD removal was slow, but removal from telomeres was 1.5-fold faster compared to the bulk genome. Complete 6-4 PP removal was rapid and achieved by 6 hours post exposure in both bulk genomic DNA and telomeres. Telomerase was not required for telomeric photoproduct reduction, since telomerase negative U2OS cells also exhibited 6-4 PP removal from telomeres at rates similar to the bulk genome. To determine whether nucleotide excision repair (NER) was responsible for telomeric photoproduct removal, we measured 6-4 PPs in telomeres isolated from UVC irradiated *XPA* mutant fibroblasts lacking NER. No significant reduction in 6-4 PPs was observed in telomeres or bulk genomic DNA by 12 hours post exposure.

Furthermore, we found that unrepaired photoproducts strongly inhibited binding of the essential telomeric protein TRF1 to telomeric DNA *in vitro*. Our findings provide new evidence that NER restores damaged telomeric DNA.

2.2 **SIGNIFICANCE**

Ultraviolet (UV) light generates DNA photoproducts in the genome that can cause mutations or chromosome breaks by interfering with DNA replication. Telomeres at chromosome ends are essential for genome stability, and we discovered that UV photoproducts strongly inhibit binding of telomeric protein TRF1 to telomeric DNA. Nucleotide excision repair (NER) removes UV photoproducts from genomic DNA, but whether this pathway functions at telomeres was unresolved. We developed a direct quantifiable assay to measure UV photoproducts at telomeres purified from UV irradiated human cells. Using this approach we discovered the two most common photoproducts form at telomeres, and are removed at rates similar to the bulk genome. Telomeric photoproduct removal requires XPA protein, providing direct evidence that NER restores damaged telomeres.

2.3 **INTRODUCTION**

Genomic stability is essential for cellular health and survival. Since DNA damage from environmental and endogenous sources is inevitable, mechanisms for subsequent repair and restoration to undamaged DNA are required. Ultraviolet (UV) light exposure generates DNA photoproducts in which two adjacent pyrimidines are covalently joined to form cyclobutane pyrimidine dimers (CPD) or pyrimidine (6-4) pyrimidone photoproducts (6-4 PP) [108]. Unrepaired photoproducts are highly mutagenic and interfere with DNA replication and transcription [109, 110]. Cellular mechanisms for managing photoproducts include global genome repair, transcription coupled repair or translesion DNA synthesis [107, 111, 112]. Mammalian nucleotide excision repair (NER) accomplishes CPD and 6-4 PP removal using an array of 30 different proteins [107]. Mutations in any one of seven NER proteins, including XPA protein, cause NER deficiency and the severe sunlight sensitivity and skin cancer prone disorder xeroderma pigmentosum (XP) [79]. Global genome NER involves damage recognition and verification, dual strand incisions flanking the lesion, repair synthesis and strand ligation [113]. Transcribed genes are repaired more rapidly than non-transcribed genes by the transcription-coupled NER pathway, which initiates when the RNA polymerase stalls at the lesion [112]. Finally, DNA polymerase η can accurately bypass CPDs during DNA replication to enable replication fork progression [114]. These mechanisms are essential for preserving the genome in the face of bulky lesions.

Both UV irradiation and telomere shortening are associated with skin aging and increased skin cancer risk [79, 115]. Critically short or dysfunctional telomeres at

chromosomal ends trigger cell growth arrest or apoptosis that drive aging-related diseases and pathologies, or chromosomal alterations that drive carcinogenesis [116, 117]. Furthermore, shortened telomeres were observed in sunlight or UVB exposed skin tissue from humans and mice [89, 104, 118] suggesting a link between sunlight exposure and telomere maintenance. Human telomeres at chromosome ends consist of about 1500 tandem TTAGGG repeats, terminating with a 3' single stranded overhang that averages 100 nucleotides in length [9, 119]. Previous studies demonstrate that telomeric repeats are susceptible to CPD formation following UV exposure [86, 87]. The 6-member shelterin protein complex at telomeres interacts with, and regulates, enzymes in every known DNA repair pathway including the NER endonuclease XPF-ERCC1 [92, 120]. Shelterin prevents inappropriate telomere processing by DNA repair enzymes, and inhibits homology directed repair and DNA double strand break repair at telomeres [9, 94]. However, whether NER proteins function at damaged telomeres remains unresolved. Previous indirect approaches for lesion detection at telomeres led to equivocal results and were limited to CPD analysis in wild type cell lines [86, 87].

Here we describe a novel direct approach to study NER at telomeres in which we isolated telomeres from UVC irradiated human cells and detected UV photoproducts using lesion specific antibodies and DNA blotting. Using this approach we discovered that both CPDs and 6-4 PPs form at telomeres, but at levels approximately 2-fold lower compared to the bulk genome. We observed CPDs were removed from telomeres 1.6-fold faster than from the bulk genome, while 6-4 PPs were removed at similar rates. Furthermore, DNA photoproducts persisted at telomeres in NER deficient cells from an XP-A patient.

Unrepaired photoproducts strongly inhibited shelterin TRF1 protein binding to telomeric DNA *in vitro*, suggesting that an accumulation of unrepaired lesions over time could compromise telomere integrity. To our knowledge, these studies provide the first evidence that NER is active at telomeres, and that NER functions to restore telomeric DNA that is damaged by UV light.

2.4 **MATERIALS AND METHODS**

2.4.1 **Gel shift assays**

Recombinant 6x-histidine tagged human TRF1 protein was purified from a baculovirus insect cell expression system as described [39]. Oligonucleotides (Table 1) for substrate preparation were purchased from Midland Certified Reagents Co. The CTRL or UV oligonucleotides were 5' end labeled with [γ-^{32}P]- ATP and Optikinase enzyme, and annealed to oligonucleotide TLS in a 1:2 molar ratio in 50 mM LiCl as described [39]. TRF1 DNA binding assays were performed as previously described [39], with substrate and protein amounts as indicated in the figure legends. The reactions were separated by gel electrophoresis on a 5% 29:1 (bisacrylamide:acrylamide) native gel at 4^{o}C and 140V for about 2 hours in 1X TBE buffer and visualized with a Typhoon 9400 Phosphoimager. Bound and unbound substrates were quantitated using ImageQuant software, and the percent bound was calculated as previously described [39] after correcting for background in the no enzyme control.

2.4.2 **Cell culture and exposures**

Telomerase immortalized human foreskin fibroblasts BJ-hTERT cells were obtained from ATCC. The SV40-immortalized NER deficient human skin fibroblasts (GM04312) derived from an XP-A donor (XP20S) was obtained from the Coriell Cell Repository. This cell line harbors homozygous inactivating mutations in gene encoding XPA protein. Cells were grown at 37^{o}C and 5% CO_2 in DMEM complete media containing 10% fetal bovine serum, penicillin (50 units/ ml) and streptomycin (50 μg/ ml) (Life Technologies). UVC irradiation was performed via a 254 nm wavelength emitting germicidal lamp on cells at 80% confluency in dishes lacking media. UVC exposures were measured with a UVX31 meter (UVP, Upland, CA). After exposures cells were incubated in fresh media, then washed with PBS and harvested at various repair time points.

2.4.3 **Cell viability and proliferation assays**

For short term proliferation assays the cells were UVC irradiated (10 J/m^2) or not in 60 mm dishes, incubated in fresh media, and then counted in duplicate at various repair time points (0 to 72 hours) using a Beckman Coulter Z1 Cell Counter. The average cell number for each repair time point was divided by the cell number at 0 hour recovery. Cell viability was determined by trypan blue exclusion. Percent viability was calculated as [1.00 – (number of blue cells ÷ number of total cells)] × 100. For long term cell viability assays cells were irradiated with UVC (0, 5 or 10 J/m^2) or not (untreated) and incubated in fresh media. After 6 hours of recovery the cells were collected by trypsinization and

counted, and then subcultured by seeding equal numbers of cells per 10-cm culture dish in duplicate. Following a seven day subculture, the cells were then counted.

2.4.4 **Genomic DNA and telomere purification**

Genomic DNA was isolated from harvested cells using the Qiagen 20/G or 100/G DNA isolation kit. Approximately $20x10^6$ cells were harvested from eleven 100 mm dishes to yield about 100 μg of bulk genomic DNA per repair time point. Telomeres were isolated as previously described with some modification [119]. Double stranded genomic DNA (100 μg) was digested overnight with *Alu*I, *Hin*fI, *Hph*I and *Mnl*I (0.5 U/μg) restriction enzymes in 250 μl reaction volume to release intact telomeric fragments. Reactions were adjusted to 1x SCC and 0.1% Triton X-100, and the digested DNA was then annealed with a biotinylated oligonucleotide (3.5 pmoles) by controlled stepwise cooling from 80°C to 25°C (1.2°C/min) using a thermocycler. Then streptavidin-coated magnetic beads (18 μl, Invitrogen, M-280) pre-washed with 1x PBST and blocked with 5x Denhardt's solution, were incubated with the annealed samples overnight in a rotator end-over-end at 6 rpm and 4°C. Beads were collected against the side of the tubes by applying a magnet (Invitrogen), and unbound supernatants and subsequent washes were collected. The beads were washed three times with 1x SSC/0.1% Triton X-100, twice with 0.2x SSC and once with elution buffer [1mM Tris pH 7.5, 1mM EDTA, 10mM LiCl]. Beads were resuspended in 100 μl elution buffer and telomeres were slowly eluted by heating the tubes at 50°C for 40 minutes. Telomeric DNA in the various fractions was quantitated by ImageQuant analysis of PhosphorImager scans of spot blots hybridized

with a mix of ^{32}P-(CCCTAA)$_4$ and ^{32}P-(TTAGGG)$_4$ radiolabeled oligonucleotides as described [121]. The fraction of telomeric DNA recovered was calculated as [bound ÷ (bound + unbound fraction)]; the unbound fraction was the total collected supernatant and wash fractions. The concentration of genomic DNA and recovered purified telomeres was quantitated using a Thermo Scientific NanoDrop 3300 fluorospectrometer which accurately measures concentrations in the picogram/µl range.

2.4.5 **Telomere restriction fragment analysis**

Terminal restriction fragment analysis was performed as described previously [122, 123] with modifications. Undigested genomic DNA (1 µg), digested genomic DNA (3 µg) or purified telomeres (1 ng) were separated by molecular weight by gel electrophoresis on a 0.6% agarose gel. Gels were dried, stained with SYBR Green and imaged with a Typhoon fluorescent imager to visualize the molecular weight marker and undigested genomic DNA. Next, the gel was denatured in NaOH solution, neutralized, and hybridized with a ^{32}P-(TTAGGG)$_4$ oligonucleotide probe. Gels were subsequently washed and visualize via a Typhoon phosphorimager. Telomere length measurement was performed using ImageQuant and the Telorun method (http://www4.utsouthwestern.edu/cellbio/shay-wright/research/sw_lab_methods.htm) as described [122]. The exACTGene 24kb Max DNA molecular weight ladder was from Fisher Scientific.

2.4.6 **Immuno-spot blot detection of DNA photoproducts**

Immuno-spot blots of purified genomic, lambda and telomeric DNA were performed using the GE Manifold spot blot apparatus as described previously [124]. For each experiment nanogram amounts of telomeric DNA was loaded with the corresponding genomic DNA (loaded in duplicates) for each recovery time point. For 6-4 PP detection, purified telomeric fractions were combined from two independent exposure experiments (100 μg genomic DNA collected from each experiment for a total of 200 μg). Positively charged Hybond H^+ membranes and Whatman filter papers (GE Healthcare Life Sciences) pre-incubated with 2x SSC buffer were assembled onto the apparatus and heat-denatured (100^{o}C, 10 minutes) DNA samples were loaded on the membrane via vacuum blotting. Membranes were removed and placed DNA face-down on filter papers saturated with denaturation buffer (1.5 M NaCl/0.5 N NaOH) followed by neutralization buffer (1 M NaCl/0.5 M Tris-HCl pH 7.0). Membranes were then vacuum dried between filter papers at 80^{o}C for 2 hours. Dried membranes were blocked for 1 hour with 5% non-fat dry milk in 1x PBST and incubated overnight with primary antibody against CPDs (1:000, clone KTM53 Kamiya Biomedical) or 6-4 PPs (1:1000, clone KTM53 Cosmo Bio). The Kamiya CPD antibody reacts specifically with thymine dimers produced by UV irradiation in double- or single-stranded DNA while the Cosmobio 6-4 PP antibody binds to 6-4 PPs formed in single-stranded DNA and at every dipyrimidine sequence (TT, TC, CT, CC). Membranes were washed with PBST and incubated for 1 hour with secondary antibody (anti mouse-HRP). Amersham ECL Primer (GE Healthcare) was used to enhance the peroxidase activity on the membranes that were immediately exposed to X-ray films (Phoenix Research products). Antibody signal intensities were quantified by

ImageJ software. Blots were subsequently hybridized with a mix of ^{32}P radiolabelled $(CCCTAA)_4$ and $(TTAGGG)_4$ probes for telomeric DNA, visualized by Phosphorimager and quantified by ImageQuant as previously described [121]. Finally, blots were then hybridized with a ^{32}P labeled probe complementary to Alu repeat DNA (Table 1), and processed as described for the telomeric probe.

2.4.7 **Quantitative PCR detection of DNA photoproducts**

Quantitative PCR (qPCR) based quantification of DNA lesions on λ DNA (New England Biolabs) exposed *in vitro* to UVC irradiation was carried out based on a previously established method [125, 126]. The qPCR assay to quantify DNA lesions is based on the principle that any DNA lesion that greatly impedes or blocks progression of DNA polymerase will inhibit the extension step. Quantification of lesion frequency is based on the Poisson equation, which requires the assumption that DNA lesions are randomly distributed. The lesion frequency per DNA strand (average for both strands) is calculated as: *lesion frequency/amplified strand*: $\lambda = -\ln(A_D/Ao)$, where A_D=Amplification of damaged template, Ao=Amplification of non-damaged template.

2.4.8 **Statistical analysis**

All statistical analyses were done using OriginPro 8 software. A two-factor Analysis of Variance (ANOVA) was used to determine whether the difference between the curves for telomeric and genomic CPD repair was significant (Fig. 8B) and to determine

significance of differences between telomeric and genomic 6-4 PPs at 0 hour (Fig. 10B). A two-tailed heteroscedastic Student's t-test was used to determine significance of differences between the genomic CPDs and telomeric CPDs at 0 hour (Fig. 8B). A one-factor ANOVA with multiple comparisons was used to determine significance of differences between genomic CPDs within time points for all repair experiments.

Table 1. Oligonucleotides used in the study

Oligo name	**Sequence (5' ->3')**
Ctrl	GTGGATCCGTACTTAGGGTTAGGGTTAACACGAATTCGA
UV	GTGGATCCGTACTTAGGGT<>TAGGGTTAACACGAATTCGA
TPL	TCGAATTCGTGTTAACCCTAACCCTAAGTACGGATCCAC
Capture oligo (Telomere)	Bio-ACTCC $(CCCTAA)_3$
Capture oligo (Scrambled)	Bio-ACTCC$(CATCAG)_3$
^{32}P- Telomere	$(TTAGGG)_4$ and $(CCCTAA)_4$
^{32}P - $(Alu)_n$	GGCCGGGCGCGGTGGCTCACGCCTGTAATCCCAGCACTTTGGG AGGCCGAGGCGGGCGGA

2.5 **RESULTS**

2.5.1 **Purification of telomeres from human cells**

To study NER at telomeres we established an assay to directly measure photoproducts in telomeres isolated from UV exposed cells. Since telomeres represent less than 0.026% of the human genome, we required large amounts of genomic DNA to obtain sufficeint telomeres for analysis. We chose highy proliferative BJ skin fibroblasts engineered to express exogenous telomerase at an early passage prior to significant telomere shortening [127]. Telomeres were isolated from UVC irradiated and untreated human cells by annealing a biotinylated oligonucleotide that was complementary to the G-rich telomeric single strand overhang [119]. The telomere/oligonucleotide complexes were captured with streptavidin-coated magnetic beads and washed, followed by the analysis of purified telomeres by spot blotting onto membranes (Fig. 6A). To obtain telomeric fragments, and to minimize the presence of sub-telomeric DNA, we digested the bulk genomic DNA with a cocktail of four frequent cutter restriction enzymes that do not recognize or cleave telomeric sequences [123]. Agarose gel resolution revealed that the bulk genome was completely digested to fragments of $\leq$ one kb (Fig. 7). To examine the integrity of the purified telomeres we resolved the telomeric fragments obtained prior to purification (Fig. 6B, lane 3, digested) and after purification (lane 4, purified), on a 0.8% agarose followed by Southern blotting and hybridization with a radiolabeled telomere specific probe. This analysis revealed that the average telomere length in our BJ-hTERT cell line is 17 $\pm$ 1.1 kb (mean $\pm$ SD from three independent experiments), and that the purified telomeres remained intact, although they migrated slightly slower than

the unpurified telomere fragments (compare lanes 3 and 4, Fig. 6B). We suspect the elution of the telomeres at 50°C may allow for some partial duplex melting and potential secondary structure formation that could retard the fragments during migration. This analysis indicates that any reduction in photoproducts observed in the repair experiments could not be attributed to telomere degradation during the isolation procedure.

To test the efficiency and specificity of telomere pulldown, we performed capture assays in the absence of biotinylated oligonucleotde (mock), with a biotinylated non-telomeric oligonucleotide (scrambled) or a biotinylated oligonucleotide containing $(CCCTAA)_3$ telomeric sequence (Table 1). From 100 μg of digested genomic DNA each, we recovered no detectable DNA for the mock, 2.6 nanogram (ng) for the scrambled control, and 10 ng for the telomeric oligonucleotide (Fig. 6C). Supernatant, wash and eluents from the three capture experiments were loaded onto a membrane and hybridized with a radiolabelled telomeric probe. The signal intensity obtained for 5 ng of the eluent from the telomere capture oligonucleotide, compared to that obtained for 5 ng of input DNA, indicates very strong enrichment for telomeres (Fig. 6C). The average efficiency of telomere purification was 33 ± 0.06% (3 independent experiments), calculated as [bound ÷ (bound + unbound)], and agreed with previous reports [119]. This value closely matches the recovery efficiency of 38% calculated by measuring DNA yields (see Materials and Methods for calculation). The actual telomere yield of 10 ± 1.3 ng was divided by maximal telomere yield (26 ng) from 100 μg of genomic BJ-hTERT DNA (average from five independent experiments). Similar telomere yields of 10 ± 3 ng were

obtained from cells following UVC irradiation at 10 J/m^2, indicating that UV photoproduct formation did not alter the efficiency of telomere isolation.

In order to estimate the purity of the eluted telomeres we loaded various amounts of input (genomic DNA) and 10 ng of purified telomere eluent, followed by hybridization with a radiolabeled probe against Alu repeat DNA (Fig. 6D). Alu repeats are short interspersed elements that comprise ~10% of the genome and are commonly used as a negative control for identifying telomere binding proteins in ChIP assays [128, 129]. Based on signal intensities quantified for genomic DNA, the total amount of non-telomeric DNA present in the telomere eluent is approximately 1.2 ± 0.2 ng (mean ± SD from two independent experiments) (Fig. 6E). This indicates that at least 90% of the DNA present in the eluent is enriched telomeres.

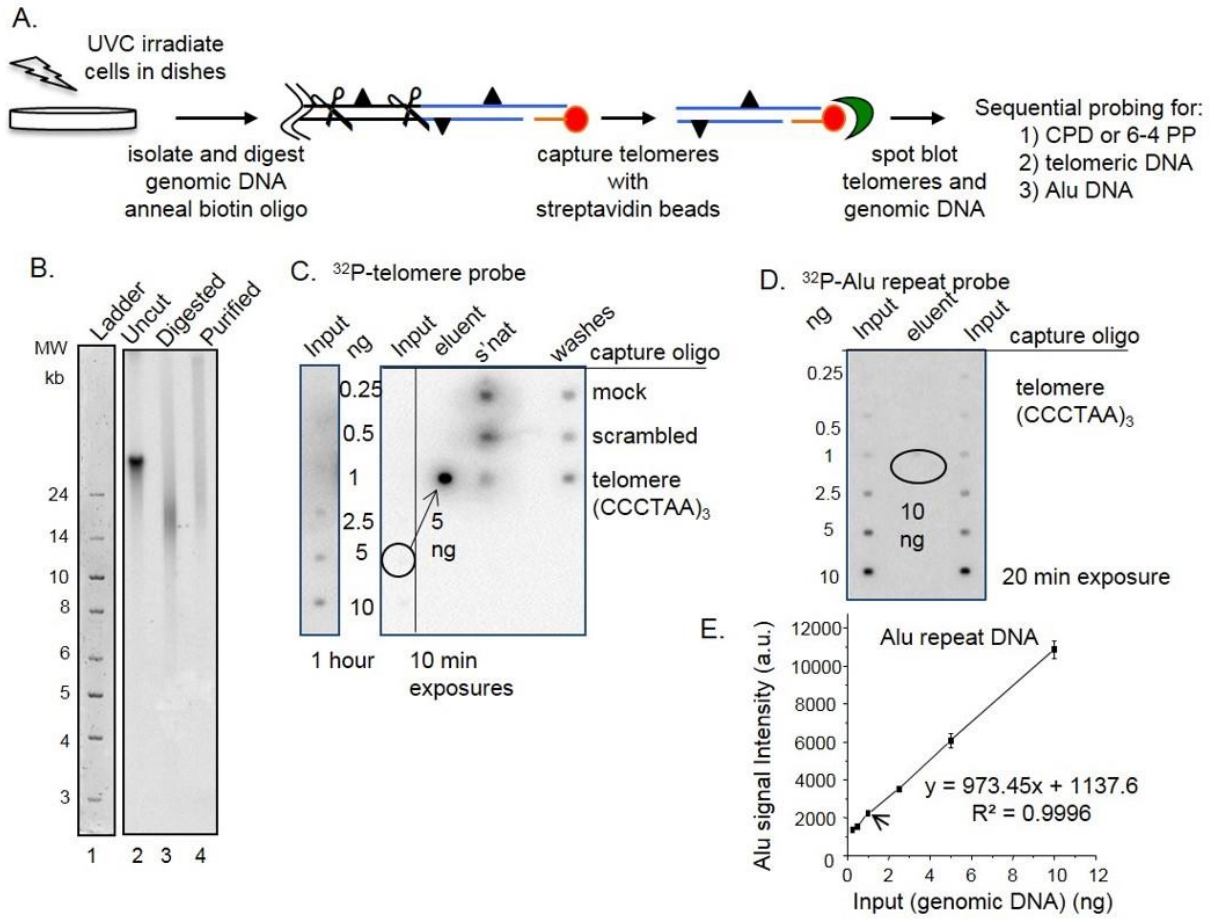

(*A*) Schematic of telomere capture assay. Telomeres (blue lines) are released by digesting the genome (scissors) and captured by annealing a biotinylated oligonucleotide (red) that binds to the telomeric single strand overhang and to streptavidin beads (green). Triangles denote photoproducts. (*B*) Undigested (lane 2) and digested (lane 3) genomic DNA, and isolated telomeres (lane 4) from BJ-hTERT cells were electrophoresed on a 0.6% agarose gel that was subsequently hybridized with a radiolabeled telomeric probe (lane 2-4). The ladder was visualized by SYBR Green staining (lane 1). (*C*) Specificity of telomere capture. Telomeres were isolated using three different conditions: mock (no oligonucleotide), scrambled (non-telomeric oligonucleotide) and telomere oligonucleotide (Table 1). Various amounts of digested genomic DNA (input), 50% of the unbound (s'nat) and 50% of the combined washes were loaded on the membrane. 50% of the eluent for the telomere oligo (5 ng) and total eluent for the mock (0 ng) and scrambled oligo (2.6 ng) was loaded. The membrane was hybridized with radiolabeled telomeric probes and exposed to a phosphoimager screen for the indicated times. (*D*) Telomere purity. Various amounts of digested genomic DNA (input) and 10 ng of the telomere eluent were loaded on a membrane that was hybridized with a radiolabeled Alu repeat DNA probe. (*E*) Alu signal intensities from the genomic DNA were plotted against the DNA amounts loaded. Values and error bars represent the mean and SD from two independent experiments. The Alu signal intensity for 10 ng of telomere eluent corresponded to about 1.2 ng (arrow).

Figure 6: Telomere isolation assay

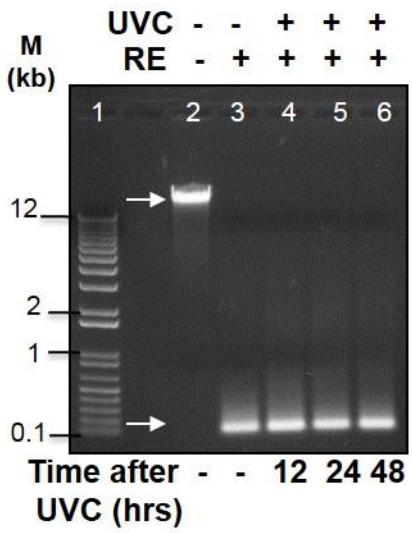

Genomic DNA isolated from untreated or 10 J/m^2 UVC exposed BJ-hTERT cells and recovered at various time points (12 – 48 h) was digested overnight with a cocktail of four restriction enzymes as described in Materials and Methods. Aliquots of uncut or digested DNA (400 ng) were resolved on a 0.8% agarose gel at 110 V for 1 hour. Ethidium bromide staining reveals that the genomic DNA was digested to fragments < 1 kb in length.

Figure 7: Restriction enzyme digestion of genomic DNA

2.5.2 **BJ-hTERT telomeres exhibit formation and removal of CPDs and 6-4 PPs**

Photoproduct removal in genomic and telomeric DNA of NER proficient BJ-hTERT cells exposed to 10 J/m^2 UVC was quantified at various recovery times by immuno-spot blot assay. This exposure generated approximately 3.6 CPDs per 10 kb of genomic DNA (Fig. 11), in general agreement with previous reports [37, 50]. This value was derived by comparing signal intensities from CPD immunodetection in genomic DNA to those obtained from lambda DNA standards for which the UV lesion frequencies were determined by quantitative PCR [125] (Fig. 11). We confirmed previous reports that CPDs form in telomeric DNA [86, 87]. However, the CPD signal for equal amounts (7 ng) of loaded bulk telomeric DNA at 0 hour recovery was on average 2.6-fold (± 0.32) lower compared to that for bulk genomic DNA (Fig. 8A, top panel). This equates to about 1.4 CPD/10 kb of telomeric DNA, or 2.3 CPDs per 17 kb telomere. The CPD signal decreased progressively with increasing recovery time after the 10 J/m^2 UVC exposure for both bulk genomic and telomeric DNA, however, the reduction was 1.5-fold more rapid for telomeric DNA (Fig. 2B). The rate difference was based on the slopes calculated from the linear portions of the curves (0 to 24 hrs). The difference between the curves for telomeric versus genomic CPD repair is statistically significant ($p = 0.0034$, two-factor ANOVA). Subsequent hybridization with the radiolabelled telomeric probe confirmed successful enrichment of telomeric DNA in the purified samples and equal loading of telomeric DNA for each recovery time point (Fig. 8A). Membrane stripping led to telomere loss, therefore, membranes were subsequently hybridized with the radiolabeled Alu repeat DNA probe to confirm equal loading of the genomic DNA samples.

To ensure that the reduction in CPDs was not due to dilution through cell division, we examined cell proliferation by obtaining cell counts for each repair time point after the 10 J/m^2 UVC exposure. UVC irradiation normally triggers transient cell cycle arrest [130]. Untreated BJ-hTERT cells doubled in number by 48 hours, while the UVC exposed cells failed to double even after 72 hours recovery (Fig. 9A). However, about 95% of the cells harvested collected via trypsinization for the repair assay were alive as determined by trypan blue staining (Fig. 9B). These results confirm that repair assays were conducted on viable cells, and that the observed reductions in photoproducts were not due to cell division.

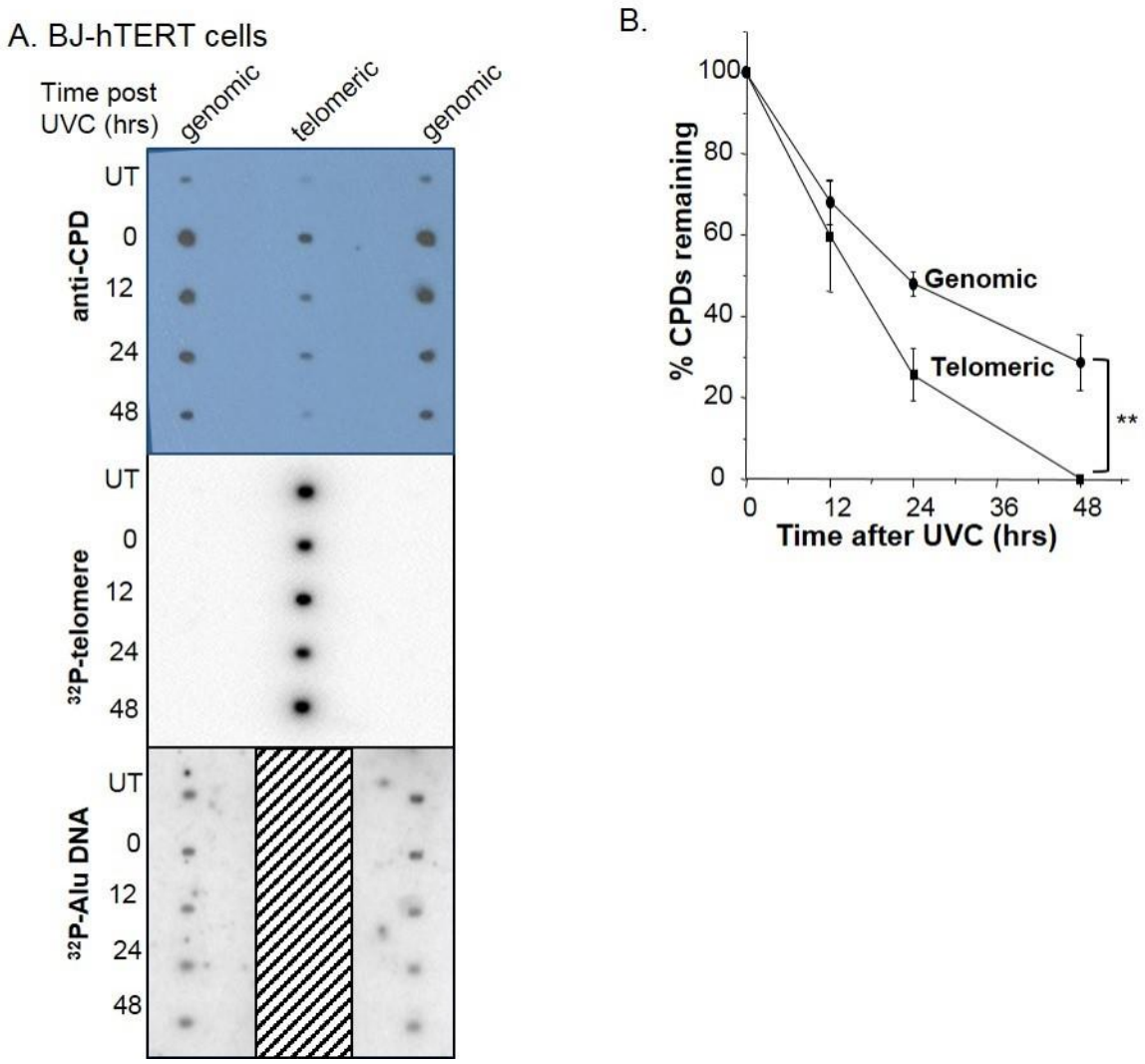

(*A*) Cells were untreated or exposed to 10 J/m^2 UVC followed by harvesting at various repair times (0 - 48 h). Telomeres were isolated from purified genomic DNA (100 μg each time point) and loaded on blots (7 ng, lane 2) with equal amounts of genomic DNA (7 ng, loaded in duplicate lanes 1 and 3). The blot was sequentially probed with a CPD antibody, a radiolabeled telomere probe, and a radiolabeled Alu repeat probe. The telomere probes remained bound (hashed box) since membranes could not be stripped without losing DNA. (*B*) The CPD signal intensity was quantitated, normalized to 0 hour, and plotted against recovery time. Values are the mean and SE from three independent experiments. The difference between the curves is statistically significant (**, p = 0.0034) by two-factor ANOVA.

Figure 8: Quantification of CPD formation and removal in telomeres from UVC exposed BJ-hTERT cells

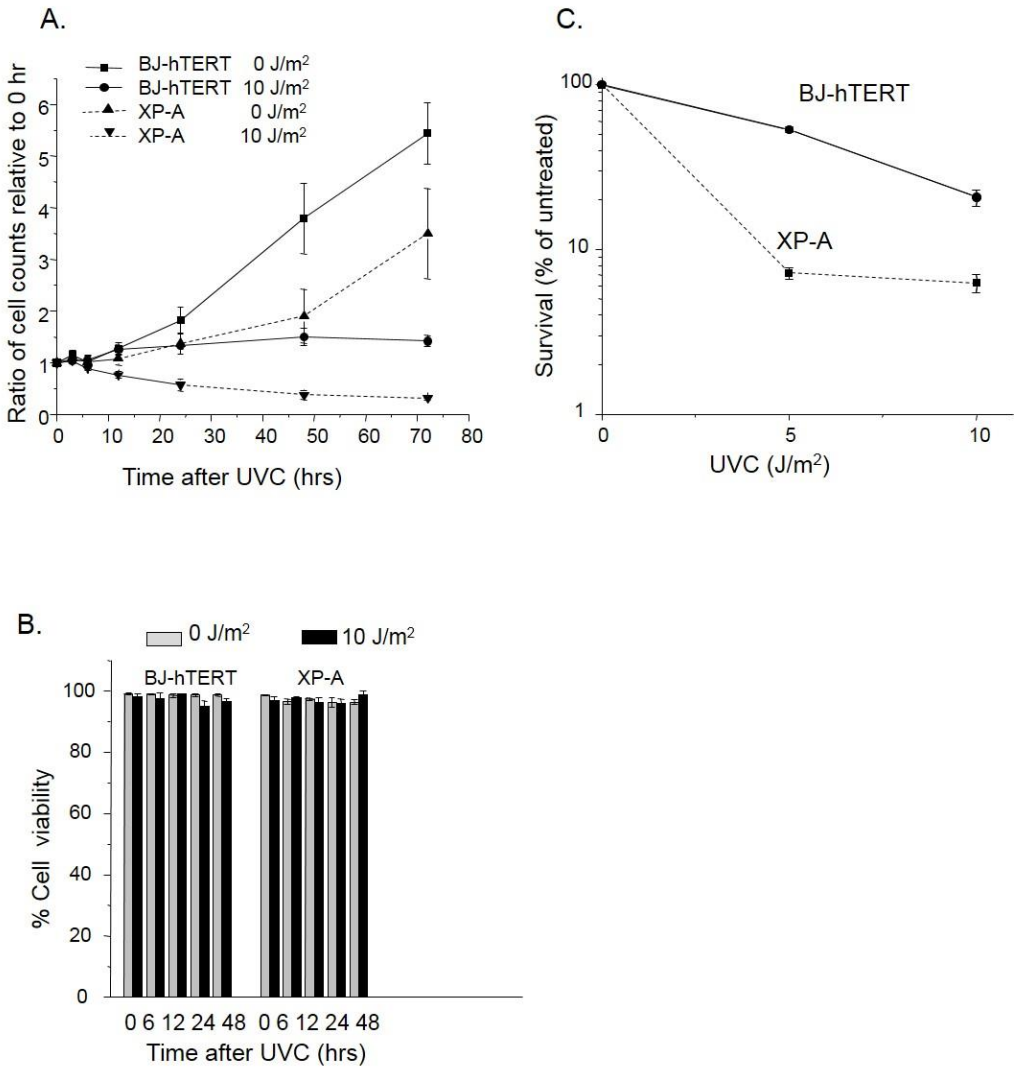

(*A*) Cells were exposed to 10 J/m^2 UVC, incubated in fresh media, and then counted after each recovery time point (0-72 h). Cell counts were normalized to the 0 h and plotted against recovery time. Values and error bars are from means and SE from three independent experiments. *(B)* Cells were exposed to 10 J/m^2 UVC, incubated in fresh media, and then harvested after each recovery time point (0-48 h) by trypsinization after washing. Cells were counted manually on a hemocytometer for total cells and Trypan blue positive dead cells. Percent viability was calculated as described in Materials and Methods. Values represent the mean and SE from three independent experiments. (*C*) Cells were exposed to 0, 5, or 10 J/m^2 UVC, recovered for 6h, sub-cultured and counted after 7 days of incubation. Survival was calculated as percent of untreated and plotted against UVC dose. Values and error bars are means and SE from three independent experiments.

Figure 9: UVC sensitivity and proliferation of BJ-hTERT and XP-A cells

The other common photoproduct 6-4 PP had not been previously examined at telomeres. 6-4 PP lesions induce greater distortion in the duplex DNA and are repaired more rapidly than CPDs, however, they are formed at a lower frequency [131, 132]. The 10 J/m^2 UVC exposure generated about 1.4 6-4 PPs per 10 kb of genomic DNA (Fig. 11). Therefore, higher amounts of loaded purified telomeres (15 ng isolated from 200 μg genomic DNA) were required for reliable 6-4 PP detection. Following 10 J/m^2 UVC, the 6-4 PP signal was on average 1.9-fold (± 0.32) lower for bulk telomeric DNA, compared to equal amounts (15 ng) of bulk genomic DNA (Fig. 10A). This equates to approximately 0.74 6-4 PPs/10 kb telomeric DNA, or 1.2 6-4 PPs per 17 kb telomere. 6-4 PPs were removed at similar rates in bulk genomic DNA compared to telomeric DNA, and were removed more rapidly than CPDs (Fig. 10B). About 20% of the 6-4 PPs remained in both genomic and telomeric DNA by 3 hours and only ~6% remained by 6 hours post UVC exposure. Hybridization with telomeric and Alu repeat specific probes confirmed equal loading of telomeric DNA and genomic DNA, respectively, for all time points (Fig. 10A). The difference between the genomic CPDs and telomeric CPDs formed at 0 hour is statistically significant (**, $p = 0.0031$) by two-tailed heteroscedastic Student's T test.

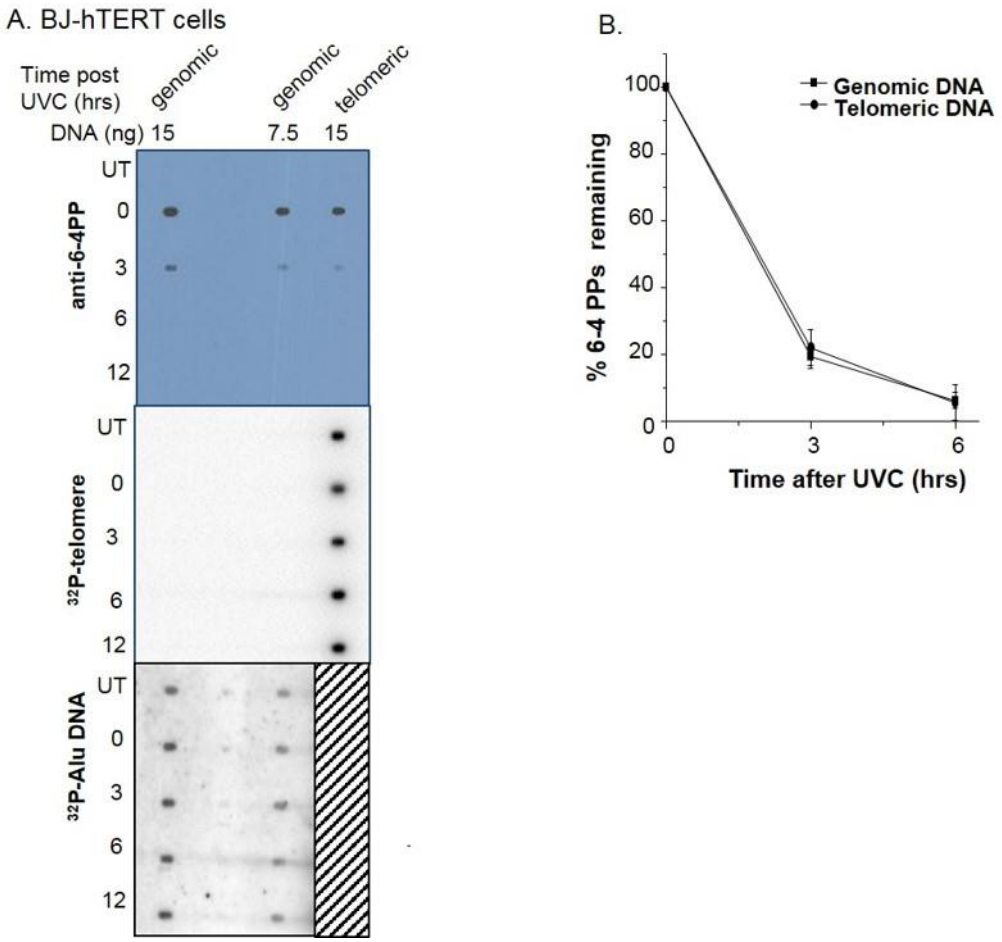

(*A*) Cells were untreated or exposed to 10 J/m^2 UVC followed by harvesting at various repair times (0 - 12 h). Telomeres were isolated from purified genomic DNA (100 μg each time point) and combined from two separate experiments to obtain 15 ng (lane 2) for loading. Genomic DNA was loaded at 7.5 ng (lane 1) and 15 ng (lane 2). The blot was sequentially probed with a 6-4 PP antibody, a radiolabeled telomere probe, and a radiolabeled Alu repeat probe. (*B*) The 6-4 PP signal intensity was quantitated, normalized to 0 hour, and plotted against recovery time. Values are the mean and SE from four independent experiments for genomic DNA and two experiments for telomeric DNA. Differences between genomic and telomeric 6-4 PPs at 0, 3 and 6 hours after UVC exposure were not statistically significant by two-factor ANOVA.

Figure 10: Quantification of 6-4 PP formation and removal in telomeres from UVC exposed BJ-hTERT cells

A

UVC J/m²	No. of lesions / 10 kb	No. of CPDs / 10 kb (*0.75)	No. of 6-4PPs /10 kb (*0.25)
0	0	0	0
5	1.67	1.25	0.42
10	3.33	2.497	0.62
20	6.46	4.84	1.615

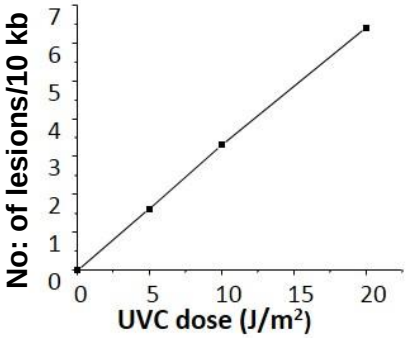

B.

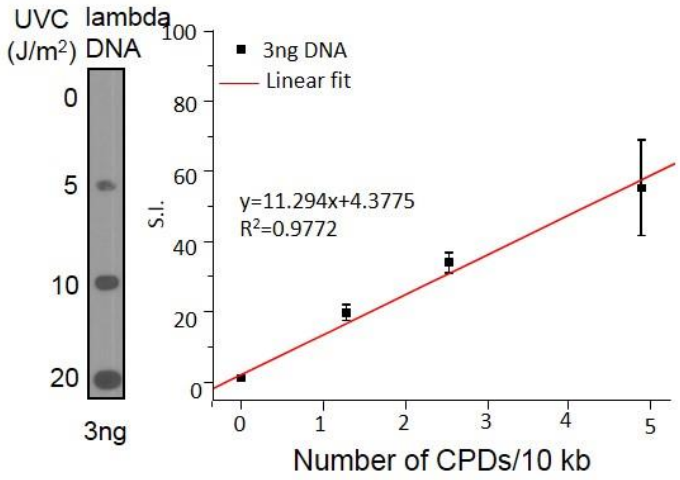

C.

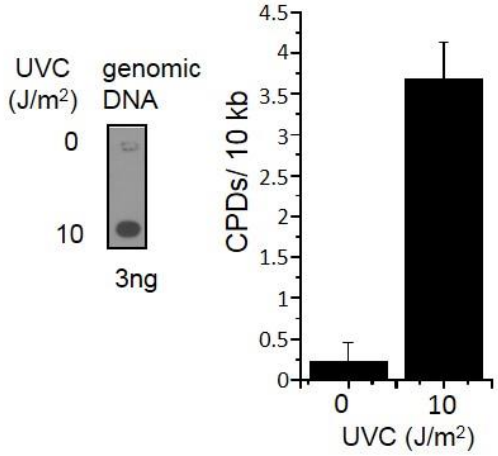

D.

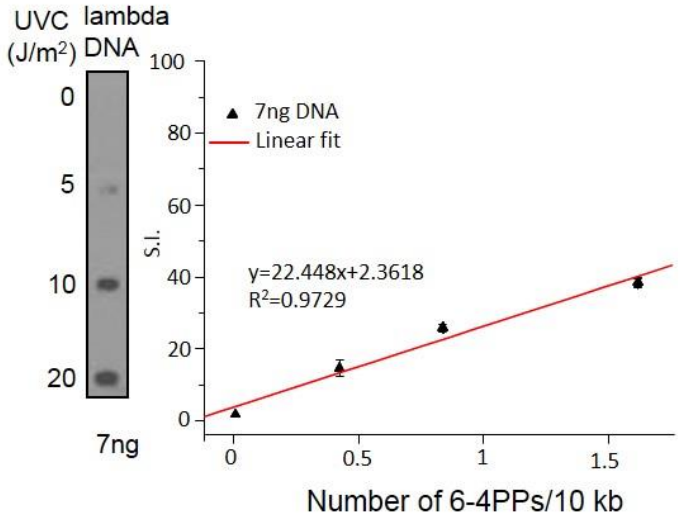

E.

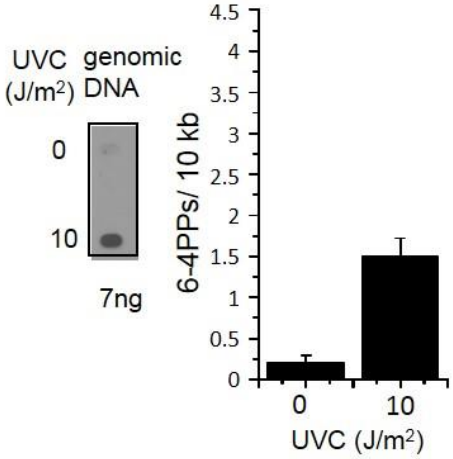

(*A*) Lambda DNA standards were prepared by exposing naked DNA to 0, 5, 10 or 20 J/m^2 UVC. Total UV photoproducts were measured by qPCR. The number of CPDs and 6-4 PPs were deduced by applying the previously reported ratio of three CPDs for one 6-4 PPs formed. (*B*) Lambda DNA standards (3 ng) were loaded in triplicate on a membrane and immunoblotted for CPDs. Signal intensities were plotted as a function of the CPD number to generate a standard curve. (*C*) The CPD signal intensity was measured for BJ-hTERT genomic DNA from untreated or 10 J/m^2 UVC exposed cells (3 ng) loaded on the same blot as the lambda DNA standards. The number of CPDs (right panel) was deduced from from the lambda standard curve. (*D*) Lambda DNA standards (7 ng) were loaded in triplicate and immunoblotted for 6-4 PPs. Signal intensities were plotted as a function of 6-4 PPs number to generate a standard curve. (*E*) The 6-4 PP signal intensity was measured for BJ-hTERT genomic DNA from untreated or 10 J/m^2 UVC exposed cells (7 ng) loaded on the same blot as the lambda DNA standards. The number of 6-4 PPs (right panel) was deduced from the lambda standard curve. Values for lambda DNA standard curves represent the mean and SE from three independent blots, and values from genomic DNA represent mean and SE from three independent experiments.

Figure 11: Estimation of CPDs and 6-4 PPs in BJ-hTERT genomic DNA after UVC exposure

2.5.3 **Removal of 6-4 PPs at telomeres depends on XPA protein**

To determine whether photoproduct removal at telomeres requires NER, we repeated the telomere capture and immuno-spot blot assays in cells lacking repair. NER deficent skin fibroblasts were obtained from an XP-A individual and were immortalized by SV 40 transformation [133]. We first confirmed that the XP-A cells were more sensitive to UVC compared to repair proficient BJ-hTERT cells by conducting a long-term survival assay [134]. For this experiment cells were exposed to UVC and allowed to recover for 6 h, then sub-cultured for 7 days and counted (Fig. 9C). Although sensitive to UVC, the XP-A cells harvested shortly after UVC irradiation for the repair assays were at least 95% viable as determined by trypan blue staining (Fig. 9B). Genomic DNA isolated from XP-A cells lacked 6-4 PP and CPD repair up to 3 or 12 hours, respectively, post UVC exposure (Figs. 12A and 13A). Similarly, there was no significant change in the amount of 6-4 PPs in bulk telomeres by 3 hours, compared to 0 hours, post UVC exposure (Figs. 12A and C). We repeated this experiment except that we allowed the cells to recover for 12 hours, and still did not observe a significant reduction in 6-4 PPs in either bulk genomic or telomeric DNA (Figs. 12B and C). These results validate our approach for the ability to detect a lack of repair in telomeres, and provide evidence that NER is active at telomeres and removes photoproducts.

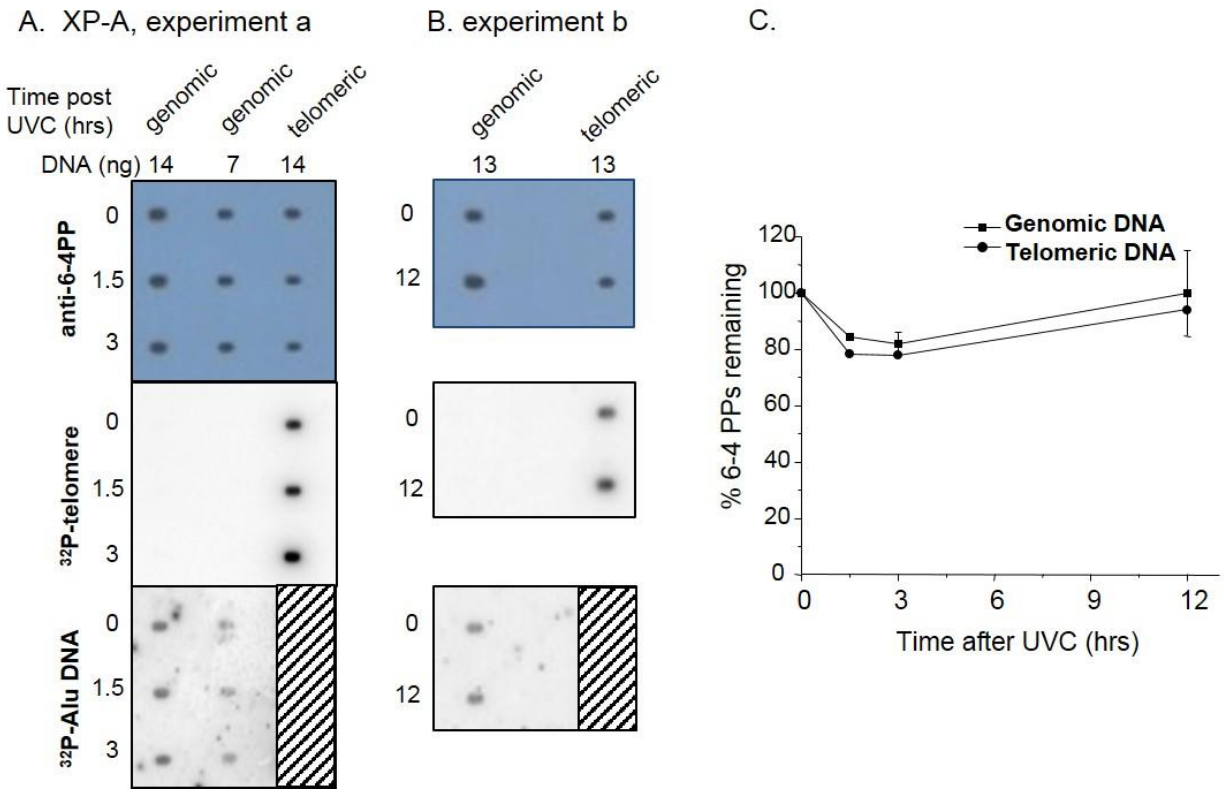

(*A*) Cells were exposed to 10 J/m^2 UVC and harvested at various repair times (0, 1.5 and 3 h, experiment a; 0 and 12 h, experiment b). Telomeres were isolated from purified genomic DNA (100 μg each time point) and combined from two separate experiments to obtain 13-14 ng (lane 2) for loading. Genomic DNA was loaded at amounts indicated. The blots were sequentially probed with a 6-4 PP antibody, a radiolabeled telomere probe, and a radiolabeled Alu repeat probe. (*B*) The 6-4 PP signal intensity was quantitated, normalized to 0 hour, and plotted against recovery time. Genomic DNA values represent the mean and SE from two independent experiments, and values for telomeres are from blots shown in *A*. (experiments a and b). Differences between 6-4 PPs repaired at 0, 3 and 12 hour in genomic DNA after UVC exposure were not statistically significant by one-factor ANOVA with multiple comparisons.

Figure 12: XPA protein is required for 6-4 PP removal from telomeres

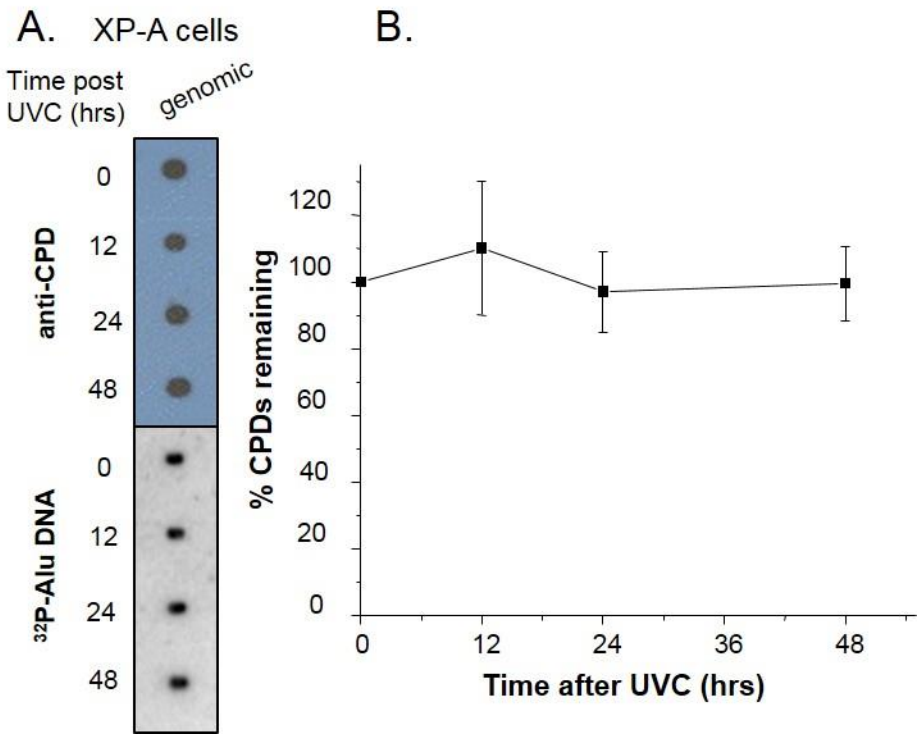

(A) Cells were exposed to 10 J/m^2 UVC followed by harvesting at various repair times. Genomic DNA was loaded (10 ng) in duplicate on a membrane which was sequentially probed with CPD antibody and then a radiolabeled Alu repeat probe. *(B)* The CPD signal intensity was quantitated, normalized to 0 hour, and plotted against recovery time. Values and error bars are means and SE from three independent experiments. Differences between CPDs at 0, 12, 24 and 48 hours in genomic DNA after UVC exposure were not statistically significant by one-factor ANOVA with multiple comparisons.

Figure 13: Quantification of CPD formation and removal in genomic DNA from UVC exposed XP-A cells

Finally, 6-4 PP removal from telomeric DNA was not dependent on telomerase. We observed nearly complete removal of 6-4 PP in both bulk genomic and bulk telomeric DNA by 12 hours post UVC in the telomerase negative human osteosarcoma cell line U2OS (Fig. 14). The initial amount of 6-4 PPs formed in telomeric DNA from U2OS cells was about 2-fold lower compared to bulk genomic DNA, similar to BJ-hTERT cells (Fig. 14). Repair rates of both 6-4 PP and CPDs in genomic DNA were slower in U2OS cells compared to BJ-hTERT (Figs. 14-15). In summary, we observed that 6-4 PPs form at telomeres following UVC exposure and are removed at rates similar to the bulk genome.

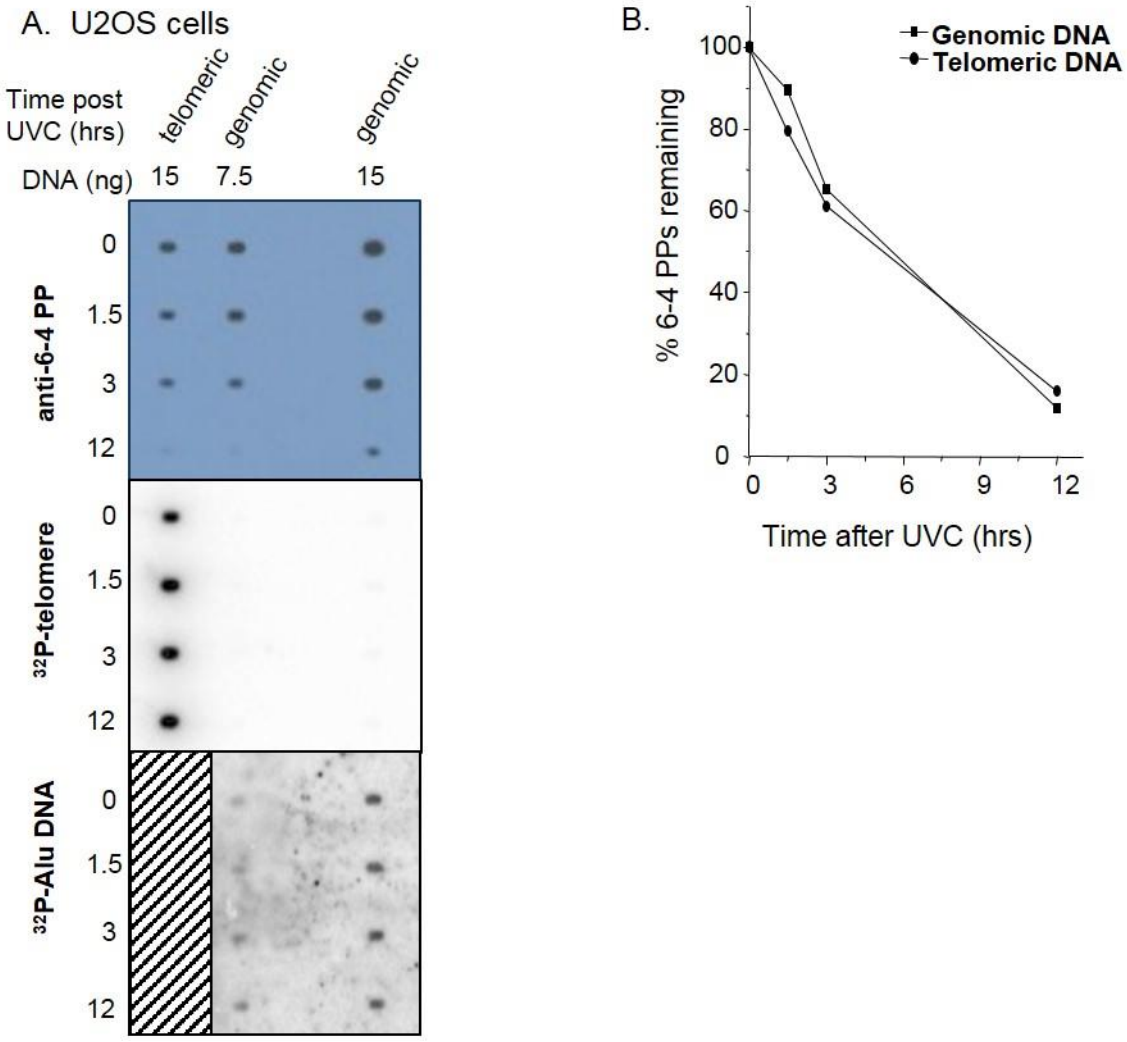

(*A*) Cells were untreated or exposed to 10 J/m^2 UVC and harvested at various repair times (0 - 12 h). Telomeres were isolated from purified genomic DNA (200 μg each time point) and loaded on a membrane (15 ng) (lane 3). Genomic DNA was loaded at 15 ng (lane 1) and 7.5 ng (lane 2). The blot was sequentially probed with a 6-4 PP antibody, a radiolabeled telomere probe, and a radiolabeled Alu repeat probe. (*B*) The 6-4 PP signal intensity was quantitated, normalized to 0 hour, and plotted against recovery time.

Figure 14: Quantification of 6-4 PPs formation and removal in telomeric DNA from UVC exposed U2OS cells

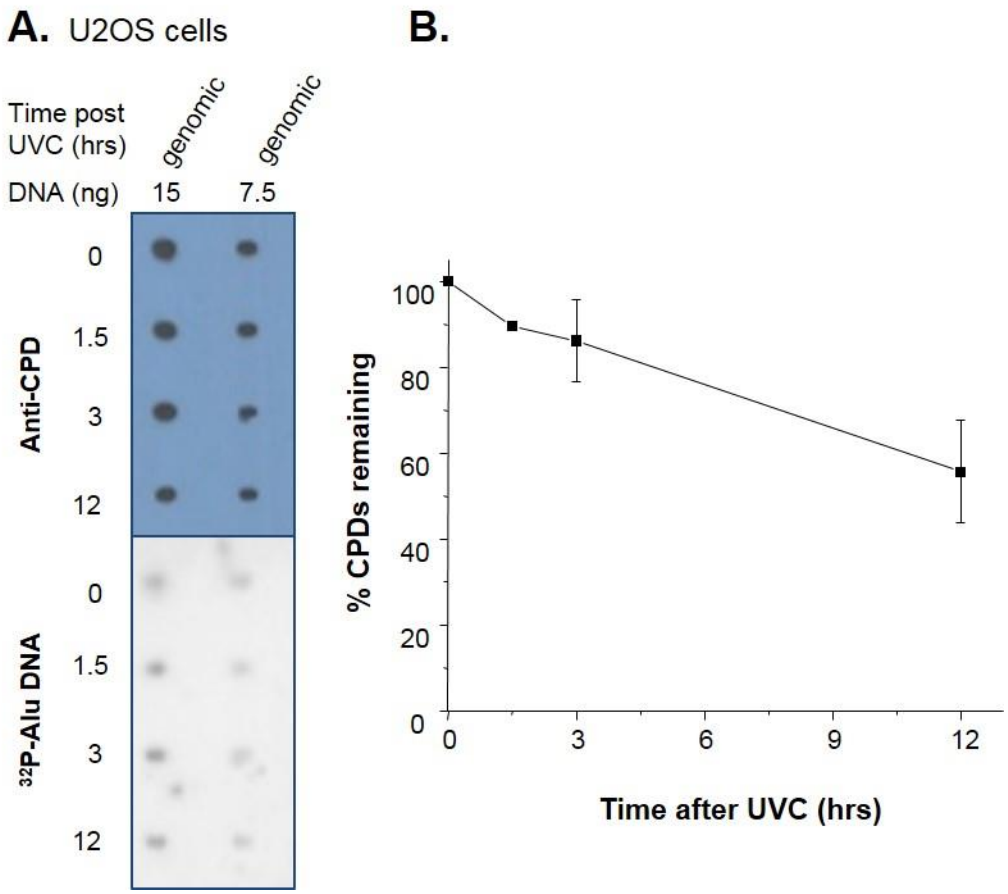

(A) Cells were exposed to 10 J/m^2 UVC and harvested at various repair times. Genomic DNA was isolated and loaded (15 or 7.5 ng) on a membrane which was sequentially probed with CPD antibody and then a radiolabeled Alu repeat probe. *(B)* The CPD signal intensity was quantitated, normalized to 0 hour, and plotted against recovery time. Values and error bars are means and SE from three independent experiments, except the 1.5 h time point which was from a single experiment. Differences between CPDs at 0, 3 and 12 hours after UVC exposure were not statistically significant with one-factor ANOVA with multiple comparisons.

Figure 15: Quantification of CPD formation and removal in genomic DNA from UVC exposed U2OS cells

2.5.4 **An unrepaired cyclobutane pyrimidine dimer inhibits TRF1 binding**

We showed that photoproducts persist in cells lacking NER (Fig. 12). Telomeres could potentially tolerate an accumulation of unrepaired DNA lesions if such lesions fail to disrupt shelterin binding. However, previous reports show that 8-oxoguanine decreases TRF1 and TRF2 binding to telomeric duplexes by 50% *in vitro* [39]. To determine whether unrepaired photoproducts also inhibit TRF1 binding, we performed gel shift assays with purified TRF1 and a 39 bp duplex DNA substrate containing the minimal consensus binding sequence for a TRF1 homo-dimer [39]. A damaged substrate was constructed by replacing the central adjacent thymines with a CPD lesion (Table 1). We tested a CPD since it distorts the helix less than a 6-4 PPs [112] and is commercially available. Migration of telomeric substrates through the agarose gel was retarded due to TRF1 binding to the duplex (Fig. 16A). The presence of a single CPD lesion within the telomeric substrate caused a prominent decrease in TRF1 binding to the substrate (lanes 7 to 10); 14-fold (93%) decrease within the linear range of the binding curve (25 nM TRF1) compared to the control (Fig. 16B). These data suggest that persistent CPDs at the telomeres could alter shelterin binding, underscoring the potential importance of repair at telomeres.

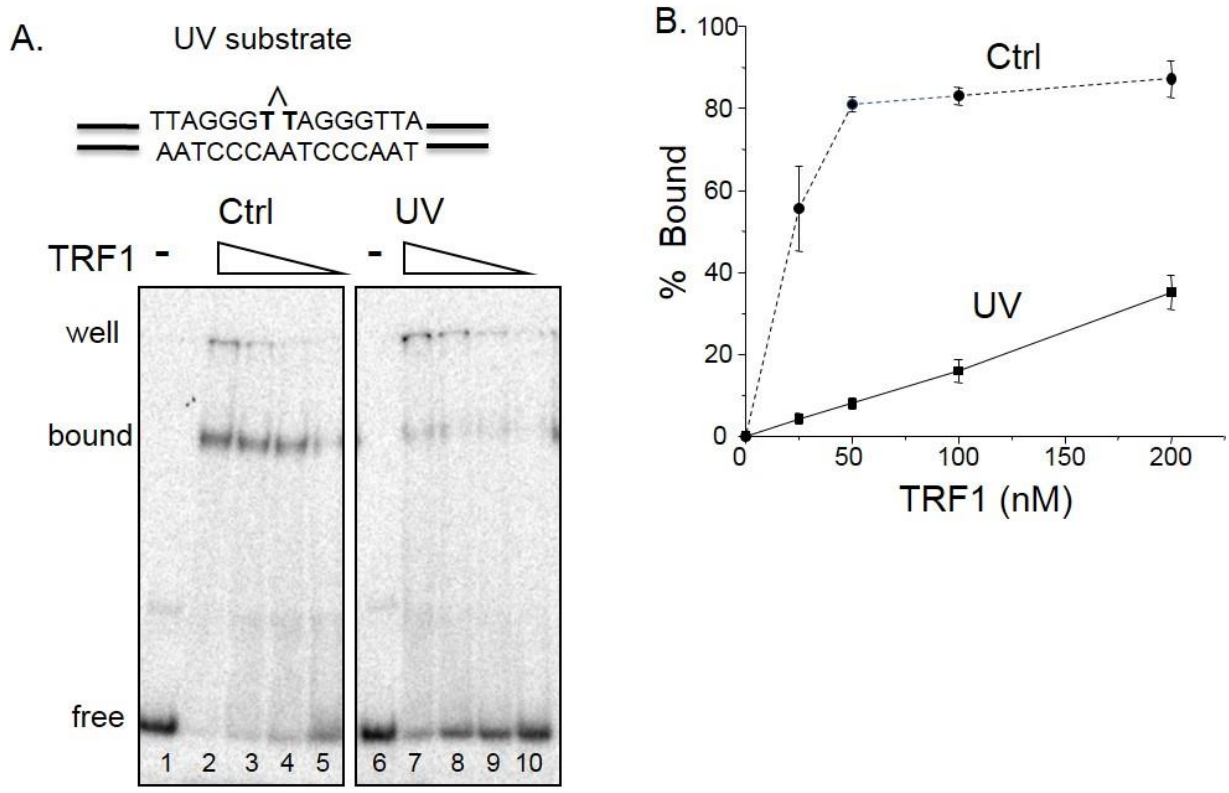

The TRF1 homo-dimer binding sequence and site specific CPD (∧) is shown. (*A*) Substrates (2.5 nM) consisting of annealed Ctrl/TPL or UV/TPL duplexes were incubated with decreasing TRF1 concentrations (200, 100, 50 or 25 nM) for 20 minutes in binding buffer, and reactions were run on a 5% acrylamide native gel. Bound and unbound (free) substrate are indicated. (*B*) The percent bound was calculated and plotted against TRF1 concentration. Circle and dotted line, control (Ctrl); square and solid line CPD containing substrate (UV). Values and error bars indicate the mean and SD from three independent experiments.

Figure 16: A cyclobutane pyrimidine dimer inhibits TRF1 binding to telomeric DNA

2.6 **DISCUSSION**

In this study we established an assay for directly visualizing and quantifying photoproduct formation and removal in bulk telomeres isolated from various UVC irradiated cell lines. Using this approach we confirmed CPD formation in telomeres, and discovered that telomeres are also susceptible to 6-4 PP formation (Figs. 8 and 10). The frequency of photoproducts at telomeres was about 2-fold lower compared to the bulk genome, suggesting that shelterin may partly shield the telomeres from damage. Using the telomere isolation and immunoblotting approach we observed that CPDs and 6-4 PPs are removed from telomeres, and that lesion reduction requires the NER protein XPA, but does not depend on telomerase activity. We discovered that a single unrepaired CPD strongly inhibited shelterin TRF1 binding to telomeric DNA *in vitro*, suggesting that unrepaired lesions at telomeres could be deleterious if they accumulate. To our knowledge this study provides the first direct evidence that NER is functional at telomeres and is required to restore damaged telomeric DNA.

Our result that CPDs and 6-4 PPs are less abundant at telomeres compared to the bulk genome suggests that shelterin may partly protect the telomeres from UV irradiation. This is particularly interesting in light of evidence that naked telomeric DNA *in vitro* is more susceptible to UVC-induced CPD formation compared to control DNA containing similar numbers of dipyrimidine sites [86]. However, shelterin may act similarly to some transcription factors which can inhibit photoproduct formation at bound promoters upon cellular UV irradiation [135]. Furthermore, we cannot rule out the possibility that photoproduct formation at telomeres may be higher compared to specific sites within the

genome. For example, previous work reported more CPDs at telomeric fragments compared to fragments from the *p53* tumor suppressor gene and 28S ribosomal DNA (rDNA) gene after cellular UVC exposure [86]. Thus, the shelterin complex at telomeres may modulate susceptibility to photoproduct formation.

Global genome repair (GGR) removes photoproducts and bulky lesions from both transcribed and silent genomic regions, whereas transcription-coupled repair (TCR) is a specialized mechanism limited to lesion removal on the template DNA strands of actively transcribed genes [112]. Therefore, our analysis of photoproduct removal from the bulk genome represents primarily GGR rates and is consistent with CPD and 6-4 PP rates reported elsewhere for human cells [86, 87, 136]. However, telomeres are transcribed from the C-rich strand into non-coding RNAs called TERRA which are required for telomere homeostasis [85, 137]. Therefore, photoproduct removal rates from telomeres may include TCR of CPDs at CT or CC dipyrimidines on the actively transcribed telomeric strand. This may explain why we observed a 1.5-fold faster removal of CPDs from bulk telomeres compared to bulk genomic DNA (Fig. 8). TCR of 6-4 PPs is often obscured because these lesions are rapidly and efficiently repaired by GGR [112, 132, 138], in agreement with our result that 6-4 PP removal rates are similar in bulk telomeres compared to bulk genomic DNA (Fig. 10).

Using our telomere capture and immuno-spot blot approach we observed that only 25% of the detectable CPDs remain at telomeres by 24 hours of repair, and that they disappear by 48 hours, in BJ-hTERT fibroblasts (Fig. 8). This rate is higher than that

reported previously for telomere CPD removal in primary fibroblasts derived from normal young individuals, in which 50% of the telomeric CPDs remained by 24 hours similar to repair rates in non-transcribed strands [87]. However, direct comparison is difficult since the UV dose used was higher (20 J/m^2) than in our experiments, and the primary fibroblasts lacked telomerase and possessed shorter telomeres; all factors that may influence telomere repair rates. For example, if efficient telomere repair relies on transcription or TCR, perhaps differences in the levels of telomere transcription among cell lines may influence the efficiency of telomere repair. Importantly, both our approach and this previous approach [87] yielded the similar result that UV-induced CPDs are removed from telomeres during recovery. These approaches have in common the detection of CPDs in telomere restriction fragments either by antibody staining of isolated telomeres (this study) or by T4 endonuclease cleavage of unpurified telomere fragments [87].

Telomeres released by restriction enzymes retain some sub-telomeric DNA that may be resistant to digestion. We attempted to minimize sub-telomeric DNA by using multiple restriction enzymes that are known to cut within the sub-telomeric regions [123]. This region contains degenerate telomeric repeats and is estimated to average ~3.5 kb in BJ-hTERT cells [139]. Therefore, approximately 20% of the purified telomere fragments could contain sub-telomeric DNA. We cannot rule out the possibility that some of the CPD and 6-4 PP removal in the purified telomeres is due to repair in sub-telomeric regions. However, if the telomeres were resistant to repair then photoproducts should have remained visible since the majority of the isolated telomeres consists of telomeric

DNA (Figs. 8, 10 and 12). In constrast, we failed to detect CPDs after 48 hours and 6-4 PPs after 6 hours of repair in telomeres from BJ-hTERT cells (Figs. 8 and 10). Another possibility is that telomeres are refractory to CPD and 6-4 PP formation and that lesions are limited to the sub-telomeric region. This is highly unlikely due to the small size of the target; 10 J/m^2 induces at least one CPD per 10 kb and 6-4 PPs are about three-fold less frequent [63, 140]. Furthermore, a previous approach reported CPDs in telomeric DNA by using quantitative PCR to measure telomeric DNA, which excludes sub-telomeric DNA [86].

Disparity between our results and a previous study that reported no significant CPD removal from telomeres by 48 hours [86], may be explained partly by differences in cell lines or approaches. In the previous study denatured ssDNA from UV irradiated cells was chromatin immuno-precipitated with a CPD-antibody to isolate ssDNA fragments containing CPDs, followed by gene and telomeric DNA identification using quantitative PCR [86]. We used the reverse approach in which we isolated bulk telomeres first, and then blotted them on a membrane for lesion detection with the CPD or 6-4 PP antibodies. Telomeres present a challenge for lesion detection because the DNA must be denatured for the antibodies to recognize the lesion, and single stranded telomeric G-rich repeats can fold into G-quadruplex structures [141]. Using our approach the telomeres are denatured in a membrane and fixed to avoid secondary structure formation, therefore, we do not suspect that G-quadruplex formation could prevent lesion detection. Furthermore, our approach is able to detect 6-4 PPs in telomeres at all time points in NER-deficient cells (Fig. 12). Perhaps, a subset of telomeres retain photoproducts but

are beyond the detection limit of our assay, and may be detectable by the more sensitive qPCR approach [86]. Another difference is that we used skin fibroblasts that are telomerase positive and an osteosarcoma cell line that maintains telomeres by ALT, rather than primary fibroblasts. A limitation of our assay is that it requires a large amount of genomic material and thus, highly proliferative cells. However, telomerase does not enable 6-4 PP removal from telomeres (Fig. 14) and previous studies also showed CPD removal from telomeres occurs in primary fibroblasts [87]. Another factor may be related to differences in transcriptional activity levels at telomeres among cell lines, which would influence lesion removal at telomeres by TCR as mentioned earlier.

2.7 **BIOLOGICAL IMPLICATIONS**

The finding that 6-4 PPs persist at telomeres in NER deficient cells, but are removed in NER proficient cells, provides strong evidence that NER is active at telomeres. Previous studies of CPD formation and removal at telomeres in normal cells could not rule out the possibility that lesion removal was accomplished by another mechanism [87]. Shelterin protein TRF2 prevents inappropriate cleavage of the telomeric 3' ssDNA overhang by the key NER nuclease XPF-ERCC1 [92]. Our data indicates this TRF2 inhibitory effect does not extend to NER. Thus, both NER (this study) and base excision repair are active at telomeres [40], while homologous recombination repair and non-homologous end joining are suppressed at telomeres [9, 94]. Together with reports that UV exposure apparently alters telomere lengths in tissue [89, 104, 118], our finding provides evidence that repair of photoproducts is likely important for telomere preservation. Consistent with

this, we observed that UVC irradiation induces telomere aberrations that are exacerbated in cells lacking lesion bypass by polymerase η, indicating that unrepaired photoproducts can interfere with telomere replication [142]. Furthermore, we observed that an unrepaired CPD inhbited TRF1 binding to telomeric DNA by 14-fold, which is much greater than the 2-fold inhibition caused by an 8-oxoguanine lesion on the identical substrate [39]. This strongly suggests that lack of lesion repair at telomeres could be deleterious if unrepaired lesions increase in density overtime. Our discovery that NER is active at telomeres is consistent with the prediction that UV photoproducts disrupt telomere function and therefore, need to be removed.

3 INVESTIGATING ROLES FOR NUCLEOTIDE EXCISION REPAIR IN PROTECTING TELOMERES FROM DEFECTS INDUCED BY UV IRRADIATION

3.1 INTRODUCTION

Unrepaired DNA photoproducts generated by exposure to UV light have the potential to cause deleterious effects at telomeres in several ways. First, UV photoproducts can cause replication stress at telomeres, leading to telomere defects [142]. Recent evidence from our lab indicates that 5 J/m^2 UVC exposure induces telomere aberrations in human skin fibroblasts, and that the amount of UV-induced telomere aberrations are greater in XPV cells compared to wild type [142]. XPV cells lack the translesion synthesis enzyme polymerase η, which efficiently and accurately bypasses UV-induced CPDs to continue DNA replication (see section 1.2.4). UV is capable of inducing several kinds of telomere aberrations [142]. These include telomere losses (missing or critically short telomeres), telomere doublets (or 'fragile' telomeres) and sister telomere fusions. Importantly, telomere doublets are believed to result from altered condensed chromatin arising from regions of unreplicated ssDNA due to stalled or broken replication forks, and are induced by factors that also cause breakage at common fragile sites in chromosomes [11]. Moreover, unrepaired UV photoproducts can interfere with shelterin integrity, as strongly supported by our finding (see section 2.5.4) that a CPD lesion can severely inhibit TRF1 binding to telomeric duplexes. Thus, these studies provide evidence that removal of UV photoproducts at telomeres is critical for preserving telomeric structure and integrity.

Previous studies in mice suggest that a functional NER pathway may be required to preserve telomeres in skin following UV exposure. XPC is a protein that participates in the global genome NER pathway for repair of DNA photoproducts [88]. In the recent study by Stout and Blasco [89] (mentioned previously in section 1.2.7), the dorsal skin of wild type and *Xpc*$^{-/-}$ knock out mice was chronically exposed to 1.8 kJ/m^2 UVB radiation. Then telomere lengths and the percent of critically short telomeres in skin were measured by quantitative fluorescent in situ hybridization (qFISH) using telomeric probes. The authors observed that chronic UVB exposure caused accelerated telomere shortening in the skin of wild type mice that was exacerbated in *Xpc*$^{-/-}$ knock out mice. These findings, however, do not show unambiguously that NER was responsible for protecting telomeres from UV-induced shortening, because UVB causes oxidative damage in addition to photoproducts, and the XPC protein participates in base excision repair (BER) of oxidative damage [90, 91].

A functional XPA protein is indispensable for removal of UV-induced DNA photoproducts by the NER pathway, and loss of XPA can lead to several cellular abnormalities caused by defects in repairing DNA lesions [143]. However, unlike XPC, there is no current evidence that XPA participates in BER. XPA is a zinc metalloprotein that binds to ssDNA bearing the damage or chemically altered nucleotide and participates in the lesion verification step of NER (see section 1.2.5). XPA also recruits structure specific endonuclease XPF-ERCC1 to the pre-incision repair complex, which makes an incision 5’ to the lesion to release the strand containing the damage [144]. XPA knockdown mice lack NER to repair UV photoproducts in their genome, are highly susceptible to UVB-

induced skin and eye tumors as well as enhanced inflammation and immunosuppression, but are otherwise normal [145]. However, UVB induction of skin cancer in these mice requires exposure to shaved regions.

In this study we set out to test the hypothesis that a functional NER pathway suppresses the formation of UVC-induced telomeric defects. In order to address this hypothesis, we performed telomere FISH on metaphase chromosomes from an NER deficient XPA mutant cell line (XP-A), compared to an isogenic XPA complemented cell line (XPAC), to score for telomere defects after 0, 5 and 10 J/m^2 UVC exposure. We predicted that the XPAC cells would be proficient for NER and would exhibit a lower number of UV-induced telomere aberrations compared to the XP-A cells which are deficient in UV photoproduct repair. Previous evidence suggested that unrepaired UV photoproducts can cause replication stress at telomeres, leading to telomere defects [142]. However, we did not observe differences in the type and number of telomere aberrations induced by UVC exposure between the XP-A and XPAC cells. We found that the XPAC cells are proficient for photoproduct repair in genomic DNA, however, the repair rate was greatly reduced compared to wild type BJ-hTERT cells (see section 3.3.3). Western blotting of cell lysates revealed that the XPAC cells express much higher amounts of XPA protein compared to BJ-hTERT cells. We concluded that the abnormal excess of XPA protein in XPAC cells might have hindered normal rates of photoproduct repair, which precluded our ability to determine whether or not NER protects against UV-induced telomere defects. However, our studies revealed that UVC irradiation of NER deficient cells causes an increase in telomeres loss and fragility.

3.2 **MATERIALS AND METHODS**

3.2.1 **Cell culture and exposures**

XPAC and XP-A isogenic cell lines were obtained from Coriell Institute (Camden NJ). The XPAC cell line (GM15876) was derived from the SV-40 transformed XP-A skin fibroblast cell line (GM04312). The XP-A cell line was obtained from an XP-A patient donor that harbored a G-to-C transversion at the 3-prime splice acceptor site of intron 3 of the *XPA* gene. The XP-A patient was found to be homozygous for the mutation. The XPAC cell line was created by transfecting an expression vector containing the full length cDNA of the *XPA* gene into the XP-A cell line to correct for the protein deficiency [133]. Cells were grown at 37^{o}C and 5% CO_2 in DMEM complete media containing 10% fetal bovine serum, penicillin (50 units/ ml) and streptomycin (50 μg/ ml) (Life Technologies). UVC irradiations were performed for XPAC cells exactly as described in Section 2.4.2 for BJ-hTERT and XP-A cells.

3.2.2 **Cell viability and proliferation assays**

Similar to BJ-hTERT and XP-A cells (see section 2.4.3), for short term proliferation assays XPAC cells were UVC irradiated (10 J/m^2) or untreated in 60 mm dishes, incubated in fresh media, and then counted in duplicate at various repair time points (0 to 72 hours) using a Beckman Coulter Z1 Cell Counter. The average cell number for each repair time point was divided by the cell number at 0 hour recovery. Cell viability was determined by Trypan Blue exclusion. Percent viability was calculated as [1.00 –

(number of blue cells ÷ number of total cells)] × 100. For long term cell viability assays, the cells were irradiated with UVC (2, 5 or 10 J/m^2) or not (untreated) and incubated in fresh media. After 6 hours of recovery the cells were collected by trypsinization and counted, and then subcultured by seeding equal numbers of cells per 10-cm culture dish in duplicate. Following a seven day subculture, the cells were counted again.

3.2.3 **Telomere fluorescent *in Situ* hybridization assays**

XP-A and XPAC cells ($5x10^5$) were seeded in 35 mm dishes and grown overnight. Cells were then exposed to the UVC dose (0, 5 or 10 J/m^2) as indicated in the figure legend, and allowed to recover for 6 hours in fresh media. Metaphase chromosomes were then prepared and stained as described previously [146]. Briefly, following recovery, cells were incubated in 0.05 μg/mL colcemid for 10 hours to accumulate cells arrested in metaphase. Cells were then harvested, incubated in 75 mM KCl hypotonic solution, fixed in 3:1 methanol:acetic acid fixative solution and dropped onto slides to spread the metaphase chromosomes. Telomeres were hybridized with a Cy3 labeled peptide nucleic acid (PNA) probe for 2 hours with the sequence $(CCCTAA)_3$ complementary to the telomeres as described previously [147]. PNAs are sequence specific probes routinely used in hybridization assays since they lack a negatively charged phosphate backbone and have high affinity for DNA. Z-stack images were obtained using a Nikon Ti90 epi-fluorescence microscope equipped with PlanApo 60×/1.40 oil immersion objective. Analysis of telomere signal free ends, fusions and aberrations was performed using NIS Elements (Nikon Inc., NY). Images were then visually inspected and scored for telomere aberrations.

3.2.4 **Genomic DNA purification and immune-spot blot detection of DNA photoproducts**

Genomic DNA was isolated from harvested cells using the Qiagen 20/G DNA isolation kit. Approximately $5x10^6$ cells were harvested from two 100 mm dishes to yield about 20 μg of bulk genomic DNA per repair time point. Immuno-spot blots of purified genomic DNA were performed using the GE Manifold spot blot apparatus as previously described [124] and exactly as was described in Section 2.4.6 for BJ-hTERT and XP-A cells.

3.2.5 **Western blotting for XPA protein**

To confirm XPA complementation in XPAC cells, cell lysates were obtained from cells grown in 75 cm^2 dishes, collected by trypsinization and washed with cold PBS. Cells were resuspended in whole cell lysis buffer [50 mM Tris [pH 7.4], 150 mM NaCl, 5 mM EDTA, 1% Nonidet P-40, and protease inhibitor cocktail (1 μg/ml chymostatin, 1 μg/ml pepstatin, 1 μg/ml aprotinin, 1 μg/ml leupeptin, 0.4 μl/ml AEBSF)]. After incubation of the cell lysates for 30 minutes on ice, the lysate was centrifuged at 15000 xg for 20 minutes at 4ºC. Bradford assay (Thermoscientific) was performed according to the manufacturer's protocol to quantitate total protein in the lysates. Protein (30 μg) from XP-A, XPAC and BJ-hTERT cells was loaded onto a pre-cast NuPAGE® Novex® 10% Bis-Tris Gels polyacrylamide gel and run using NuPAGE® MOPS SDS running buffer. Proteins were separated by size via gel electrophoresis and then transferred onto a PVDF membrane. The membrane was blocked with 5% non-fat dry milk in 1X PBST (0.5% Tween 20) and then incubated with primary antibody against XPA (FL-273,

Santacruz Biotechnology, 1:200 dilution). Post incubation with horseradish peroxidase-conjugated (HRP) secondary antibodies (1:10000), membranes were washed with 1xPBST and visualized using enhanced chemiluminescent plus (GE Amersham). The membrane was then stripped and reprobed with an antibody against Glyceraldehyde-3-Phosphate Dehydrogenase (GAPDH) (0411, Santa Cruz Biotechnology, 1:200) as a loading control.

3.2.6 **Statistical methods**

Statistical analyses were performed using OriginPro 8 software. One-factor ANOVA along with Holm-Sidak test for comparison of means was used to determine the significance of differences between the three UVC exposure conditions (0, 5 and 10 J/m^2) (Fig. 18). One-factor ANOVA with multiple comparisons of means was used to determine significance of differences between the five repair time-points (0, 6, 12, 24, 48 hours) for CPDs and 6-4 PPs post UVC exposure in XPAC cells (Fig. 19). The statistically significant level was set at $p<0.05$.

3.3 **RESULTS**

3.3.1 **UVC sensitivity of XPAC cells compared to XP-A cells**

Complementation of XP-A cells with functional XPA protein should increase resistance to UVC irradiation [148]. To confirm this, we examined the effect of UVC irradiation on

long term cell proliferation and survival in XPAC cells. Following UVC exposures and 6 h recovery, cells were sub-cultured and recovered for seven days and then counted. We observed that the XPA complemented XPAC cells were less sensitive to the UVC exposure, compared to the isogenic NER deficient XP-A cells (Fig. 17A) (XP-A data from Chapter 2 is shown here again for comparison with XPAC).

Next we examined cell proliferation in XPAC cells shortly after 10 J/m^2 UVC exposure to ensure that any decrease in photoproducts during the repair time points was not due to dilution through cell division. UVC exposed XPAC cells, unlike untreated XPAC cells, failed to double even after 72 hours recovery (Fig. 17B). No obvious difference in UVC-induced inhibition of cell proliferation, or reductions in cell counts, was detected between the XPAC and XP-A cells in this short term proliferation assay (Fig. 17B)(XP-A data from Chapter 2 shown for comparison). We performed cell viability assays using trypan blue exclusion staining, and consistent with results obtained for BJ-TERT and XP-A cells (see Chapter 2), we observed that about 95% of the XPAC cells collected via trypsinization for subsequent repair analysis failed to stain with trypan blue dye and were thus, viable (Fig. 17C). These results confirm that genomic DNA repair assays were conducted on viable XPAC cells, and that any observed reductions in photoproducts were not due to cell division.

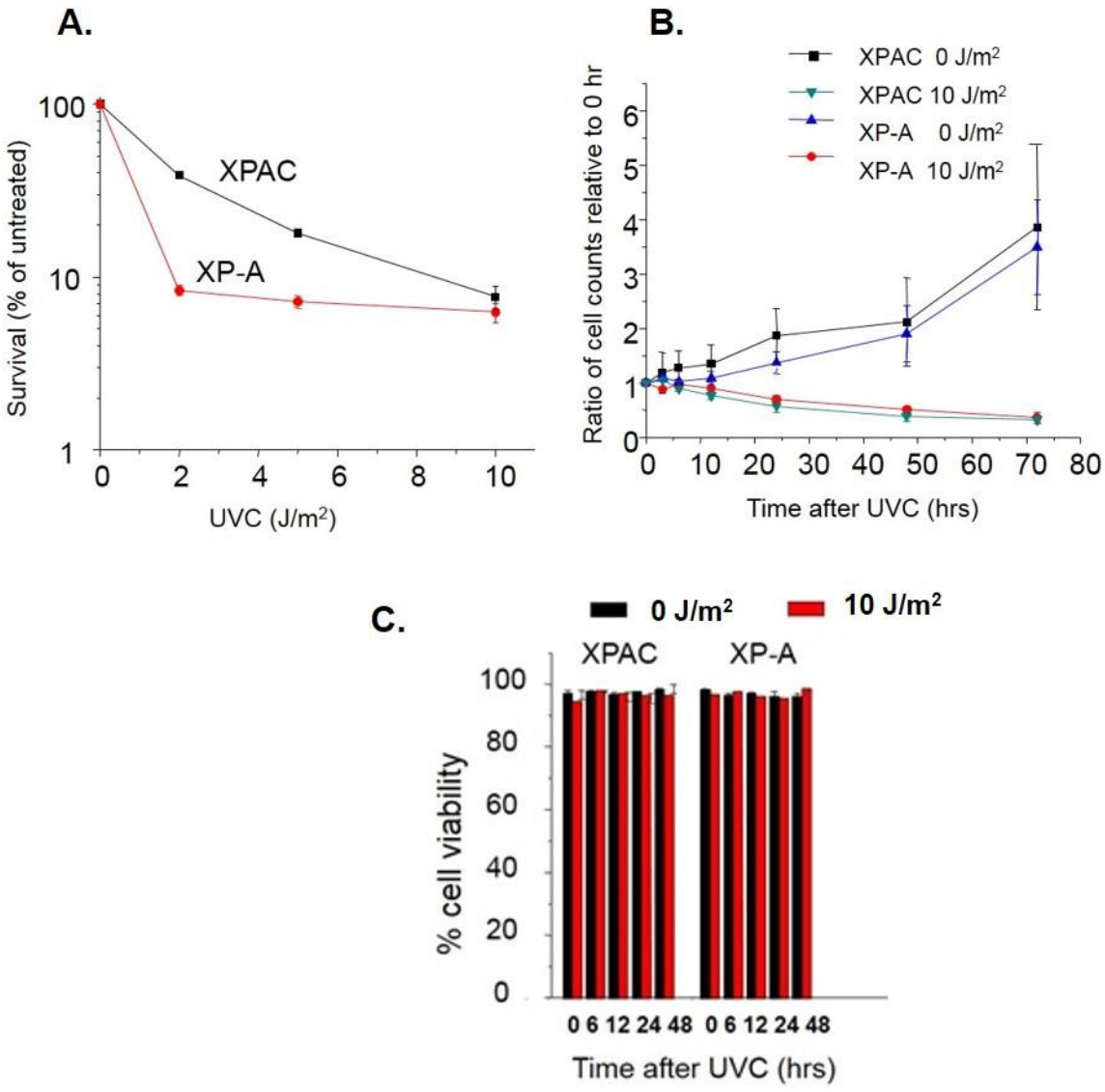

(A) Cells were exposed to 0, 2, 5 or 10 J/m^2 UVC, sub-cultured and counted after seven days. Survival was calculated as the percent of untreated and plotted against UVC dose. Values and error bars are means and SE from three independent experiments. (B) Cells were exposed to 10 J/m^2 UVC and counted at various recovery times. Cell counts were normalized to 0 h and plotted against recovery time. Values and error bars are means and SE from three independent experiments. (C) Cells were exposed to 10 J/m^2 UVC, incubated in fresh media, washed and then harvested after each recovery time point by trypsinization. Cells were counted manually on a hemocytometer for total cells and trypan blue positive dead cells. Values are mean and SE from three independent experiments.

Figure 17: UVC induces sensitivity and inhibits proliferation of XPAC cells

3.3.2 **UVC causes an increase in telomere aberrations in XP-A and XPAC cells**

A previous study by Brash and Rochette [86] showed that chronic UVB exposure does not induce reductions in average telomere lengths. However, UV photoproducts might not form in every telomere and UV exposure may affect individual telomeres without causing detectable alterations in mean telomere lengths. Since unrepaired photoproducts are capable of creating replication blocks [149], we expected that replication stress associated telomeric defects would result in the absence of photoproduct removal by NER.

To determine if UVC is able to cause telomeric defects in cells proficient and deficient in NER as well as to determine if NER proficiency in cells protects telomeres from forming aberrations, we performed the Telo-FISH assay as described in Materials and methods in isogenic cell lines XP-A and XPAC. Briefly, we exposed XP-A and XPAC cells to 0, 5 or 10 J/m^2 UVC, allowed recovery for 6 hours, and treated the cells with colcemid which inhibits spindle fiber formation and arrests cells in metaphase. We then visualized telomeres at chromosome ends via *in situ* hybridization using a fluorescent PNA probe that binds specifically to telomeres. 30 metaphase spreads were analyzed for each treatment and Z stack images were acquired. The Z stack images represent a series of eight 0.25 μm slices acquired at different focal planes to ensure that a missing telomere is not just out of focus. Telomere losses manifest as signal free ends (SFEs) that lack PNA staining at the termini of one or both chromatids, telomere doublets (TDs) represent more than one telomeric PNA signal at a chromatid end, and sister telomere fusions (STFs) appear as a single fused PNA signal at two adjacent sister chromatid telomeres.

We mainly scored for telomere doublets (TDs) and telomere loss or signal free ends (SFEs) since telomere fusions (STFs) were found to be very rare. The number and type of aberrations for both cell lines were plotted against UVC dose and statistical analysis performed to test for significant differences between the three treatments using one way ANOVA and Holm-Sidak test (OriginPro 8). If NER activity at telomeres is required for preserving damage telomeres, we predicted that XPAC cells should be NER proficient and have a lower amount of telomere aberrations compared to NER deficient XP-A cells.

We made five important observations following our analyses (see Fig. 18). First, we observed that background SFEs in untreated cells for both cell lines was high. Second, UVC exposure increased the number of telomere aberrations in both cell lines in a dose dependent manner with 10 J/m^2 causing the highest number of telomere defects overall. Third, there was a greater induction of SFEs compared to TDs in both the cell lines for most cases. Fourth, there was a two-fold increase in SFEs in both the cell lines treated at 10 J/m^2 UVC compared to corresponding untreated cells. This difference was found to be statistically significant, as was the difference between SFEs in untreated and 5 J/m^2 UVC treated cells for both XP-A and XPAC cell lines. Finally, the induction of SFEs and TDs for both 5 J/m^2 and 10 J/m^2 UVC treatments was similar that between the XP-A and XPAC cell lines. However, the difference between TDs after 10 J/m^2 compared to untreated was only statistically significant for the XP-A cell line. Thus, contrary to our original expectation, we failed to observe differences in number of UVC-induced telomere aberrations between XP-A and XPAC cell lines. In summary, we observed that

the incidence of UVC-induced telomere aberrations was not lower in XPA complement XPAC cell line, compared to NER deficient XP-A cells.

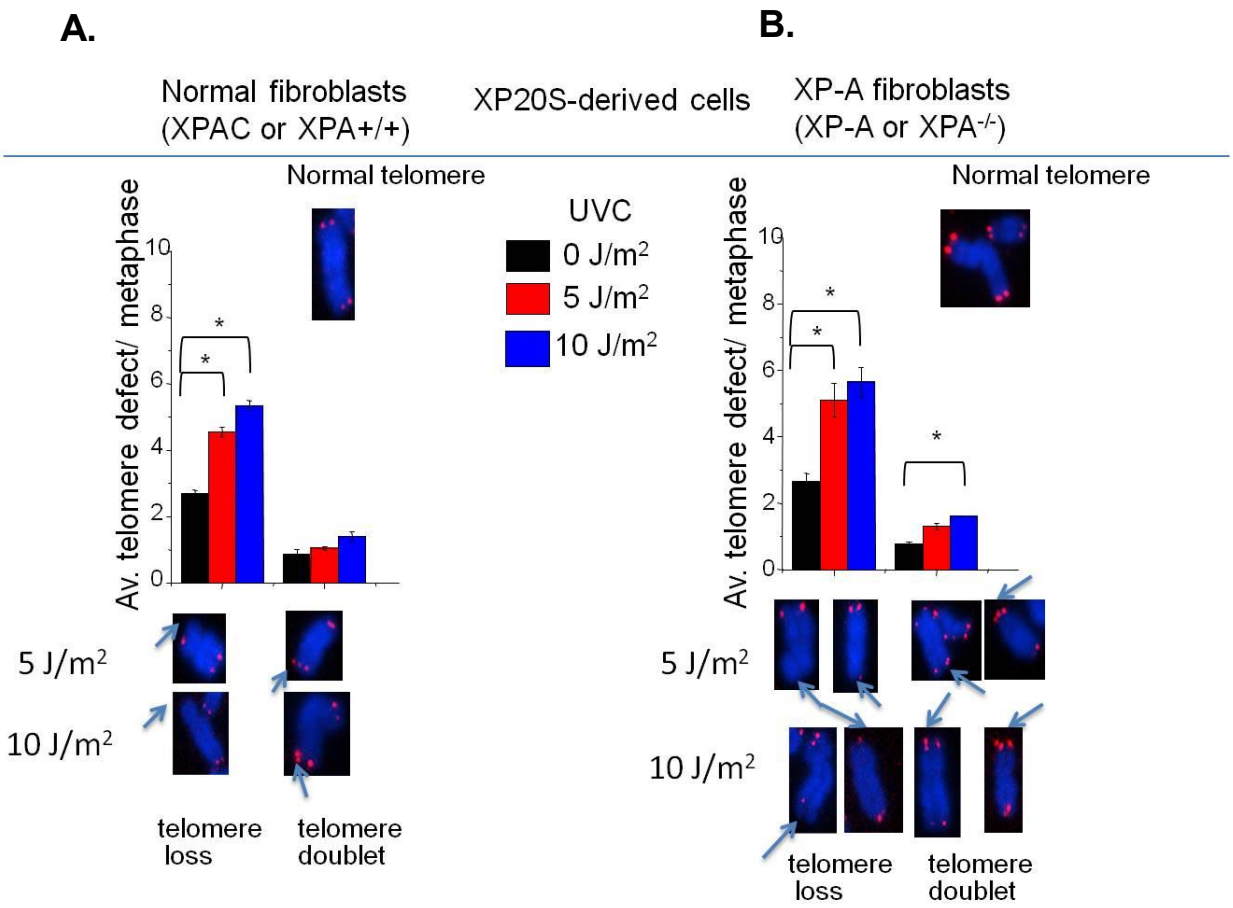

Courtesy: Laura Congelio and Connor Murphy.
Statistical analysis: Dhvani Parikh

Telomere aberrations were enumerated as telomere loss (signal free ends) or telomere doublets (fragile telomeres). (A) (Left) Representative images of telomere FISH of untreated (normal) and treated XPAC cells (5 J/m^2 or 10 J/m^2 UVC) (B) (Right) Representative images of telomere FISH of untreated (normal) and treated XP-A cells (5 J/m^2 or 10 J/m^2 UVC). Z-stacked images (0.25 µm steps) were acquired for each metaphase and analyzed. Average telomere defect per metaphase after 0, 5 or 10 J/m^2 UVC irradiation and 6 h recovery for both cell lines was plotted. Blue arrows indicate either telomere losses (signal free ends) or telomere doublets (multiple telomere signals per chromosome). Results are from 30 metaphases for each UV treatment in each cell line. The data represent mean ± SE from two individual experiments. Bars with * are significantly different ($p<0.05$, one-factor ANOVA, OriginPro 8 software).

Figure 18: UVC induces telomere aberrations in XPAC and XP-A cells

3.3.3 **CPDs and 6-4 PPs are poorly removed from genomic DNA of XPAC cells**

We next wanted to test if the XPAC cells are proficient for NER. The reason for this was that although we did not observe a difference in UV-induced telomere aberrations between XPAC and XP-A cells, we did observe a difference in survival after UVC exposure between the two cell lines (see section 3.3.1) (Fig. 17A). Furthermore, previous studies provided evidence that the XPAC cells express an adequate amount of XPA to perform repair [133]. Moreover our repair assays were standardized to detect reliably a lack of repair. Therefore, we performed repair assays on genomic DNA isolated from XPAC cells exposed to 10 J/m^2 UVC using the immune spot blot assay as previously described for BJ-hTERT and XP-A cells in Chapter 2. We also performed Alu probing to confirm equal genomic DNA loading for all samples.

We observed slow genomic CPD and 6-4 PP removal in XPAC cells when post UVC exposure of 10 J/m^2 (Fig. 19). This was quantified as 20% CPD repair and 50% 6-4 PP repair after 48 hours of UVC recovery. This was in stark contrast with our results for BJ-hTERT cells which show 70% genomic CPD repair by 48 hours and nearly complete removal of genomic 6-4 PPs by 3 hours post UVC (see Chapter 2, section 2.5.2). XPAC cells also showed 5% genomic CPD repair and 30% genomic 6-4 PP repair by 12 hours post UVC (Fig. 19). We also observed that XP-A cells to exhibit lack removal of genomic 6-4 PPs by 12 hours (see section 2.5.3). Therefore, XPAC cells removed UV photoproducts faster than XP-A cells, but much slower than immortalized BJ-hTERT cells. This indicates that XPAC cells are proficient for NER but the repair rates are abnormally slow.

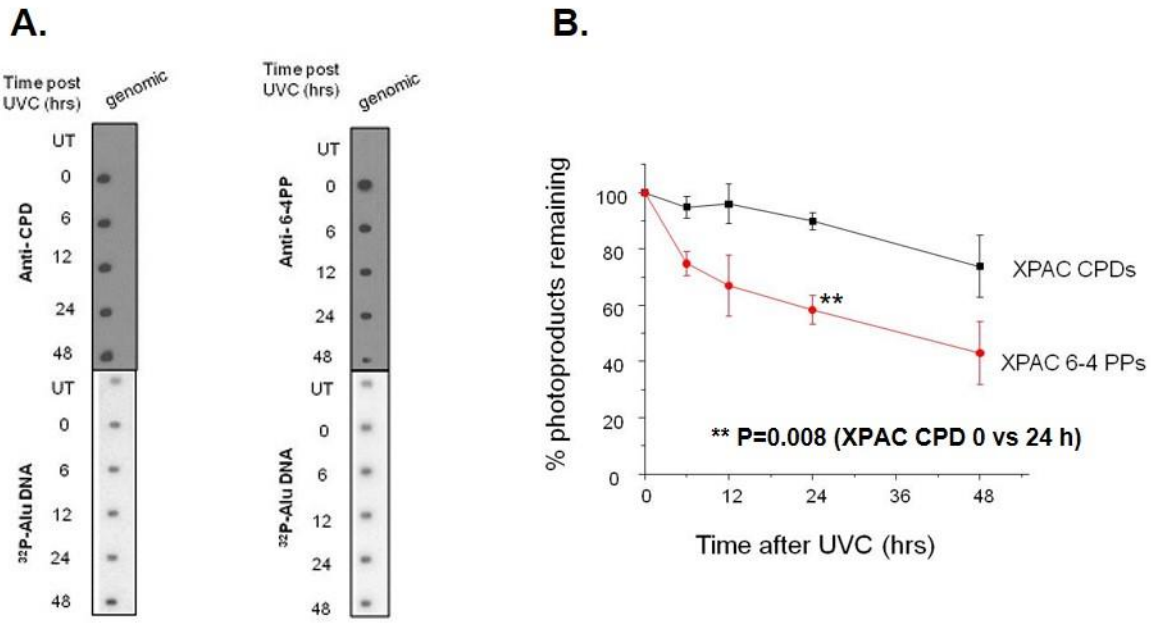

6-4 PP experiment courtesy: Elise Fouquerel

(A) Cells were untreated or exposed to 10 J/m^2 UVC followed by harvesting at various times (0-48 h). Genomic DNA for all repair time points was isolated and loaded in triplicate (7.5 ng). The blots were sequentially probed with a CPD antibody or 6-4 PP antibody as indicated, and then a radiolabeled Alu repeat DNA probe. (B) The CPD or 6-4 PP signal intensity was quantitated, normalized to 0 hour and plotted against recovery time in the graph (right). Values are means and SE from two independent experiments. P-values are derived from one-factor ANOVA (see statistical analysis in methods). The difference between 6-4 PPs at 0 hour and 24 hour in XPAC cells is statistically significant (**p = 0.008).

Figure 19: Quantification of CPD and 6-4 PP formation and removal in genomic DNA from UVC exposed XPAC cells

3.3.4 **XPAC cells express abnormally high levels of XPA protein**

Since XPAC cells did not exhibit a difference in telomere aberrations and showed unusually slow repair of genomic DNA photoproducts by 48 hours (Figs. 18 and 19), western blotting analysis was performed to examine the level of XPA protein in the XPAC cell line compared to the BJ-hTERT and XP-A cell lines (Fig. 20). Protein lysates from each cell line were resolved by SDS-PAGE and then transferred to a membrane which was probed with an XPA antibody. The membrane was then stripped and tested for loading with the constitutively expressed protein glyceraldehyde-3-phosphate dehydrogenase (GAPDH). We observed that the XPA protein levels appear to be several fold higher in XPAC cells compared to BJ-hTERT cells (Fig. 20). We did not detect XPA protein in the XP-A cells.

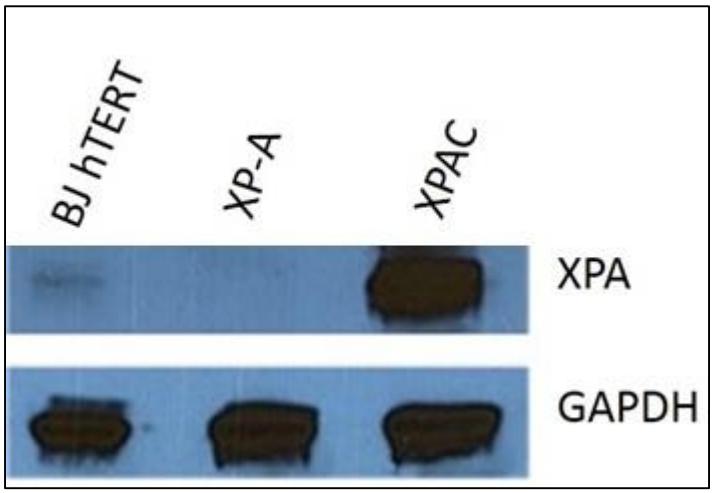

Courtesy: Melinda Sager & Connor Murphy

XPA protein were analyzed in three cell lines for comparison: BJ-hTERT, XP-A and XPAC. Membranes were first probed with rabbit polyclonal XPA antibody and then stripped and re-probed with mouse monoclonal anti-GAPDH antibody for a loading control.

Figure 20: Western blotting analysis of BJ-hTERT, XP-A and XPAC cells for the presence of XPA protein

3.3.5 **Discussion**

In this study we set out to determine whether NER protects against UVC-induced telomere aberrations by comparing isogenic cells lines that differed in XPA protein expression, and thus, NER proficiency. However, during the course of our study we discovered the surprising result that the XPA proficient cell lines exhibited abnormally slow NER.

A previous study by Levy *et al*. in 1995 utilized the identical cell lines as in our study, XPA deficient (XP2OS or XP-A) and XPA complemented (XP2OS-pCAH19WS or XPAC) [133], to compare relative repair capacities post UVC damage in the two cell lines. For this, they transfected UVC damaged plasmids into the XP-A and XPAC cell lines, and after three days they observed that the XPAC cells showed improved transcriptional activity via enhanced expression of the plasmid reporter gene chloramphenicol acetyl transferase (CAT) [133] compared to XP-A cells. UV-induced photoproducts block CAT transcription and successful expression of the CAT gene requires removal of these UV photoproducts from the UV damaged plasmid. Removal of UV photoproducts would require a functional NER pathway with adequate XPA expression and thus, XPAC cells replete with XPA should be able to perform NER and thus lead to the CAT transcription. The observation that XPAC cells had a 100-fold higher CAT expression compared to XP-A cells led to the conclusion by the authors that the XPAC cells were repairing the UVC damaged plasmid [133]. Furthermore, plasmids that were exposed to UVC (200 to 1000 J/m^2) and transfected into XP-A and XPAC, were poorly recovered from XP-A cells following two days of replication, compared to the XPAC cells [133]. Expression of XPA

in XPAC cells restored recovery of plasmid to up to 9% of the untreated control. The XP-A cells in comparison showed only 0.01% plasmid recovery [133]. These represent indirect methods for assessing repair capacity, but support the conclusion that the XPAC cells are NER proficient.

Our results agree with previous studies that the XPAC cells are NER proficient, but our results revealed abnormal rates of repair, while repair rates were not measured directly in the previous report. In our studies we utilized a direct immuno-spot blot based assay to quantitate repair of CPDs and 6-4 PPs in genomic DNA of cells exposed to UVC as a function of time (see section 3.2.4). We observed that while XPAC cells were able to repair CPDs and 6-4 PPs, this rate of repair was lower than BJ-hTERT cells expressing wild type XPA protein (see Fig. 19 and Fig. 8, genomic DNA). Importantly, XPAC cells were able to remove CPDs and 6-4 PPs in genomic DNA as opposed to XP-A cells that lacked CPD and 6-4 PP repair (see Fig. 12, genomic DNA and Fig. 19). Furthermore, we observed that XPAC cells showed a 40% survival after 2 J/m^2 UVC and 20% survival after 5 J/m^2 UVC exposure as opposed to a rapid survival decline to 10% for XP-A cells for the same UVC doses (Fig. 17A). Based on these observations, it is reasonable to attribute the observed resistance of XPAC cells compared to XP-A, cells to the presence of XPA protein and NER activity.

There could be a variety of reasons that the XPAC cells in our studies showed reduced rates of repair compared to the BJ-hTERT cells. We ruled the possibility that the XPAC cells were obtained lost XPA protein expression. In western blotting experiments we

confirmed that the XPAC cells retained XPA expression, whereas the XP-A cells lacked XPA expression. However, these experiments revealed that the XPAC cells possess much higher amounts of XPA protein as compared to wild type BJ-hTERT cells (Fig. 20). Thus, it is possible that excessive XPA protein expressed in the XPAC cells may be inhibiting the cellular NER mechanism by binding to and sequestering other repair factors downstream in the NER pathway. Since the XPAC cells are NER proficient, but just show slower repair, it is possible that sufficient repair of UV-damaged plasmids occurred in the two and three day time period for the plasmid transcription and replication assays to reach near normal levels of CAT transcription and plasmid recovery [133]. This may explain why Levy and colleagues did not detect a deficiency in repair capacity in the XPAC cells using these indirect assays [133]. Alternatively, it is also possible that XPAC gene may have undergone mutation in the cell line we obtained, leading to production of a non-functional XPA protein in the XPAC cells, perhaps due to reversion to the original XP-A cell line. Studies on various XPA complemented cell lines have reported a high frequency of reversion ($5x10^{-5}$) to the UV sensitivity phenotype of XP-A cell lines [150]. Re-sequencing analysis can be performed on XPAC cells to ascertain whether the XPA gene is mutated.

In our Telo-FISH assay for scoring telomere aberrations, we observed that UVC induced a 2-fold increase in telomere losses in the XP-A and XPAC cell lines (Fig. 18). We expected to observe a lower number of UV-induced telomeres aberrations in the XPA expressing cells based on the prediction that the presence of NER would protect telomeres after UV exposure in XPAC cells. However, we did not observe differences

between UV-induced telomere aberrations in XP-A compared to XPAC cells overall. We suspect that this is due to the abnormally slow rate of lesion removal in XPAC cells, such that significant lesions would have remained at the telomeres at the time of harvesting for telomere analysis. Nevertheless, we were able to confirm that UVC exposure is damaging to telomeres in both cell lines. We observed that a UVC dose of 10 J/m^2 in XP-A cells causes telomere losses to increase from 2.5 to 4.5 per metaphase (Fig. 18). These increases are observed in the complemented XPAC cell line as well, and are statistically significant compared to the untreated controls. In summary, we were unable to conclude from the XPAC cell lines we utilized that presence of NER protects telomeres from UVC-induced aberrations.

In order to definitively determine if normal NER activity protects against UV-induced telomere aberrations we will need to repeat this study in isogenic wild type NER proficient and NER deficient cells lines. For this, we propose to generate a cell line derived from wild type BJ-hTERT which are stably deficient in XPA protein by using small hairpin RNAs that specifically silence XPA expression (i.e. stable knockdown). We will perform western blotting to confirm that the XPA protein is indeed greatly reduced in the XPA knock down cell line, and that this leads to increased cellular sensitivity to UVC exposure. If this is the case, then we expect that these cells would be deficient in NER capacity and consequently would show persistence of UV photoproducts at genomic and telomeric DNA during recovery time points in our immune-spot blot repair assay, indicating a lack of repair. This pair of cell lines would be appropriate for addressing the question of

whether wild type NER activity reduces the levels of UVC-induced telomere losses and fragile telomeres, compared to NER deficient cells.

4 FINAL DISCUSSION

4.1 SUMMARY OF FINDINGS

Genomic stability is as important a life process for cellular survival as is metabolism. Since DNA damage from environmental and endogenous sources is inevitable, subsequent repair and restoration to undamaged DNA is essential. Prior to our study, it was known that ubiquitous ultraviolet (UV) light exposure generates the mutagenic DNA photoproduct CPD at telomeres [86, 87], but it was unknown if UV also generates 6-4 PPs at telomeres and if the photoproducts are repaired at telomeres by the NER pathway. The purpose of this research was to investigate specifically if CPDs and 6-4 PPs form at telomeres and if NER removes UV damage at telomeres (see section 1.3). We observed repair of UV-induced photoproducts from telomeres in the NER proficient cell lines BJ-hTERT and U2OS, and we failed to observe telomere repair in the NER deficient cell line XP-A (see section 2.5.2. and section 2.5.3). The importance of these findings was underscored by our discovery that a CPD lesion disrupted TRF1 binding to telomeric DNA *in vitro*, suggesting that UV photoproducts could disrupt shelterin integrity (see section 2.5.4).

A previous study that measured telomeric CPD repair utilized an iPod (immunoprecipitation of damaged DNA) assay which is a polymerase chain reaction (PCR) based assay [86]. Briefly, primary lung fibroblasts were exposed to 10 J/m^2 UVC or primary skin fibroblasts were exposed to 20 J/m^2 UVC. Genomic DNA was isolated,

sonicated and denatured, and the resulting ssDNA fragments containing CPDs were immunoprecipitated using an anti-CPD antibody [86]. The underlying principle of the assay was that the amount of UV-induced CPD damage within the cellular DNA should be proportional to the amount of DNA fragments immunoprecipitated using the CPD antibody. Finally, the DNA in the immunoprecipitated (IP'ed) fractions was amplified via quantitative PCR using primers specific for telomeric DNA, certain genes, or mitochondria DNA [86]. The resulting amplified products were visualized on an agarose gel and the signal intensities were quantified. The authors observed that the amount of amplified CPD-contained telomeric fractions from cells exposed to UVC did not vary with different recovery times from 0-48 hours [86]. However, the amount of amplified genomic *p53* and 28S gene fractions decreased after 24 and 48 hours of repair time. The authors concluded that the decrease in IP'ed fraction was due to cellular CPD repair in the *p53* and 28S genes [86]. Additionally, they concluded that the observed lack of change in the amount of telomeric IP'ed fractions over 48 hours of repair time was because telomeres were refractory to CPD repair. Their data implied that the amount of CPDs in all telomeric fractions isolated at different times remained the same. Thus, the study concluded that telomeres are refractory to CPD repair as opposed to our experiments that showed telomeric repair of both CPDs and 6-4 PPs by 48 hours [86].

Multiple reasons may account for the discrepant results that we observed compared to results obtained by Rochette and Brash regarding telomeric repair. One potential explanation relates to the ability of telomeric DNA to form secondary structure. Both the damaged and undamaged DNA would have become single stranded in solution due to the denaturation step in the iPoD assay. The resulting ssDNA can form secondary

structures such as G quadruplexes in the G-rich repeats and i-Motif structures in the C-rich repeats [151]. Since CPDs cause a distortion in the DNA, it is possible that the secondary structures in undamaged DNA, which also distort DNA, were recognized non-specifically by the CPD antibodies. This might explain why the authors obtained a relatively high telomeric signal intensity from untreated cells in the IP'd DNA, compared to the largely undetectable signals for the *p53* and 28S genes recovered from untreated controls. Alternatively, the CPD antibodies may not be able to access and bind to the CPDs in telomeric ssDNA fragments that were folded into secondary structure. Thus, it is possible that the CPD antibodies bound nonspecifically to secondary structures of undamaged DNA while failing to access the photoproducts within the damaged folded DNA, which would interfere with accurate quantification of CPD containing telomeric DNA [86]. Furthermore, a small portion of the damaged telomeric DNA that did not fold into secondary structures may have been accessible to the CPD antibodies and subsequently amplified via qPCR. Thus, it is possible that while the majority of the telomeres were being repaired in the cells, this small unrepaired fraction of the total telomeres was detected by the sensitive PCR assay but was beyond the limit of detection in our telomeric immuno-spot blot assay. We circumvented the problem of potential secondary structure formation in telomeric DNA in our assay, by denaturing telomeres in the nylon membrane and then fixing the telomeric DNA onto the membrane by baking at 80°C prior to immunoblotting.

Another important difference between our study and that conducted by Rochette and Brash is the choice of cell lines used. The primary fibroblasts used by Rochette and

Brash lack mechanisms to maintain telomere lengths. It is possible that the telomeric photoproduct removal that we observed in BJ-hTERT cells and U2OS cells may involve the telomere length maintenance mechanisms operating in these cells. BJ-hTERT cells express telomerase to maintain their telomeres while U2OS cells lack telomerase, but rather use the recombination-based alternative lengthening of telomeres (ALT) pathways to maintain telomeres. It is possible that telomeres undergoing length maintenance mechanisms are more accessible to repair proteins and perhaps ALT in U2OS cells might account for the slower rate of telomeric repair in U2OS cells than that observed for BJ-hTERT cells (see sections 2.5.3 and 2.5.3). This hypothesis is debatable because Kruk *et al.* reported in 1995 using telomere restriction fragment (TRF) analysis, that telomeric CPDs in normal primary fibroblasts (GM 38A, Coriell Cell Repository) are repaired at a rate similar to the CPD repair rate of non-transcribing genes [87]. The telomeric repair observed in these primary skin fibroblasts lacking telomere maintenance mechanisms would have occurred independently of ALT or telomerase. In order to determine whether telomeric photoproduct repair is indeed enabled or enhanced by telomere maintenance mechanisms, it would be necessary to measure both telomeric CPD and telomeric 6-4 PP repair rates in primary cells exposed to UVC using our direct telomeric immuno-blot assay.

Cell lines from different tissues of origin may possess differences in telomeric repair capacities [152]. Interestingly, the study that concluded that telomeres lacked CPD repair [86] was performed in two different cell lines; a fibroblast cell line derived from lung tissue and exposed to 10 J/m^2 UVC and a skin fibroblast cell line derived from breast tissue

and exposed to 20 J/m^2 UVC. In contrast, our studies that support telomeric photoproduct repair were performed in a foreskin tissue derived fibroblast cell line 10 J/m^2 UVC. Comparison between the cell lines of similar tissue origin (skin fibroblasts) is difficult because the dose of UVC that was used to create damage was different. The higher dose of UVC used in the Rochette and Brash study (20 J/m^2 instead of 10 J/m^2) [86] may have caused a higher level of telomeric photoproducts. Perhaps at this higher level of damage, a fraction of telomeres may remain unrepaired at 48 hours. Thus, differences in both cell types and UVC dose may have contributed to differences in results from the study that concluded telomeres are refractory to repair [48] compared to our study in which we observed telomere repair. It would be valuable to compare telomeric repair rates using our direct telomeric immuno-blot assay in lung and skin primary fibroblasts both exposed to a minimally lethal dose of 10 J/m^2 UVC.

4.2 **LIMITATIONS OF THE ASSAY**

A major limitation of our telomeric immune-spot blot assay is the requirement for copious amounts of purified genomic DNA as starting material. About 20x10^6 cells grown in eleven 100 mm dishes are needed to yield at least 100 ug of genomic DNA from which we obtained an average yield of 10-11 ng pure telomeric DNA for each repair time point. However, a significant advantage of our standardized assay is its inherent capability to *directly* identify and quantify varied types of telomeric damage such as oxidative base damage using sensitive antibodies that identify oxidative lesions such as 8-oxoguanines.

Also, environmental toxic bulky polycyclic aromatic hydrocarbon adducts and anti-tumor agent cisplatin adducts form in DNA but it is unknown if they occur at telomeres *in vivo* and if they are repaired. Our repair assay would thus be helpful in directly determining their formation and rate of removal using existing damage specific antibodies (Trevigen Anti-BPDE antibody for PAH adducts, Abcam Anti-Cisplatin modified DNA antibody for cisplatin adducts are currently available).

4.3 **FUTURE DIRECTIONS**

Of the six shelterin proteins, TRF1, TRF2 and POT1 directly bind to telomeric DNA while TPP1, TIN2 and RAP1 interact with those proteins, as opposed to binding DNA [7]. TRF1 and TRF2 share a common TRFH domain and a C-terminal Myb domain that binds double stranded telomeric DNA, while POT1 binds to single stranded DNA through its N terminal OB folds [7]. It is possible that the binding inhibition we observed for TRF1 in the presence of a CPD lesion is limited to TRF1 alone and does not extend to other shelterin proteins. Therefore, it would be valuable to test TRF2 and POT1 binding as well to telomeric DNA substrates harboring a CPD lesion. We predict that CPD lesions will similarly inhibit TRF2 binding to dsDNA and POT1 binding to ssDNA in telomeres.

To test the effect of CPD lesions on TRF1 and TRF2 binding to DNA *in vivo*, chromatin immunoprecipitation (ChIP) assays can be utilized. We expect that the yield of lesions in telomeres following an acute dose of UVC would be insufficient to displace a detectable amount of TRF1 or TRF2 proteins. To circumvent this problem we would use plasmids

containing six telomeric repeats, as described previously [153], with defined lesions. Briefly, we would first transfect plasmids containing telomeric repeats into cells. These plasmids would be constructed using an oligonucleotide with a pre-synthesized site specific CPD lesion incorporated into the telomeric repeats [154]. As a control, plasmids constructed with templates lacking DNA lesions would be used. Post transfection of these plasmids into cells, TRF1 and TRF2 shelterin proteins inside the cells should bind to the telomeric repeats in these plasmids, as observed previously for other plasmids harboring telomeric repeats [155]. Next, we will test if the presence of CPD lesions within the telomeric repeats of the plasmids will affect TRF1 and TRF2 binding to the telomeric sequences. For this, we will perform ChIP using antibodies against TRF1 and TRF2 to immunoprecipitate (IP) cross-linked telomeric DNA-protein complexes. Sonication of cross-linked telomeric DNA-protein complexes prior to immunoprecipitation will create smaller sized fragments of plasmid DNA bound to TRF1/TRF2. After reverse cross linking of these complexes to remove associated TRF1/TRF2 proteins the telomeric DNA fragments can be identified and amplified via quantitative PCR. The qPCR assay would use primers that are complementary to the plasmid sequences flanking the telomeric DNA on both sides. Therefore, only the telomeric repeats from the plasmid would be amplified and not the telomeric sequences at the chromosome ends. If CPD lesions indeed inhibited TRF1/TRF2 binding to telomeric DNA in cells, then we expect to recover lower yields of telomeric DNA in the TRF1/TRF2 immunoprecipated fractions from cells transfected with CPD contained plasmids, compared to non-lesion containing plasmids. Our observation that telomeric CPD repair was more rapid that CPD repair in the bulk genome raises the possibility that telomeric CPD repair was achieved by transcription

coupled repair (TCR). This is because the bulk of the genome is repaired by global genome repair, which is slower than TCR. The TCR pathway at telomeres is plausible because telomeres are actively transcribed into TERRA via action of transcription protein RNA polymerase II [85]. As described earlier, Cockayne syndrome A (CSA) and Cockayne syndrome B (CSB) are key proteins involved in TCR at the initial lesion recognition step in the pathway [156]. It is possible that disruption of these proteins may affect the repair rate we observe in telomeres. To test for this possibility, we will use a lentiviral system to generate stable knockdown of CSA or CSB protein levels in BJ-hTERT cells via expression of small hairpin RNAs (shRNA) that target the CSA or CSB transcripts, respectively [157]. The shRNA will suppress expression of CSA or CSB, and cells expressing the antibiotic resistance gene in the vector will be selected by growth in media containing antibiotic. Since shRNAs can sometimes bind to and silence un-intended transcripts or mRNA, causing off-target effects, four-five shRNAs having slightly different sequences will be tested instead of a single shRNA. Western blotting will be performed to confirm decrease protein levels of CSA/CSB in cells expressing the shRNAs. We will then expose these TCR deficient and the corresponding control cells to UVC, and perform the telomere repair assays as we described previously, to observe if there is a difference in the telomeric CPD repair rate in TCR deficient compared to TCR proficient cells (see section 2.5.2). Similar to CSA/CSB knockdown cell lines, we can also generate an XPC knockdown cell line via shRNAs against the XPC protein in BJ-hTERT cells. XPC is required for global genome NER, but not for TCR [158]. This XPC knockdown cell line will serve as a negative control for telomeric TCR.

In summary, we expect to obtain the following results upon performing the telomeric repair experiments in TCR and GGR deficient cell lines. If TCR is functional at telomeres, we expect to observe a decrease in repair rates of telomeric CPDs in CSA/CSB deficient cell lines compared to CSA/CSB proficient cell lines exposed to UVC (see section 2.5.2). Conversely, if telomeres are repaired by TCR, and not GGR, then we do not expect to observe a difference in telomeric repair rates between XPC proficient and XPC deficient cell lines exposed to UVC.

To confirm the lack of telomeric repair we observed in XP-A cells, an isogenic cell line to BJ-hTERT which lacks NER can be utilized. This BJ-hTERT XPA knockdown cell line can be generated by using shRNAs against XPA protein in BJ-hTERT cells similar to the CSA/CSB knockdown cells lines mentioned above. Telomeric repair experiments performed in these cells will allow for direct comparison between BJ-hTERT NER deficient and BJ-hTERT NER proficient cells. We expect that the BJ-hTERT XPA knockdown cells will show a lack of telomeric repair similar to what we observed in XP-A cells (see section 2.5.3).

The presence of NER at telomeres indicates that bulky lesions within shelterin coated telomeric DNA are accessible to NER proteins, suggesting that a dynamic interplay may occur between shelterin and NER proteins during repair. To test if shelterin proteins might modulate removal of CPD lesions on telomeric and non-telomeric substrates, we can perform *in vitro* NER assays using cell extracts in presence or absence of shelterin. For this, we will construct double stranded plasmids with telomeric and non-telomeric

sequences and place site-specific CPD lesion within the sequences using established protocols [159]. Naked substrates or substrates pre-coated with shelterin proteins will be incubated with cell extracts containing all the NER factors required for successful removal of the lesion. The excised lesions containing fragments released in the course of NER reactions can be visualized using radioactive end labeling, analyzed by denaturing gel electrophoresis and quantitated by phosphorimager scanning. If shelterin interaction with NER proteins promotes lesion removal at telomeres, then we expect to observe higher amounts of NER excision products for shelterin coated substrates than for naked substrates.

4.4 **BIOLOGICAL IMPLICATIONS**

Since NER is functional at telomeres, removal of photoproducts at telomeres is important for genome integrity. Accumulation of UV photoproducts has the potential to cause replication stress at telomeres, telomere shortening and telomere defects. Particularly, critically short telomeres can induce persistent DNA damage responses at telomeres which can trigger cell death or senescence in presence of tumor suppressor gene *p53* [19]. Pre-malignant cells lacking functional *p53* and with short dysfunctional telomeres can override senescence causing genomic instability, which is a hallmark for cancer [23, 160]. Unrepaired photoproducts at telomeres therefore, have the potential to drive senescence or cancer by causing telomere dysfunction in cells. In individuals whose skin may be chronically exposed to UV in sunlight, telomeric photoproducts can either be repaired or accumulate over time. NER capacities can differ among different individuals

[152] and in individuals with a lower telomeric NER capacity to remove UV photoproducts, an accumulation of telomeric photoproducts may cause telomere shortening or telomere dysfunction over a period of time. Short dysfunctional telomeres in turn can lead to accelerated senescence leading to skin aging or in a *p53* deficient background, drive skin cancer. Thus, individuals who have a lower cellular NER capacity may have an increased susceptibility to UV-induced telomere shortening that can lead to UV driven skin aging or skin cancer. Knowledge about telomere repair in organisms can serve as an important biomarker for aging and disease. Levels of telomere repair *in vivo* can inform about mechanisms by which environmental toxicants such as UV in sunlight can function as gerontogens to accelerate skin aging or drive skin cancer [161]. Biomarkers of toxicology for aging and cancer that are not tissue specific (relate to several organs) and have a causal role in promoting aging or cancer have a need to be defined [161]. Our quantitative telomere repair assay that measures damage accumulation and repair capacities in different cells can serve as a valuable tool to develop biomarkers for decreased telomeric repair capacities in individuals and therefore, serve as an indicator of accelerated aging or pre-cancerous conditions. For example, we would expect that upon induction of UV photoproducts in the skin of individuals prone to accelerated aging or skin cancer, our repair assay would demonstrate persistence of damage at telomeres in cells of these individuals over time that would indicate a compromised DNA repair efficiency. We expect that if telomere lengths are measured from skin nevi biopsies of these individuals, the telomeres might be found to be shortened since cells with low NER capacity would be unable to fully prevent telomere shortening caused due to UV-induced replication stress. Our studies

will thus, aid in development of biomarkers for toxicology in skin photo-aging and skin cancer.

4.5 **STUDY CONCLUSIONS**

Our current study fills an important gap in existing knowledge about UV photoproduct formation and removal at telomeres. We show for the first time that 6-4 PPs are formed at telomeres after UV exposure and removed at rates comparable to bulk genomic DNA repair. Our findings open up a new area in basic science for investigation of the type of nucleotide excision repair pathway that might be active at telomeres. Going further, our study provides novel opportunities to investigate roles of dysfunctional telomeres in driving UV-induced carcinogenesis in a background of NER deficiency such as the xeroderma pigmentosum disorder.

APPENDIX: PRELIMINARY STUDY ON NER AND SHELTERIN INTERACTIONS

SHELTERIN INHIBITS NER PROTEIN XPF-ERCC1 CLEAVAGE OF A STEM LOOP SUBSTRATE

Introduction

XPF-ERCC1 is a structure specific heterodimeric endonuclease that incises 5' to the lesion in order to release the strand containing the bulky damage in the NER pathway (see section 1.2.5). XPF-ERCC1 localizes to telomeres and associates with the telomeric protein complex as shown by immunoprecipitation studies [92]. Previous cellular data indicates that XPF-ERCC1 cleaves the telomeric 3' single strand overhang in the absence of TRF2 protein [92]. Moreover, residues that lie within the active site of XPF nuclease form part of a putative TRF2 docking motif that mediates protein interactions with TRF2 [162]. Transgenic mice that over express TRF2 in the skin exhibit increased susceptibility to UVB induced skin pathologies and cancer, similar to xeroderma pigmentosum, and telomere loss in skin cells, which was mediated by XPF-ERCC1 endonuclease [93]. Thus, there is some evidence for interactions between XPF-ERCC1 and shelterin protein TRF2, although whether TRF2 and XPF-ERCC1 can directly modulate each other's activity has not been tested. To examine this premise we conducted an activity assay for purified XPF-ERCC1 in presence of purified TRF2 protein *in vitro*. We observed a progressive decrease in XPF-ERCC1 activity on a stem loop substrate as a function of increasing TRF2 concentration. Our data provides preliminary

evidence to support the hypothesis that shelterin proteins interact with NER proteins to modulate their activity to preserve telomere integrity.

Materials and Methods

The stem–loop substrate (XPF SL) that was shown to be an optimal substrate for XPF-ERCC1 cleavage was obtained from Orlando Scharer (Stony Brook University School of Medicine). XPF SL is a 46 base pair substrate with the sequence (GCCAGCGCTCGG$(T)_{22}$CCGAGCGCTGGC) containing a "stem" and a " loop" region in its structure. The 22 thymines (T's) form the loop that mimics the bubble structure created around the DNA lesion during bulky lesion repair by the NER pathway. The rest of the 24 bases are paired into the stem structure (see model in Fig. 21). 10 pmol of the XPF SL substrate containing a fluorescent dye Cy5 as the 3' end was annealed in a 200 ul reaction buffer (10 mM Tris pH 8.0, 50 mM NaCl, 1 mM $MgCl_2$) by initial heating at 90^{o}C for 10 minutes and cooling at room temperature for 2 hours, as previously described [163]. Purified recombinant human XPF-ERCC1 was generated from a baculovirus infected Sf9 insect cells using a histidine (His6) tag as previously described by Scharer lab [164] and was generously provided by Orlando Scharer. Recombinant N-terminal His_6-tagged TRF2 was purified using a baculovirus/insect cell expression system and an AKTA Explorer FPLC (GE Healthcare) as described previously [165].
Purified full length human TRF2 (400, 1600, or 3200 fmols) and XPF-ERCC1 heterodimer (400 fmol) were pre-incubated in endonuclease buffer for 5 min at 30^{o}C prior to addition of Cy5 3' end labeled XPF SL substrate (100 fmol) to the reaction mix . The

endonuclease buffer consisted of 25 mM Tris pH 8.0, 40 mM NaCl, 0.5 mM β-mercaptoethanol, 2 mM $MgCl_2$, 0.5 mg/ml BSA and 10% glycerol in 15 μl final reaction volume. The reactions were incubated at 37°C for 30 minutes and stopped via addition of 80% formamide/10 mM EDTA and heating at 95°C for 10 minutes. Reactions were electrophoresed on a 15% 19:1 (bisacrylamide:acrylamide) denaturing gel in 0.5X TBE buffer, visualized on Typhoon 9400 imaging system (Amersham Biosciences) and quantitated by ImageQuant software.

Results

XPF-ERCC1 incises at the 5' side of the stem loop substrate (S) releasing a 9-10 basepair fragment that is represented in the gel as P (product). In our experiments, XPF-ERCC1 exhibited a maximum cleavage of about 15% of the stem loop substrate in the absence of TRF2. This incision activity reduces to below detectable levels in presence of a 4 fold molar ratio of TRF2 homodimer to XPF ERCC1 heterodimer.

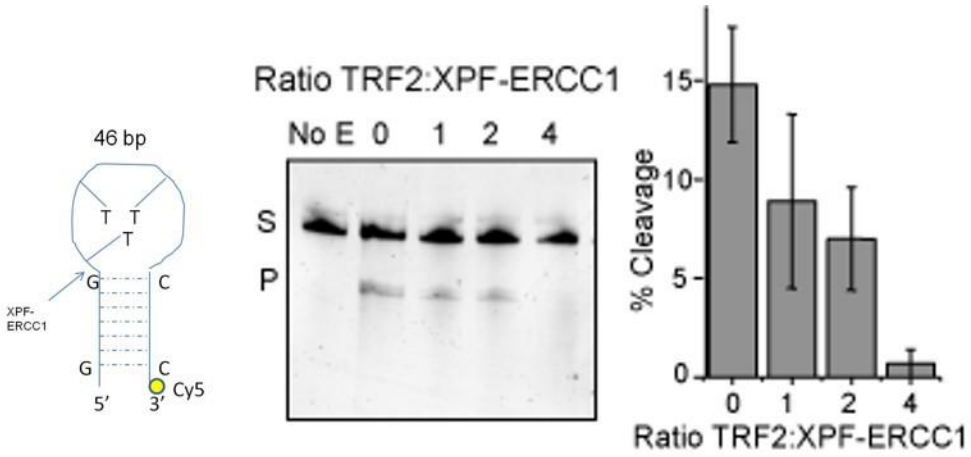

Reactions contained a Cy5-labeled stem-loop substrate and 400 fmol XPF-ERCC1. Number = molar ratio of TRF2 homodimer to XPF-ERCC1 heterodimer. S=substrate and P=product. Reactions were run on 14% denaturing gel. Values and error bars are the mean and SE from 3 independent experiments.

Figure 21: Inhibition of XPF-ERCC1 activity on stem-loop substrate by TRF2

Discussion and conclusion

A previous publication reported that XPF is required for TRF2 mediated telomere shortening and that XPF controls both TRF2 and telomere length as a negative regulator [166]. When wild type XPF was introduced into XPF-deficient cells, TRF2 association with telomeric DNA decreased by 40%. Moreover, XPF when overexpressed in XPF-proficient cells induced telomere shortening [166]. XPF- ERCC1 also was shown to associate with TRF2 at telomeres, and to remove the 3' overhang from uncapped telomeres [92]. Whether the interaction between TRF2 and XPF-ERCC1 is direct, or is mediated by another protein, is not known. This is the first study to provide preliminary evidence for functional interactions between TRF2 and XPF-ERCC1 and its possible effect on the activity of XPF-ERCC1. Using a telomeric substrate to test this interaction might further shed light on the dynamics between NER and shelterin proteins at telomeres, however, it is possible that TRF2 and XPF-ERCC1 may interact directly at sites distal from the telomeres too.

BIBLIOGRAPHY

1. Gall, J.G., *Telomeres*. 1995, Cold Spring Harbor, New York: Cold Spring Harbor Press.
2. Szostak, J.W. and E.H. Blackburn, *Cloning yeast telomeres on linear plasmid vectors.* Cell, 1982. **29**(1): p. 245-55.
3. Olovnikov, A.M., *[Principle of marginotomy in template synthesis of polynucleotides].* Dokl Akad Nauk SSSR, 1971. **201**(6): p. 1496-9.
4. Zakian, V.A., *Telomeres: beginning to understand the end.* Science, 1995. **270**(5242): p. 1601-7.
5. Blackburn, E.H., et al., *Recognition and elongation of telomeres by telomerase.* Genome, 1989. **31**(2): p. 553-60.
6. Greider, C.W. and E.H. Blackburn, *A telomeric sequence in the RNA of Tetrahymena telomerase required for telomere repeat synthesis.* Nature, 1989. **337**(6205): p. 331-7.
7. de Lange, T., *Shelterin: the protein complex that shapes and safeguards human telomeres.* Genes Dev, 2005. **19**(18): p. 2100-10.
8. Griffith, J.D., et al., *Mammalian telomeres end in a large duplex loop.* Cell, 1999. **97**(4): p. 503-14.
9. Palm, W. and T. de Lange, *How shelterin protects mammalian telomeres.* Annu Rev Genet, 2008. **42**: p. 301-34.
10. Doksani, Y., et al., *Super-resolution fluorescence imaging of telomeres reveals TRF2-dependent T-loop formation.* Cell, 2013. **155**(2): p. 345-56.
11. Sfeir, A., et al., *Mammalian telomeres resemble fragile sites and require TRF1 for efficient replication.* Cell, 2009. **138**(1): p. 90-103.
12. Denchi, E.L. and T. de Lange, *Protection of telomeres through independent control of ATM and ATR by TRF2 and POT1.* Nature, 2007. **448**(7157): p. 1068-71.
13. Sfeir, A. and T. de Lange, *Removal of shelterin reveals the telomere end-protection problem.* Science, 2012. **336**(6081): p. 593-7.
14. Bae, N.S. and P. Baumann, *A RAP1/TRF2 complex inhibits nonhomologous end-joining at human telomeric DNA ends.* Mol Cell, 2007. **26**(3): p. 323-34.
15. Wu, L., et al., *Pot1 deficiency initiates DNA damage checkpoint activation and aberrant homologous recombination at telomeres.* Cell, 2006. **126**(1): p. 49-62.
16. Sfeir, A., et al., *Loss of Rap1 induces telomere recombination in the absence of NHEJ or a DNA damage signal.* Science, 2010. **327**(5973): p. 1657-61.
17. van Steensel, B., A. Smogorzewska, and T. de Lange, *TRF2 protects human telomeres from end-to-end fusions.* Cell, 1998. **92**(3): p. 401-13.
18. Nandakumar, J., E.R. Podell, and T.R. Cech, *How telomeric protein POT1 avoids RNA to achieve specificity for single-stranded DNA.* Proc Natl Acad Sci U S A, 2010. **107**(2): p. 651-6.
19. d'Adda di Fagagna, F., et al., *A DNA damage checkpoint response in telomere-initiated senescence.* Nature, 2003. **426**(6963): p. 194-8.

20. Jeyapalan, J.C. and J.M. Sedivy, *Cellular senescence and organismal aging.* Mech Ageing Dev, 2008. **129**(7-8): p. 467-74.
21. Hemann, M.T., et al., *The shortest telomere, not average telomere length, is critical for cell viability and chromosome stability.* Cell, 2001. **107**(1): p. 67-77.
22. Kaul, Z., et al., *Five dysfunctional telomeres predict onset of senescence in human cells.* EMBO Rep, 2012. **13**(1): p. 52-9.
23. Hanahan, D. and R.A. Weinberg, *Hallmarks of cancer: the next generation.* Cell, 2011. **144**(5): p. 646-74.
24. Lopez-Otin, C., et al., *The hallmarks of aging.* Cell, 2013. **153**(6): p. 1194-217.
25. de Lange, T., *Activation of telomerase in a human tumor.* Proc Natl Acad Sci U S A, 1994. **91**(8): p. 2882-5.
26. Cesare, A.J. and R.R. Reddel, *Alternative lengthening of telomeres: models, mechanisms and implications.* Nat Rev Genet, 2010. **11**(5): p. 319-30.
27. De Bont, R. and N. van Larebeke, *Endogenous DNA damage in humans: a review of quantitative data.* Mutagenesis, 2004. **19**(3): p. 169-85.
28. Friedberg, E.C., G.C. Walker, and W. Siede, *DNA repair and mutagenesis*. 1995, Washington, D.C.: ASM Press. xvii, 698 p., 8 p. of plates.
29. International Agency for Research on Cancer., *Exposure to artificial UV radiation and skin cancer : this report represents the views and expert opinions of an IARC working group that met in Lyon, France 27-29 June 2005*. IARC working group reports. 2005, Lyon, France: International Agency for Research on Cancer. p.
30. Thornhill, M.H., *The sun, the ozone layer and the skin: the role of ultraviolet light in lip and skin cancer.* Dent Update, 1993. **20**(6): p. 236-40.
31. Taylor, H.R., et al., *Effect of ultraviolet radiation on cataract formation.* N Engl J Med, 1988. **319**(22): p. 1429-33.
32. Diffey, B.L., *Stratospheric ozone depletion and the risk of non-melanoma skin cancer in a British population.* Phys Med Biol, 1992. **37**(12): p. 2267-79.
33. Besaratinia, A., S.I. Kim, and G.P. Pfeifer, *Rapid repair of UVA-induced oxidized purines and persistence of UVB-induced dipyrimidine lesions determine the mutagenicity of sunlight in mouse cells.* FASEB J, 2008. **22**(7): p. 2379-92.
34. Shibutani, S., M. Takeshita, and A.P. Grollman, *Insertion of specific bases during DNA synthesis past the oxidation-damaged base 8-oxodG.* Nature, 1991. **349**(6308): p. 431-4.
35. Michaels, M.L., et al., *Evidence that MutY and MutM combine to prevent mutations by an oxidatively damaged form of guanine in DNA.* Proc Natl Acad Sci U S A, 1992. **89**(15): p. 7022-5.
36. Matsumoto, Y. and K. Kim, *Excision of deoxyribose phosphate residues by DNA polymerase beta during DNA repair.* Science, 1995. **269**(5224): p. 699-702.
37. Friedberg, E.C. and E.C. Friedberg, *DNA repair and mutagenesis*. 2nd ed. 2006, Washington, D.C.: ASM Press. xxix, 1118 p.
38. Kurz, D.J., et al., *Chronic oxidative stress compromises telomere integrity and accelerates the onset of senescence in human endothelial cells.* J Cell Sci, 2004. **117**(Pt 11): p. 2417-26.
39. Opresko, P.L., et al., *Oxidative damage in telomeric DNA disrupts recognition by TRF1 and TRF2.* Nucleic Acids Res, 2005. **33**(4): p. 1230-9.

40. Wang, Z., et al., *Characterization of oxidative guanine damage and repair in mammalian telomeres.* PLoS Genet, 2010. **6**(5): p. e1000951.
41. Vallabhaneni, H., et al., *Defective repair of oxidative base lesions by the DNA glycosylase Nth1 associates with multiple telomere defects.* PLoS Genet, 2013. **9**(7): p. e1003639.
42. Madlener, S., et al., *Essential role for mammalian apurinic/apyrimidinic (AP) endonuclease Ape1/Ref-1 in telomere maintenance.* Proc Natl Acad Sci U S A, 2013. **110**(44): p. 17844-9.
43. Setlow, R.B., *The photochemistry, photobiology, and repair of polynucleotides.* Prog Nucleic Acid Res Mol Biol, 1968. **8**: p. 257-95.
44. Wacker, A., et al., *ORGANIC PHOTOCHEMISTRY OF NUCLEIC ACIDS*.* Photochemistry and Photobiology, 1964. **3**(4): p. 369-394.
45. Mitchell, D.L., J. Jen, and J.E. Cleaver, *Sequence specificity of cyclobutane pyrimidine dimers in DNA treated with solar (ultraviolet B) radiation.* Nucleic Acids Res, 1992. **20**(2): p. 225-9.
46. Kim, J.K., D. Patel, and B.S. Choi, *Contrasting structural impacts induced by cis-syn cyclobutane dimer and (6-4) adduct in DNA duplex decamers: implication in mutagenesis and repair activity.* Photochem Photobiol, 1995. **62**(1): p. 44-50.
47. Mizukoshi, T., et al., *Structural study of DNA duplexes containing the (6-4) photoproduct by fluorescence resonance energy transfer.* Nucleic Acids Res, 2001. **29**(24): p. 4948-54.
48. Brash, D.E., et al., *Photoproduct frequency is not the major determinant of UV base substitution hot spots or cold spots in human cells.* Proc Natl Acad Sci U S A, 1987. **84**(11): p. 3782-6.
49. Mitchell, D.L. and R.S. Nairn, *The biology of the (6-4) photoproduct.* Photochem Photobiol, 1989. **49**(6): p. 805-19.
50. Perdiz, D., et al., *Distribution and repair of bipyrimidine photoproducts in solar UV-irradiated mammalian cells. Possible role of Dewar photoproducts in solar mutagenesis.* J Biol Chem, 2000. **275**(35): p. 26732-42.
51. Todo, T., *Functional diversity of the DNA photolyase/blue light receptor family.* Mutat Res, 1999. **434**(2): p. 89-97.
52. Lemaire, D.G. and B.P. Ruzsicska, *Kinetic analysis of the deamination reactions of cyclobutane dimers of thymidylyl-3',5'-2'-deoxycytidine and 2'-deoxycytidylyl-3',5'-thymidine.* Biochemistry, 1993. **32**(10): p. 2525-33.
53. Douki, T. and J. Cadet, *Formation of cyclobutane dimers and (6-4) photoproducts upon far-UV photolysis of 5-methylcytosine-containing dinucleotide monophosphates.* Biochemistry, 1994. **33**(39): p. 11942-50.
54. Tommasi, S., M.F. Denissenko, and G.P. Pfeifer, *Sunlight induces pyrimidine dimers preferentially at 5-methylcytosine bases.* Cancer Res, 1997. **57**(21): p. 4727-30.
55. Tsaalbi-Shtylik, A., et al., *Persistently stalled replication forks inhibit nucleotide excision repair in trans by sequestering Replication protein A.* Nucleic Acids Res, 2014. **42**(7): p. 4406-13.
56. Andersen, P.L., et al., *Sequential assembly of translesion DNA polymerases at UV-induced DNA damage sites.* Mol Biol Cell, 2011. **22**(13): p. 2373-83.

57. Wang, Y.C., V.M. Maher, and J.J. McCormick, *Xeroderma pigmentosum variant cells are less likely than normal cells to incorporate dAMP opposite photoproducts during replication of UV-irradiated plasmids.* Proc Natl Acad Sci U S A, 1991. **88**(17): p. 7810-4.
58. Protic-Sabljic, M., et al., *UV light-induced cyclobutane pyrimidine dimers are mutagenic in mammalian cells.* Mol Cell Biol, 1986. **6**(10): p. 3349-56.
59. Glazer, P.M., S.N. Sarkar, and W.C. Summers, *Detection and analysis of UV-induced mutations in mammalian cell DNA using a lambda phage shuttle vector.* Proc Natl Acad Sci U S A, 1986. **83**(4): p. 1041-4.
60. Mouret, S., et al., *Cyclobutane pyrimidine dimers are predominant DNA lesions in whole human skin exposed to UVA radiation.* Proc Natl Acad Sci U S A, 2006. **103**(37): p. 13765-70.
61. Husain, I., J. Griffith, and A. Sancar, *Thymine dimers bend DNA.* Proc Natl Acad Sci U S A, 1988. **85**(8): p. 2558-62.
62. Park, H., et al., *Crystal structure of a DNA decamer containing a cis-syn thymine dimer.* Proc Natl Acad Sci U S A, 2002. **99**(25): p. 15965-70.
63. Mitchell, D.L., *The relative cytotoxicity of (6-4) photoproducts and cyclobutane dimers in mammalian cells.* Photochem Photobiol, 1988. **48**(1): p. 51-7.
64. Kantor, G.J. and R.B. Setlow, *Rate and extent of DNA repair in nondividing human diploid fibroblasts.* Cancer Res, 1981. **41**(3): p. 819-25.
65. Mitchell, D.L., et al., *Loss of thymine dimers from mammalian cell DNA. The kinetics for antibody-binding sites are not the same as that for T4 endonuclease V sites.* Biochim Biophys Acta, 1982. **697**(3): p. 270-7.
66. Williams, J.I. and J.E. Cleaver, *Removal of T4 endonuclease V-sensitive sites from SV40 DNA after exposure to ultraviolet light.* Biochim Biophys Acta, 1979. **562**(3): p. 429-37.
67. Fousteri, M., et al., *Cockayne syndrome A and B proteins differentially regulate recruitment of chromatin remodeling and repair factors to stalled RNA polymerase II in vivo.* Mol Cell, 2006. **23**(4): p. 471-82.
68. Groisman, R., et al., *CSA-dependent degradation of CSB by the ubiquitin-proteasome pathway establishes a link between complementation factors of the Cockayne syndrome.* Genes Dev, 2006. **20**(11): p. 1429-34.
69. Scrima, A., et al., *Structural basis of UV DNA-damage recognition by the DDB1-DDB2 complex.* Cell, 2008. **135**(7): p. 1213-23.
70. Coin, F., V. Oksenych, and J.M. Egly, *Distinct roles for the XPB/p52 and XPD/p44 subcomplexes of TFIIH in damaged DNA opening during nucleotide excision repair.* Mol Cell, 2007. **26**(2): p. 245-56.
71. Winkler, G.S., et al., *TFIIH with inactive XPD helicase functions in transcription initiation but is defective in DNA repair.* J Biol Chem, 2000. **275**(6): p. 4258-66.
72. Fuss, J.O. and J.A. Tainer, *XPB and XPD helicases in TFIIH orchestrate DNA duplex opening and damage verification to coordinate repair with transcription and cell cycle via CAK kinase.* DNA Repair (Amst), 2011. **10**(7): p. 697-713.
73. Zotter, A., et al., *Recruitment of the nucleotide excision repair endonuclease XPG to sites of UV-induced dna damage depends on functional TFIIH.* Mol Cell Biol, 2006. **26**(23): p. 8868-79.

74. Overmeer, R.M., et al., *Replication protein A safeguards genome integrity by controlling NER incision events.* J Cell Biol, 2011. **192**(3): p. 401-15.
75. Marteijn, J.A., et al., *Understanding nucleotide excision repair and its roles in cancer and ageing.* Nat Rev Mol Cell Biol, 2014. **15**(7): p. 465-81.
76. Shivji, M.K., et al., *Dual-incision assays for nucleotide excision repair using DNA with a lesion at a specific site.* Methods Mol Biol, 1999. **113**: p. 373-92.
77. Ogi, T., et al., *Three DNA polymerases, recruited by different mechanisms, carry out NER repair synthesis in human cells.* Mol Cell, 2010. **37**(5): p. 714-27.
78. Moser, J., et al., *Sealing of chromosomal DNA nicks during nucleotide excision repair requires XRCC1 and DNA ligase III alpha in a cell-cycle-specific manner.* Mol Cell, 2007. **27**(2): p. 311-23.
79. DiGiovanna, J.J. and K.H. Kraemer, *Shining a light on xeroderma pigmentosum.* J Invest Dermatol, 2012. **132**(3 Pt 2): p. 785-96.
80. Bradford, P.T., et al., *Cancer and neurologic degeneration in xeroderma pigmentosum: long term follow-up characterises the role of DNA repair.* J Med Genet, 2011. **48**(3): p. 168-76.
81. Kleijer, W.J., et al., *Incidence of DNA repair deficiency disorders in western Europe: Xeroderma pigmentosum, Cockayne syndrome and trichothiodystrophy.* DNA Repair (Amst), 2008. **7**(5): p. 744-50.
82. Wang, Y., et al., *Dysregulation of gene expression as a cause of Cockayne syndrome neurological disease.* Proc Natl Acad Sci U S A, 2014. **111**(40): p. 14454-9.
83. Rapin, I., et al., *Cockayne syndrome in adults: review with clinical and pathologic study of a new case.* J Child Neurol, 2006. **21**(11): p. 991-1006.
84. Sarthy, J.F. and P. Baumann, *Apollo-taking the lead in telomere protection.* Mol Cell, 2010. **39**(4): p. 489-91.
85. Azzalin, C.M., et al., *Telomeric repeat containing RNA and RNA surveillance factors at mammalian chromosome ends.* Science, 2007. **318**(5851): p. 798-801.
86. Rochette, P.J. and D.E. Brash, *Human telomeres are hypersensitive to UV-induced DNA Damage and refractory to repair.* PLoS Genet, 2010. **6**(4): p. e1000926.
87. Kruk, P.A., N.J. Rampino, and V.A. Bohr, *DNA damage and repair in telomeres: relation to aging.* Proc Natl Acad Sci U S A, 1995. **92**(1): p. 258-62.
88. Sugasawa, K., et al., *Xeroderma pigmentosum group C protein complex is the initiator of global genome nucleotide excision repair.* Mol Cell, 1998. **2**(2): p. 223-32.
89. Stout, G.J. and M.A. Blasco, *Telomere length and telomerase activity impact the UV sensitivity syndrome xeroderma pigmentosum C.* Cancer Res, 2013. **73**(6): p. 1844-54.
90. Kassam, S.N. and A.J. Rainbow, *Deficient base excision repair of oxidative DNA damage induced by methylene blue plus visible light in xeroderma pigmentosum group C fibroblasts.* Biochem Biophys Res Commun, 2007. **359**(4): p. 1004-9.
91. D'Errico, M., et al., *New functions of XPC in the protection of human skin cells from oxidative damage.* EMBO J, 2006. **25**(18): p. 4305-15.

92. Zhu, X.D., et al., *ERCC1/XPF removes the 3' overhang from uncapped telomeres and represses formation of telomeric DNA-containing double minute chromosomes.* Mol Cell, 2003. **12**(6): p. 1489-98.
93. Munoz, P., et al., *XPF nuclease-dependent telomere loss and increased DNA damage in mice overexpressing TRF2 result in premature aging and cancer.* Nat Genet, 2005. **37**(10): p. 1063-71.
94. Fumagalli, M., et al., *Telomeric DNA damage is irreparable and causes persistent DNA-damage-response activation.* Nat Cell Biol, 2012. **14**(4): p. 355-65.
95. Bohr, V.A., et al., *DNA repair in an active gene: removal of pyrimidine dimers from the DHFR gene of CHO cells is much more efficient than in the genome overall.* Cell, 1985. **40**(2): p. 359-69.
96. Maicher, A., et al., *Deregulated telomere transcription causes replication-dependent telomere shortening and promotes cellular senescence.* Nucleic Acids Res, 2012. **40**(14): p. 6649-59.
97. Hess, M.T., et al., *Base pair conformation-dependent excision of benzo[a]pyrene diol epoxide-guanine adducts by human nucleotide excision repair enzymes.* Mol Cell Biol, 1997. **17**(12): p. 7069-76.
98. Braithwaite, E., X. Wu, and Z. Wang, *Repair of DNA lesions induced by polycyclic aromatic hydrocarbons in human cell-free extracts: involvement of two excision repair mechanisms in vitro.* Carcinogenesis, 1998. **19**(7): p. 1239-46.
99. Jain, V., et al., *Conformational and thermodynamic properties modulate the nucleotide excision repair of 2-aminofluorene and 2-acetylaminofluorene dG adducts in the NarI sequence.* Nucleic Acids Res, 2012. **40**(9): p. 3939-51.
100. Lukin, M., et al., *Structure and stability of DNA containing an aristolactam II-dA lesion: implications for the NER recognition of bulky adducts.* Nucleic Acids Res, 2012. **40**(6): p. 2759-70.
101. Alekseyev, Y.O., M.L. Hamm, and J.M. Essigmann, *Aflatoxin B1 formamidopyrimidine adducts are preferentially repaired by the nucleotide excision repair pathway in vivo.* Carcinogenesis, 2004. **25**(6): p. 1045-51.
102. O'Brien, T.J., B.R. Brooks, and S.R. Patierno, *Nucleotide excision repair functions in the removal of chromium-induced DNA damage in mammalian cells.* Mol Cell Biochem, 2005. **279**(1-2): p. 85-95.
103. Furuta, T., et al., *Transcription-coupled nucleotide excision repair as a determinant of cisplatin sensitivity of human cells.* Cancer Res, 2002. **62**(17): p. 4899-902.
104. Ikeda, H., et al., *Quantitative fluorescence in situ hybridization measurement of telomere length in skin with/without sun exposure or actinic keratosis.* Hum Pathol, 2014. **45**(3): p. 473-80.
105. Farmer, H., et al., *Targeting the DNA repair defect in BRCA mutant cells as a therapeutic strategy.* Nature, 2005. **434**(7035): p. 917-21.
106. Helleday, T., et al., *DNA repair pathways as targets for cancer therapy.* Nat Rev Cancer, 2008. **8**(3): p. 193-204.
107. Hoeijmakers, J.H., *DNA damage, aging, and cancer.* N Engl J Med, 2009. **361**(15): p. 1475-85.

108. Szymkowski, D.E., C.W. Lawrence, and R.D. Wood, *Repair by human cell extracts of single (6-4) and cyclobutane thymine-thymine photoproducts in DNA.* Proc Natl Acad Sci U S A, 1993. **90**(21): p. 9823-7.
109. Yoon, J.H., et al., *The DNA damage spectrum produced by simulated sunlight.* J Mol Biol, 2000. **299**(3): p. 681-93.
110. Garinis, G.A., et al., *Transcriptome analysis reveals cyclobutane pyrimidine dimers as a major source of UV-induced DNA breaks.* EMBO J, 2005. **24**(22): p. 3952-62.
111. Lange, S.S., K. Takata, and R.D. Wood, *DNA polymerases and cancer.* Nat Rev Cancer, 2011. **11**(2): p. 96-110.
112. Hanawalt, P.C. and G. Spivak, *Transcription-coupled DNA repair: two decades of progress and surprises.* Nat Rev Mol Cell Biol, 2008. **9**(12): p. 958-70.
113. Gillet, L.C. and O.D. Scharer, *Molecular mechanisms of mammalian global genome nucleotide excision repair.* Chem Rev, 2006. **106**(2): p. 253-76.
114. Masutani, C., et al., *The XPV (xeroderma pigmentosum variant) gene encodes human DNA polymerase eta.* Nature, 1999. **399**(6737): p. 700-4.
115. Armanios, M. and E.H. Blackburn, *The telomere syndromes.* Nat Rev Genet, 2012.
116. Finkel, T., M. Serrano, and M.A. Blasco, *The common biology of cancer and ageing.* Nature, 2007. **448**(7155): p. 767-74.
117. Wright, W.E. and J.W. Shay, *Telomere biology in aging and cancer.* J Am Geriatr Soc, 2005. **53**(9 Suppl): p. S292-4.
118. Emanuele, E., et al., *Topical application of preparations containing DNA repair enzymes prevents ultraviolet-induced telomere shortening and c-FOS proto-oncogene hyperexpression in human skin: an experimental pilot study.* J Drugs Dermatol, 2013. **12**(9): p. 1017-21.
119. Wright, W.E., et al., *Normal human chromosomes have long G-rich telomeric overhangs at one end.* Genes Dev, 1997. **11**(21): p. 2801-9.
120. de Lange, T., *Telomere biology and DNA repair: enemies with benefits.* FEBS Lett, 2010. **584**(17): p. 3673-4.
121. Opresko, P.L., et al., *The Werner syndrome helicase and exonuclease cooperate to resolve telomeric D loops in a manner regulated by TRF1 and TRF2.* Mol Cell, 2004. **14**(6): p. 763-74.
122. Herbert, B.S., J.W. Shay, and W.E. Wright, *Analysis of telomeres and telomerase.* Curr Protoc Cell Biol, 2003. **Chapter 18**: p. Unit 18 6.
123. Kimura, M., et al., *Measurement of telomere length by the Southern blot analysis of terminal restriction fragment lengths.* Nat Protoc, 2010. **5**(9): p. 1596-607.
124. Wani, A.A., S.M. D'Ambrosio, and N.K. Alvi, *Quantitation of pyrimidine dimers by immunoslot blot following sublethal UV-irradiation of human cells.* Photochem Photobiol, 1987. **46**(4): p. 477-82.
125. Ayala-Torres, S., et al., *Analysis of gene-specific DNA damage and repair using quantitative polymerase chain reaction.* Methods, 2000. **22**(2): p. 135-47.
126. Kad, N.M., et al., *Collaborative dynamic DNA scanning by nucleotide excision repair proteins investigated by single- molecule imaging of quantum-dot-labeled proteins.* Mol Cell, 2010. **37**(5): p. 702-13.

127. Bodnar, A.G., et al., *Extension of life-span by introduction of telomerase into normal human cells.* Science, 1998. **279**(5349): p. 349-52.
128. Batzer, M.A. and P.L. Deininger, *Alu repeats and human genomic diversity.* Nat Rev Genet, 2002. **3**(5): p. 370-9.
129. Grolimund, L., et al., *A quantitative telomeric chromatin isolation protocol identifies different telomeric states.* Nat Commun, 2013. **4**: p. 2848.
130. Heffernan, T.P., et al., *An ATR- and Chk1-dependent S checkpoint inhibits replicon initiation following UVC-induced DNA damage.* Mol Cell Biol, 2002. **22**(24): p. 8552-61.
131. Mitchell, D.L., C.A. Haipek, and J.M. Clarkson, *(6-4)Photoproducts are removed from the DNA of UV-irradiated mammalian cells more efficiently than cyclobutane pyrimidine dimers.* Mutat Res, 1985. **143**(3): p. 109-12.
132. Vreeswijk, M.P., et al., *Analysis of repair of cyclobutane pyrimidine dimers and pyrimidine 6-4 pyrimidone photoproducts in transcriptionally active and inactive genes in Chinese hamster cells.* J Biol Chem, 1994. **269**(50): p. 31858-63.
133. Levy, D.D., et al., *Expression of a transfected DNA repair gene (XPA) in xeroderma pigmentosum group A cells restores normal DNA repair and mutagenesis of UV-treated plasmids.* Carcinogenesis, 1995. **16**(7): p. 1557-63.
134. Herbert, B.S., et al., *A peroxisome proliferator-activated receptor-gamma agonist and the p53 rescue drug CP-31398 inhibit the spontaneous immortalization of breast epithelial cells.* Cancer Res, 2003. **63**(8): p. 1914-9.
135. Tornaletti, S. and G.P. Pfeifer, *UV light as a footprinting agent: modulation of UV-induced DNA damage by transcription factors bound at the promoters of three human genes.* J Mol Biol, 1995. **249**(4): p. 714-28.
136. Ford, J.M. and P.C. Hanawalt, *Expression of wild-type p53 is required for efficient global genomic nucleotide excision repair in UV-irradiated human fibroblasts.* J Biol Chem, 1997. **272**(44): p. 28073-80.
137. Luke, B. and J. Lingner, *TERRA: telomeric repeat-containing RNA.* EMBO J, 2009. **28**(17): p. 2503-10.
138. van Hoffen, A., et al., *Transcription-coupled repair removes both cyclobutane pyrimidine dimers and 6-4 photoproducts with equal efficiency and in a sequential way from transcribed DNA in xeroderma pigmentosum group C fibroblasts.* EMBO J, 1995. **14**(2): p. 360-7.
139. Steinert, S., J.W. Shay, and W.E. Wright, *Modification of subtelomeric DNA.* Mol Cell Biol, 2004. **24**(10): p. 4571-80.
140. Courdavault, S., et al., *Repair of the three main types of bipyrimidine DNA photoproducts in human keratinocytes exposed to UVB and UVA radiations.* DNA Repair (Amst), 2005. **4**(7): p. 836-44.
141. Bryan, T.M. and P. Baumann, *G-quadruplexes: from guanine gels to chemotherapeutics.* Mol Biotechnol, 2011. **49**(2): p. 198-208.
142. Pope-Varsalona, H., et al., *Polymerase eta suppresses telomere defects induced by DNA damaging agents.* Nucleic Acids Res, 2014.
143. de Vries, A., et al., *Increased susceptibility to ultraviolet-B and carcinogens of mice lacking the DNA excision repair gene XPA.* Nature, 1995. **377**(6545): p. 169-73.

144. Tsodikov, O.V., et al., *Structural basis for the recruitment of ERCC1-XPF to nucleotide excision repair complexes by XPA.* EMBO J, 2007. **26**(22): p. 4768-76.
145. Miyauchi-Hashimoto, H., K. Tanaka, and T. Horio, *Enhanced inflammation and immunosuppression by ultraviolet radiation in xeroderma pigmentosum group A (XPA) model mice.* J Invest Dermatol, 1996. **107**(3): p. 343-8.
146. Liu, F.J., A. Barchowsky, and P.L. Opresko, *The Werner syndrome protein suppresses telomeric instability caused by chromium (VI) induced DNA replication stress.* PLoS One, 2010. **5**(6): p. e11152.
147. Liu, F.J., A. Barchowsky, and P.L. Opresko, *The Werner syndrome protein functions in repair of Cr(VI)-induced replication-associated DNA damage.* Toxicol Sci, 2009. **110**(2): p. 307-18.
148. Cleaver, J.E., et al., *Unique DNA repair properties of a xeroderma pigmentosum revertant.* Mol Cell Biol, 1987. **7**(9): p. 3353-7.
149. Chan, G.L., P.W. Doetsch, and W.A. Haseltine, *Cyclobutane pyrimidine dimers and (6-4) photoproducts block polymerization by DNA polymerase I.* Biochemistry, 1985. **24**(21): p. 5723-8.
150. Schultz, R.A., D.P. Barbis, and E.C. Friedberg, *Studies on gene transfer and reversion to UV resistance in xeroderma pigmentosum cells.* Somat Cell Mol Genet, 1985. **11**(6): p. 617-24.
151. Phan, A.T. and J.L. Mergny, *Human telomeric DNA: G-quadruplex, i-motif and Watson-Crick double helix.* Nucleic Acids Res, 2002. **30**(21): p. 4618-25.
152. Nagel, Z.D., et al., *Multiplexed DNA repair assays for multiple lesions and multiple doses via transcription inhibition and transcriptional mutagenesis.* Proc Natl Acad Sci U S A, 2014. **111**(18): p. E1823-32.
153. Damerla, R.R., et al., *Werner syndrome protein suppresses the formation of large deletions during the replication of human telomeric sequences.* Cell Cycle, 2012. **11**(16): p. 3036-44.
154. Gillet, L.C., J. Alzeer, and O.D. Scharer, *Site-specific incorporation of N-(deoxyguanosin-8-yl)-2-acetylaminofluorene (dG-AAF) into oligonucleotides using modified 'ultra-mild' DNA synthesis.* Nucleic Acids Res, 2005. **33**(6): p. 1961-9.
155. Deng, Z., et al., *Telomere repeat binding factors TRF1, TRF2, and hRAP1 modulate replication of Epstein-Barr virus OriP.* J Virol, 2003. **77**(22): p. 11992-2001.
156. Fousteri, M. and L.H. Mullenders, *Transcription-coupled nucleotide excision repair in mammalian cells: molecular mechanisms and biological effects.* Cell Res, 2008. **18**(1): p. 73-84.
157. Kitsera, N., et al., *Cockayne syndrome: varied requirement of transcription-coupled nucleotide excision repair for the removal of three structurally different adducts from transcribed DNA.* PLoS One, 2014. **9**(4): p. e94405.
158. Mu, D. and A. Sancar, *Model for XPC-independent transcription-coupled repair of pyrimidine dimers in humans.* J Biol Chem, 1997. **272**(12): p. 7570-3.
159. Shivji, M.K.K., et al., *Dual-Incision Assays for Nucleotide Excision Repair Using DNA with a Lesion at a Specific Site.* DNA Repair Protocols, 1999. **113**(II): p. 20.
160. Artandi, S.E., et al., *Telomere dysfunction promotes non-reciprocal translocations and epithelial cancers in mice.* Nature, 2000. **406**(6796): p. 641-5.

161. Sorrentino, J.A., H.K. Sanoff, and N.E. Sharpless, *Defining the toxicology of aging.* Trends Mol Med, 2014. **20**(7): p. 375-84.
162. Chen, Y., et al., *A shared docking motif in TRF1 and TRF2 used for differential recruitment of telomeric proteins.* Science, 2008. **319**(5866): p. 1092-6.
163. Su, Y., et al., *Multiple DNA binding domains mediate the function of the ERCC1-XPF protein in nucleotide excision repair.* J Biol Chem, 2012. **287**(26): p. 21846-55.
164. Ahmad, A., et al., *Mislocalization of XPF-ERCC1 nuclease contributes to reduced DNA repair in XP-F patients.* PLoS Genet, 2010. **6**(3): p. e1000871.
165. Opresko, P.L., et al., *Telomere-binding protein TRF2 binds to and stimulates the Werner and Bloom syndrome helicases.* J Biol Chem, 2002. **277**(43): p. 41110-9.
166. Wu, Y., T.R. Mitchell, and X.D. Zhu, *Human XPF controls TRF2 and telomere length maintenance through distinctive mechanisms.* Mech Ageing Dev, 2008. **129**(10): p. 602-10.